THESIS

PROTEIN INTERACTORS OF ATSR1 MRNA DURING SALT STRESS

Submitted by

Vesper Burjoski

Department of Biology

In partial fulfillment of the requirements

For the Degree of Master of Science

Colorado State University

Fort Collins, Colorado

Summer 2021

Master's Committee:

Advisor: Anireddy Reddy

Patricia Bedinger
Ashok Prasad
Chris Snow

ABSTRACT

PROTEIN INTERACTORS OF ATSR1 MRNA DURING SALT STRESS

To survive adverse conditions, plants must respond physiologically to biotic and abiotic stresses. Stressors are detected via primary sensors in the cell wall and plasma membrane to elicit a host of secondary signals, such as reactive oxygen species and calcium (Ca^{2+}) flux. These secondary messengers are detected by a host of signal transduction molecules for the modulation of gene expression and physiology in response to stress. In the case of calcium, the class of proteins known as calmodulin and calmodulin-like proteins bind calcium and this complex then interacts with many proteins, including transcription factors, to activate the stress response. One calmodulin-binding protein, known as Signal Responsive 1 (SR1) or CAMTA3, is known to play a role in diverse stress response pathways, including basal plant immunity, systemic acquired resistance, cold, herbivory, and salt stress, acting as both a positive and negative regulator of resistance depending on the stress. *SR1* mRNA accumulates several-fold during salt stress due to increased stability mediated by reactive oxygen species (ROS). This accumulation requires the 3' end of the transcript and is not accompanied by corresponding increases in SR1 protein. Thus, the physiological mechanism and role of *SR1* accumulation during salt stress poses an important question in understanding how SR1 mediates salt stress response. I hypothesized that a protein factor might bind *SR1* during salt stress, possibly after undergoing an ROS-triggered conformational change to increase its RNA binding capacity, to confer increased stability to *SR1,* likely by protecting it against deadenylase-mediated degradation. Here, I describe my studies to

test this hypothesis. I created transgenic lines of Arabidopsis expressing SR1 fused to an N-terminal protein tag (3xFLAG) and a 3' RNA aptamer tag (MS2) and used these lines to perform MS2 tandem repeat affinity purification and mass spectrometry, or MS2-TRAP-MS. In the presence and absence of salt, Arabidopsis WT and transgenic seedlings were exposed to UV radiation to crosslink the RNA population to directly interacting proteins, then ground to powder in liquid nitrogen and lysed. The lysate was passed over amylose beads bearing the MS2 coat protein (MCP), which binds the MS2 RNA aptamer, to pull down *SR1-MS2* and any crosslinked proteins. RNA was removed from the population of crosslinked proteins via RNAseI digestion, and the proteins were separated on SDS gels for use in liquid chromatography mass spectrometry (LC-MS). Across all experiments and samples, LC-MS identified 395 individual Arabidopsis proteins. In the salt-treated sample, GO term enrichment revealed significantly higher prevalence of metabolically related terms, and the salt-treated sample also showed a much higher proportion of proteins predicted to be localized to the mitochondria or chloroplast. Among these proteins, only 2 were reproducibly enriched as interacting with *SR1-MS2* under salt treatment: glutamate dehydrogenase 2 (GDH2) and rubisco bisphosphate carboxylase large chain (rbcL). Both GDH2 and rbcL are multimeric metabolic enzymes: GDH2 is a mitochondrial enzyme involved in nitrogen metabolism, and rbcL is a chloroplastic enzyme that catalyzes the carboxylation of ribulose bisphosphate during photosynthesis and makes up a significant portion of a plant cell's total protein. These surprising results are discussed and evidence is amassed leading us to conclude that my results may represent real binding of *SR1-MS2,* despite the unexpected nature of the enriched proteins and the high prevalence of rbcL. Both GDH2 and rbcL are known to possess some RNA binding capacity, and it is possible that *SR1-MS2* plays a role in competing

with their other RNA binding targets under salt stress. It is also possible that *SR1-MS2* and its interactions with these proteins play a role in the stabilization of liquid-liquid phase separation in the organelles upon salt stress-induced destabilization of organellar condensates. Further experiments are needed to conclusively show that this binding is not artifactual, including yeast three-hybrid verification of the interactions, gel shift assays, and visualization of *SR1-MS2* localization during salt stress.

TABLE OF CONTENTS

1. Introduction

All organisms interact with and respond to their environments to survive. When an organism's environment is inhospitable to it, it experiences stress. Organisms mitigate stress in two ways: adaptation and acclimation (Levitt, 1980). Adaptation to stressful environments involves the systemic selection of heritable protective measures that are suited to a particular range of environmental parameters and allow an organism to avoid the experience of stress under those conditions. Endemic adaptation is usually achieved through the microevolution of populations. Acclimation, on the other hand, requires an individual organism to experience and respond to stress. Traditionally, acclimation responses were understood as reversible and non-inheritable, but the discovery of heritable, stress-responsive epigenetic modifications has blurred these lines (Krasensky and Jonak, 2012; Allis and Jenuwein, 2016).

Stress acclimation responses take two broad categories: avoidance and tolerance (Levitt, 1980). Motile organisms, such as most animals, are able to rely heavily on stress avoidance techniques, whereas sessile organisms, such as plants, must prioritize stress tolerance techniques because of their inability to leave an environment that becomes inhospitable (Mei et al., 2018). In plants, stress can be divided into two categories: biotic stress and abiotic stress (Krasensky and Jonak, 2012). Biotic stress is stress that originates from a biotic agent, such as a pathogen or herbivore. Abiotic stress is typically climatic or chemical, in the form of adverse temperatures (hot or cold), radiation, over- or under-abundance of water (flood and drought), salinity, and heavy metal toxicity. These types of stresses are estimated to account for approximately 70% of crop yield losses worldwide (Acqaah, 2009).

1.1 Plant Abiotic Stress Response

In order to respond to abiotic stressors, organisms - including plants - must have mechanisms in place to detect the presence of such stressful conditions. Much effort has been expended on the identification of primary stress sensors in plants, but to date few components can be considered as such with much confidence (Gong et al., 2020). Despite the difficulty in identifying these primary sensors, there are some viable theories as to the nature of abiotic stress perception. It's thought that many different cellular components and molecules may detect stressors simultaneously and work in coordination, as abiotic stress usually impacts a cell in a holistic manner (Zhu, 2016). Membrane-less organelles such as stress granules, nuclear speckles, liquid-liquid phase separations, and ribonucleoprotein complexes have also been earmarked as potential key components in stress perception (Boeynaems, 2018). Ribonucleoprotein complexes are likely to play crucial role due to the fact that in plants, many stress-responsive genes encode intrinsically-disordered proteins whose pre-mRNA is inadequately processed under abiotic stress, leading to ribonucleoprotein aggregation under the increased macromolecular crowding conditions that abiotic stresses often trigger (Cui and Xiong, 2015).

Although the primary sensors and signals of abiotic stress are not well understood in plants, they do share a common secondary signal that has been extremely well-studied. In reaction to most types of abiotic stress, a temporary spike in cytosolic Ca^{2+} concentrations is observed, which acts as a secondary signal in coordinating stress response (Reddy et al., 2011). This calcium signaling is discussed in detail later in this Introduction.

Perception of abiotic stress through calcium signaling or other means triggers diverse chemical, physiological, and genetic responses to ameliorate the effects of stress. These responses are characteristic of the specific type of abiotic stress perceived and represent entire fields of research unto themselves. Only those relevant to the work described in this thesis will be discussed in further detail here.

1.1.1 Drought

Drought stress response is characterized by an up to 50-fold increase in concentration of the plant hormone abscisic acid (ABA), which, briefly, triggers stomatal closing through ABA-mediated regulation of membrane transporters (Zeevaart, 1980; Raghavendra et al., 2010; Qi et al., 2018). A family of pyrobactin resistance like (PYL) proteins act as ABA receptors in conjunction with protein phosphatase 2C (PP2C) proteins, which bind to and inhibit the activity of the SNF1-related protein kinase 2 (SnRK2) family of kinases in the absence of ABA (Ma et al., 2009; Park et al., 2009). When ABA is present, the released SnRK2 kinases phosphorylate a group of transcription factors known as ABA-responsive element binding factors, which are then able to activate ABA-responsive (and thus drought-responsive) genes (Cutler et al., 2010; Qi et al., 2018; Raghavendra et al., 2010; Zhu, 2016; Gong et al., 2020).

1.1.2 Salt

What is referred to as salt stress is actually made up of two distinct types of stress: osmotic stress, leading to decreased water uptake, and ion toxicity due to the over-accumulation of toxic ions. For this reason, salt stress responses can be difficult to separate from those of drought, as both subject the plant to a hydration deficit (Gong et al., 2020). Response to salt-related ion

toxicity is coordinated through the Salt Overly Sensitive (SOS) pathway, which is composed of proteins encoded by three genes - SOS1, SOS2, and SOS3 (Zhu, 2001). The SOS pathway functions by activating SOS1, a Na^+/H^+ antiporter, in response to calcium signaling detected by SOS3, which contains three E-F hand motifs; i.e., it is a calcium sensor (Liu and Zhu, 1998; Shi et al., 2000; Liu et al., 2000; Shi et al. 2002; Shi et al., 2002b; Quintero et al., 2010). Ca2+-bound SOS3 relieves the autoinhibition of SOS2, a kinase which phosphorylates SOS1 when active (Guo et al., 2001). Phosphorylated SOS1 has enhanced antiporter activity due to relieved autoinhibition, resulting in lowered cellular concentrations of Na^+ (Quintero et al., 2010). It is thought that this Na^+ efflux functions to transport Na^+ into root xylem under salt stress, where it is carried upward to be stored in leaf vacuoles (El Mahi et al., 2019; Gong et al., 2020). Vacuolar sequestration is accomplished through tonoplast transporters such as NHX1, another Na^+/H^+ antiporter (Gaxiola et al., 1999). NHX1's activity is inhibited by a calmodulin within the vacuole, and this inhibition is released under salt stress to activate NHX1-mediated sequestration of Na^+ (Yamaguchi et al., 2003; Yamaguchi et al., 2005). Thus, calcium signaling plays a critical role at multiple points in regulation of salt-stress response (Seifikalhor et al., 2019).

1.2. Calcium Signaling

In plants – as in all eukaryotes - cellular Ca^{2+} levels form a layer of signaling that impacts hormone activity and response to biotic and abiotic stress (Berridge et al., 2000; Ranty et al., 2006; Kudla et al., 2017). Because of Ca^{2+} cytotoxicity - likely due to the fact that Ca^{2+} can precipitate phosphate and disrupt cellular energy currency - plants maintain a cytosolic Ca^{2+} concentration orders of magnitude lower than that in the apoplast and some organelles (Clapham, 1995; Reddy, 2001; Ranty et al., 2006). A wide array of Ca^{2+} channels and pumps located in

plasma and organellar membranes maintain cellular Ca^{2+} concentrations through fine adjustments of Ca^{2+} influx and efflux. In response to detection of stress by primary sensors, temporary spikes in cytosolic Ca^{2+} are evoked as a secondary signal by influx proteins, which source their Ca^{2+} from apoplastic spaces or from Ca^{2+} sequestered in organelles (Berridge et al., 2003). The dynamics of these Ca^{2+} spikes - frequency, amplitude, duration, location - are dependent on the type and severity of stress/extracellular stimulus, forming signatures characteristic of different types of stress that can be detected and distinguished by calcium binding proteins (Webb et al., 1996; Hetherington and Brownlee, 2004). Some of these binding proteins are directly regulated by Ca^{2+}, while others serve as intermediaries to signal for genetic and biochemical changes (Day et al., 2002).

One of the most notable calcium sensors is calmodulin, named for CALcium MODULating proteIN (Babu et al., 1988). In eukaryotes, calmodulins are members of a gene family some of whose members encode an evolutionarily conserved "prototypical" calmodulin. In plants, there is also an extended family of less-conserved calmodulin-related genes (McCormack et al., 2005). In fact, the members of these extended families are more numerous in plants than are true calmodulins. True calmodulins are rich in introns, whereas calmodulin-like proteins are intron-less and evolved prior to calmodulins (Mohanta et al., 2017).

The prototypical calmodulin is a member of the E-F hand family of intermediary calcium sensors, which are characterized by the presence of the E-F hand structural motif. The E-F hand motif contains an N-terminal helix, a C-terminal helix, and a Ca^{2+} coordinating loop sandwiched between the helices (Babu et al., 1988). Calmodulin has four E-F hands, arranged as two

homologous globular domains made up of two E-F hands each (Roads and Friedberg, 1997). The conformations of these two sets of E-F hands is differentially dependent on Ca^{2+} binding; superficially, their conformations are closed or only semi-open in the absence of Ca^{2+}, and undergo changes to an open configuration in the presence of Ca^{2+} (Snedden and Fromm, 2001). This exposes previously hidden hydrophobic groups, constituting a Ca^{2+} directed release of free energy that couples the Ca^{2+} binding event to cellular biochemical energy and produces calmodulin's transducer capacity (Marlow et al., 2010).

Because of its bimodal conformations, calmodulin has the capacity to bind different populations of proteins in the presence and absence of Ca^{2+}; i.e., calcium-dependent binding and calcium-independent binding. No calmodulin-binding consensus motif has been identified, but patterns in the spacing of anchoring hydrophobic residues have been noted, constituting motifs such as the IQ sequence motif (Mruk et al., 2014). Calmodulin regulation is diversified in plants compared to other eukaryotes with calmodulin, sharing only about one-third of regulatory targets with homologous targets in other calmodulin-regulated organisms (Bouché et al., 2005). Many calmodulin-binding targets have been identified, reaching nearly 25% of proteins screened and running the gamut from metabolic enzymes, protein kinases/phosphatases, cytoskeleton-associated proteins, ion transporters, chaperonins, and transcription factors (Reddy, 2001; Popescu et al., 2007).

These downstream targets of calmodulins and calmodulin-like proteins tie calmodulin-mediated calcium signaling to significant roles in a number of cellular processes. Calmodulin has been shown to play an important role in plant developmental biology, plant-microbe interactions, the

circadian clock, and abiotic stress response (Kudla et al., 2017). In coordination with Ca^{2+}, NAD^{+}, NAD kinase, and NADPase, calmodulin forms a self-sustaining loop that acts as a gear for the circadian clock for cell growth (Ruiz et al., 2018). Spikes in cellular Ca2+ have been observed in response to most abiotic stresses, each with its own flux signature in terms of amplitude, duration, and frequency (Liu et al., 2020).

Particularly, calmodulin has been shown to play a role in response to salt stress, as was mentioned earlier. A calmodulin-like protein, CML18, is involved in the Salt Overly Sensitive pathway (SOS), in which its binding to AtNHX1, a vacuolar Na^{+}/H^{+} antiporter, decreases its exchange capacity. Under salt-induced rise in pH, CML18 is released from AtNHX1, increasing its exchange capacity and thus targeting cytosolic Na+ to the vacuole (Yamaguchi et al., 2005). Transcription factors regulating salt and dehydration response genes have been found to be calmodulin-binding, and salt-inducible calmodulin isoforms were shown to modulate the DNA-binding capacity of such transcription factors (Kudla et al., 2017). In rice, overexpression of calmodulins widely impacts genes involved in salt stress response and affects carbon and energy metabolism, suggesting that calmodulin modulates the activity of several metabolic enzymes while under salt stress (Yuenyong et al., 2017; Yuenyong et al., 2018). In *Medicago truncatula*, a model calmodulin was found to be upregulated under salt stress, and overexpression of the gene resulted in greater seed germination sensitivity to osmotic stress, as well as inhibition of root and shoot growth, suggesting that the gene is involved in negative regulation of salt stress response (Zhang et al., 2018). A wide variety of calmodulins and calmodulin-like genes were studied in a wild-growing grapevine species, *Vitis amurensis*, in response to salt stress, and over half of these genes were observed to be upregulated or downregulated greatly in response to the treatment

(Dubrovina et al., 2019). Thus, the role of calmodulins and calmodulin-like proteins in salt stress response appears significant and widespread (Seifikalhor et al., 2019).

1.3. Signal Responsive 1 (SR1)

SR1 (also known as CAMTA3), is a transcription factor that binds to calmodulin in response to changes in cellular Ca^{2+} levels induced by either biotic or abiotic stress (Reddy et al., 2000; Yang and Poovaiah, 2000; Galon et al., 2010; Laluk et al., 2012; Qiu et al., 2012) (Fig. 1). SR1 is a member of a six-gene family encoding transcription factors in Arabidopsis (SRs/CAMTAs), which are characterized by the presence of a battery of shared motifs (Reddy et al., 2000; Yang and Poovaiah, 2000; Yang and Poovaiah, 2002; Bouché et al., 2002; Han et al. 2006; Song et al., 2006; Pandey et al., 2013). Calmodulin-binding in response to stress is mediated by their shared Ca^{2+}-dependent calmodulin-binding domain (Reddy et al. 2011; Poovaiah et al. 2013). In addition, they also contain Ca^{2+}-independent calmodulin-binding domains (also known as IQ domains) and the role of these domains in regulating these transcription factors is not yet elucidated. All CAMTAs bind DNA by their shared N-terminal CG-1 DNA-binding domain and immunoglobulin-like fold domain (Silva, 1994; Mitsuda et al., 2003; Yang and Poovaiah, 2002; Doherty et al., 2009). The CG-1 DNA-binding plays a key role in activating the general stress response (GSR), inducing genes whose promoters contain the *cis*-regulatory Rapid Stress Response Element (RSRE; CGCG) in coordination with members 1-4 of the SR/CAMTA family (Walley et al., 2007; Benn et al., 2014). SR1 is believed to be constitutively expressed but can rapidly activate RSRE-driven genes in a Ca^{2+}-dependent manner (Bjornson et al., 2014).

AtSR1 functions as a master regulator of the general stress response, plant immunity, cold stress response, and salt stress response in a calcium/calmodulin-dependent manner (Figure 1). It constitutively represses activators of plant immunity; the repression is released via ubiquitination- and phosphorylation-mediated nuclear export and proteasome degradation upon pathogen exposure (Lolle et al., 2017; Yuan et al., 2018; Jiang et al., 2020). At warm temperatures, AtSR1 coordinates with CAMTA1 and CAMTA2 (two other members of the same gene family) to repress salicylic acid synthesis; during cold acclimation, the repression is released (Galon et al., 2008; Doherty et al., 2009; Kim et al., 2013; Kim et al., 2017). Similarly, AtSR1, CAMTA1, and CAMTA2 coordinate to repress synthesis of pipecolic acid (Pip), which is involved in system acquired resistance (Kim et al., 2020). It also plays a role in activating the general stress response as mediated by calcium/calmodulin and the plastidial metabolite methylerythritol cyclodiphosphate (MEcPP) (Galon et al, 2010; Benn et al., 2014; Benn et al., 2016).

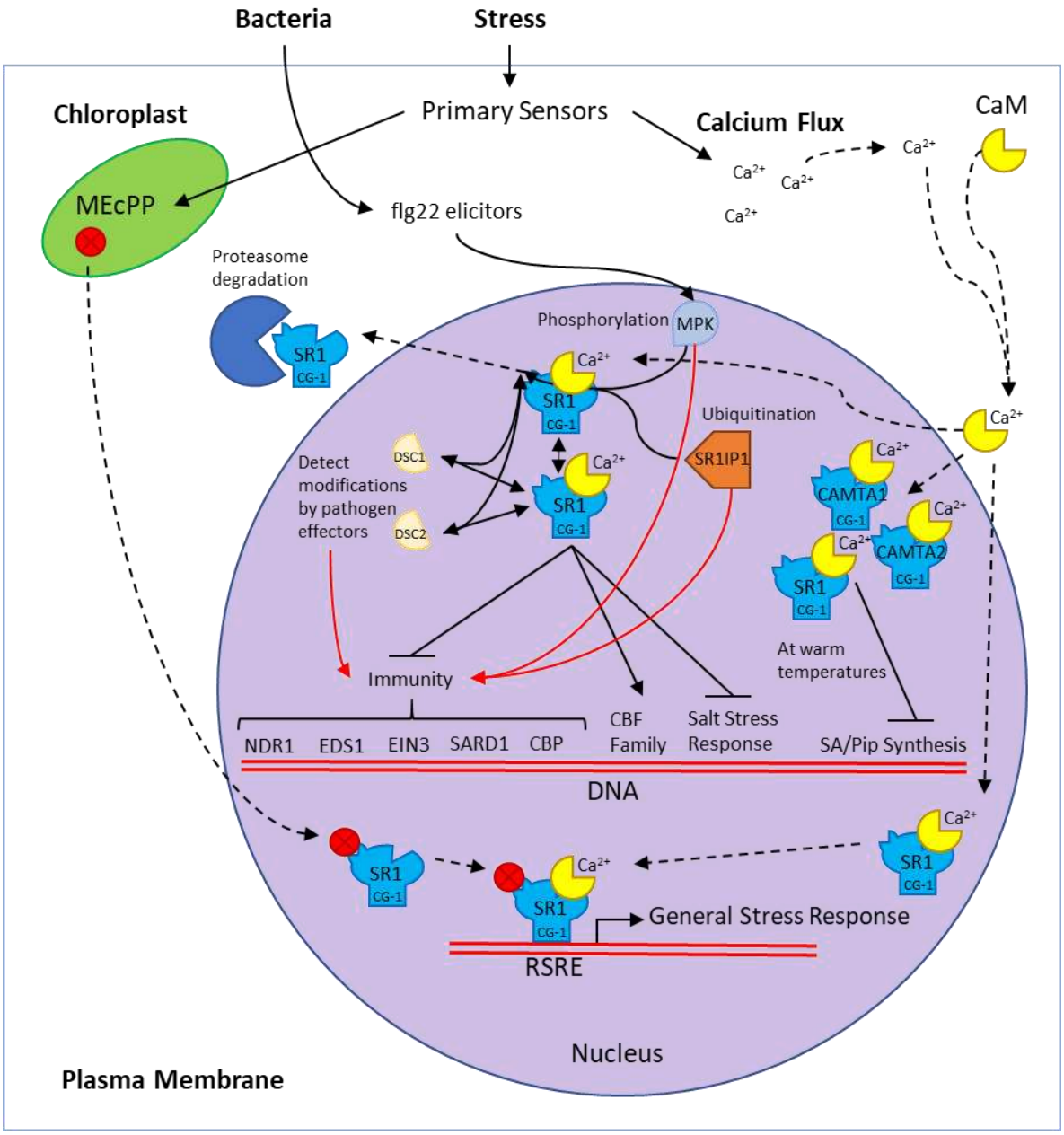

Figure 1: Summary of AtSR1 Biology

AtSR1 functions as a master regulator of the general stress response, plant immunity, cold stress response, and salt stress response in a calcium/calmodulin-dependent manner. It constitutively represses activators of plant immunity; the repression is released via ubiquitination- and phosphorylation-mediated nuclear export and proteasome degradation upon pathogen exposure (Lolle et al., 2017; Yuan et al., 2018; Jiang et al., 2020). At warm temperatures, AtSR1 coordinates with CAMTA1 and CAMTA2 (two other members of the same gene family) to repress salicylic acid synthesis; during cold acclimation, the repression is released (Galon et al., 2008; Doherty et al., 2009; Kim et al., 2013; Kim et al., 2017). Similarly, AtSR1, CAMTA1, and CAMTA2 coordinate to repress synthesis of pipecolic acid (Pip), which is involved in systemic

acquired resistance (Kim et al., 2020). It also plays a role in activating the general stress response as mediated by calcium/calmodulin and the plastidial metabolite methylerythritol cyclodiphosphate (MEcPP) (Galon et al, 2010; Benn et al., 2014; Benn et al., 2016).

SR1's role in diverse stress responses has been elucidated: it has been shown as a negative regulator of Arabidopsis plant immunity, and a positive regulator of cold and insect resistance (Galon et al., 2008; Doherty et al., 2009; Du et al., 2009; Laluk et al., 2012; Nie et al., 2012; Qiu et al., 2012; Kim et al., 2013; Truman et al., 2013). RNA-seq studies have demonstrated over 3000 SR1-regulated genes and showed that it also plays a role in negative regulation of salt stress (Prasad et al., 2016). Later work demonstrated that *SR1* mRNA accumulates several-fold under salt stress due to enhanced RNA stability, and showed that this accumulation was dependent on a 500-nucleotide region at the 3' end of the *SR1* transcript (Fig. 2, Fig. 3) (Abdel-Hameed et al., 2020). This accumulation was mediated by reactive oxygen species, a signal well-known to be induced by salt stress and to regulate downstream salt-stress responses (Fig. 3).

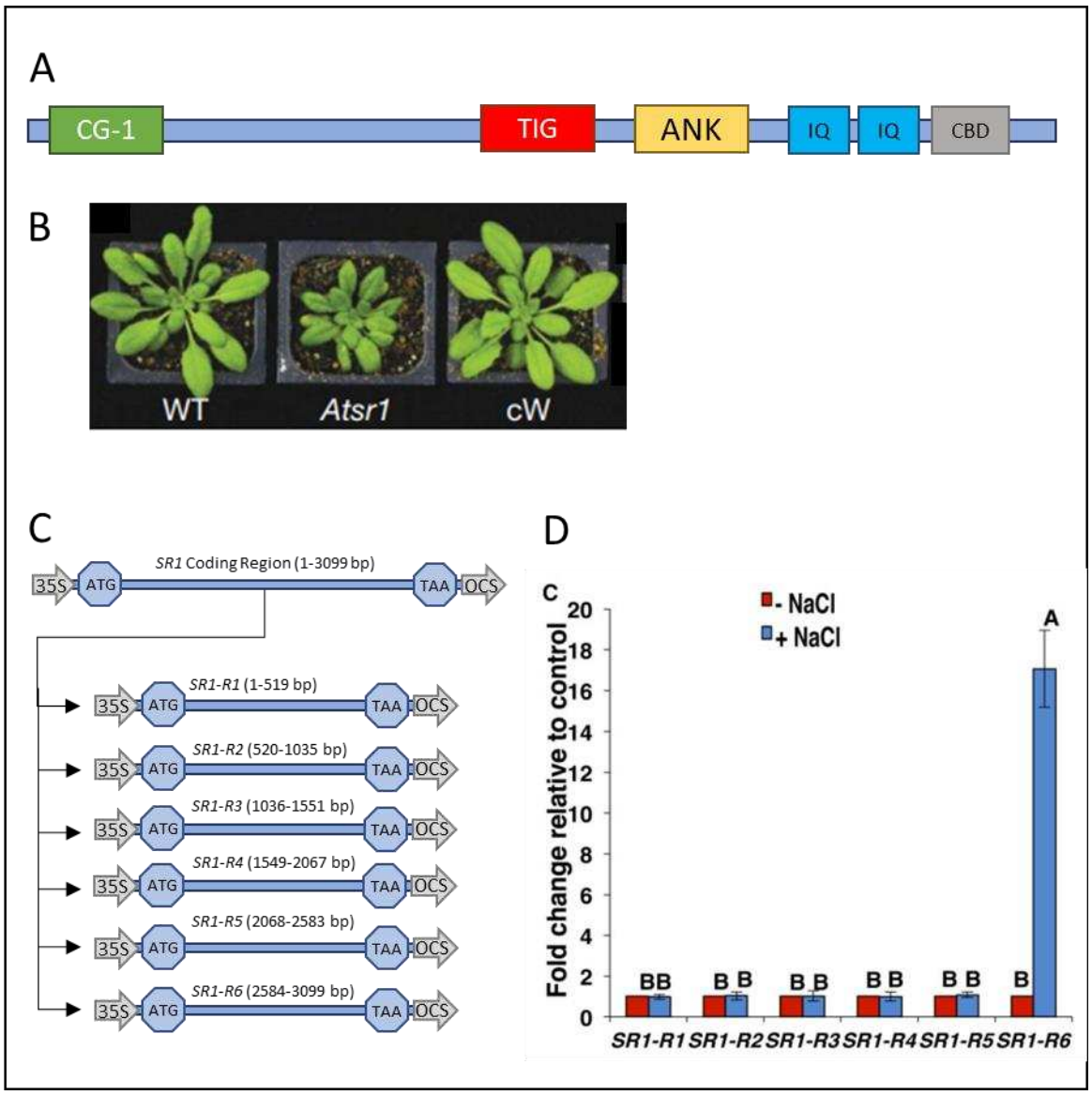

Figure 2. Summary of AtSR1 Structure and Recent Data

A - AtSR1 has an N-terminal CG-1 DNA-binding domain that mediates its function as a transcription factor, along with its immunoglobulin-like fold domain (TIG). Its IQ-IQ calmodulin-binding domain and calcium-dependent calmodulin-binding domain (CBD) mediate its Ca^{2+} regulation, which is necessary for transcriptional repression/activation. B – Phenotype of AtSR1 *Arabidopsis thaliana* knockout line, SR1-KO. When grown at 19°C, the knockout line shows slight dwarfism and chlorosis of older leaves at ~25 days after germination. Reproduced from Du et al., 2009. C – Cloning of *AtSR1* truncated constructs. Upon observation of *SR1* mRNA accumulation under salt stress, the coding sequence of *AtSR1* was subdivided into six ~500 bp fragments and expressed in *A. thaliana* to determine which portion of the coding sequence plays a role in mRNA accumulation. D – All fragments of *AtSR1* except the 3' ~500bp fragment fail to show mRNA accumulation under salt stress. The 500 bp at the 3' end are critical

for *AtSR1* mRNA accumulation under salt stress. C and D were reproduced from Abdel-Hameed et al., 2020.

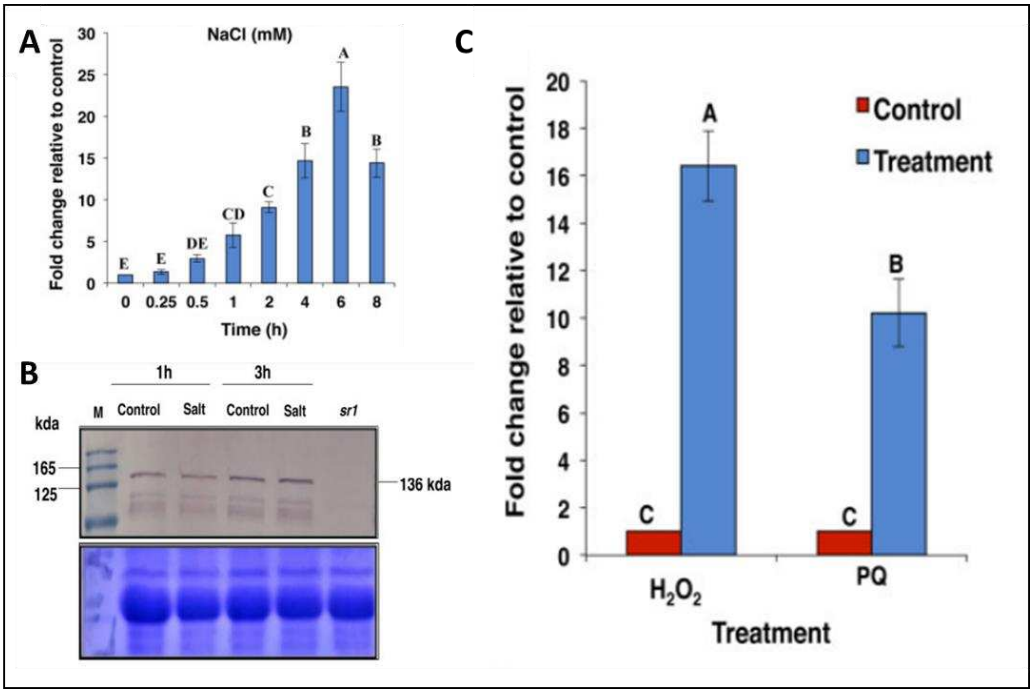

Figure 3. *AtSR1* Accumulation under Salt Stress

A - *AtSR1* accumulates under salt stress over the first 6 hours of salt treatment, followed by slight decrease by 8 hours post stress initiation. B – The SR1 protein does not show accumulation under salt stress despite the increase in mRNA levels. C – Accumulation of *AtSR1* under salt stress is mediated by reactive oxygen species, as shown by treatment with hydrogen peroxide and paraquat. Reproduced from Abdel-Hameed et al., 2020.

1.4 mRNA Stability in Plants

Along with transcriptional rates, mRNA stability is one of the major determinants of steady-state mRNA levels in eukaryotic cells (Boo and Kim, 2020). The stability of an mRNA is measured by its decay rate, or half-life, which is influenced by a number of different factors: RNA decay or degradation mechanisms, which form the basal rate of mRNA decay; sequence-specific controls, which determine each mRNA's inherent stability; and stimulus-responsive controls, which alter the turnover of mRNAs from their steady-state balance between the basal decay rate and their inherent stabilities (Gutiérrez et al., 1999).

Among stimulus-responsive controls, RNA modifications play a significant role in determining mRNA fate (Boo and Kim, 2020). RNA modifications are chemical alterations of RNA strands, which can occur either co-transcriptionally or post-transcriptionally. Such modifications can impact the fate of the RNA, including synthesis, splicing, translation, degradation, and stability (Roundtree et al., 2017; Kadumuri and Janga, 2018; Nachtergaele and He, 2018). In particular, the effect of RNA modifications on RNA stability seems to play a key role in regulating gene expression. This regulation is accomplished through three classes of proteins: writer proteins, which transfer chemical groups to target positions on RNA molecules; reader proteins, which bind to the modified nucleotides and provide recognition of the modification; and eraser proteins, which remove chemical groups from modified nucleotides and reconstitute unmodified RNA (Jonkhout et al., 2017; Roundtree et al., 2017; Kadumuri and Janga, 2018; Nachtergaele and He, 2018; Shi et al., 2019). Proteins in each of these three categories have not been identified for all known types of RNA modifications, and it is possible that certain classes of modification do not require dedicated reader proteins, or are irreversible and thus do not have eraser proteins (Boo

and Kim, 2020). Further, specific writer proteins do not produce all modifications. In the case of NAD-capping, a dedicated writer protein as-such has not been detected because the modification is performed through incorporation of a non-canonical initiating nucleoside (NAD^+) by RNA polymerase (Bird et al., 2016; Jiao et al., 2017; Walters et al., 2017; Kiledjian, 2018).

High-throughput RNA-sequencing has generated databases that suggest there are approximately 170 different types of RNA modifications in eukaryotes (Helm and Motorin, 2017; Boccaletto et al., 2017; Nachtergaele and He, 2018). The most abundant and well-studied mRNA modification is the N^6-methyladenosine, or m^6A modification, in which a methyl group is transferred to the N-6 position of the adenosine base (Shi et al., 2019; Boo and Kim, 2020). This occurs co-transcriptionally via a 4-member methyltransferase complex (Liu et al., 2014; Ping et al., 2014; Schwartz et al., 2014; Wang et al., 2014). The m^6A modification has diverse regulatory consequences in mRNA degradation, stability, translation, and miRNA processing, and can function both to stabilize and destabilize transcripts in a position-dependent manner (Chen et al., 2019; Huang et al., 2020; Lee et al., 2020). In plants, m^6A modifications in the 3' and 5' UTRs are correlated with increased stability, whereas such modifications elsewhere in the transcript seem to target it for decreased translation (Luo et al., 2014). The ECT2 protein - a YTH-domain-containing protein homologous to the human YTHDF2 protein - binds m^6A modifications in plant transcripts to increase their stability (Arribas-Hernández et al., 2018; Scutenaire et al., 2018; Wei et al., 2018). Under heat stress conditions, ECT2 also targets transcripts for relocation to stress granules, where their sequestration results in translational repression (Scutenaire et al., 2018).

m^6A modifications can also have an impact on translation of mRNAs. Modifications in the 5' UTR in stress-responsive genes mediates binding of eukaryotic initiation factor 3 (eIF3) and recruitment of the 43S ribosomal complex to activate translation (Meyer et al., 2015). Interestingly, 3'-UTR m^6A can serve a similar function, recruiting the m6a reader YTH N6-Methyladenosine RNA Binding Protein 1 (YTHDF1) and a host of other factors that work together to recruit the 43S ribosomal complex and activate translation (Wang et al., 2015). ADD m6A role in MLOs

1.5 Overview of Methods to Detect RNA-Protein Interactions and their Application to Plants

RNA-binding proteins have become a target of great interest in recent years, and many new methodologies have been developed to analyze the RNA-protein interactome. However, in plants, most research done in this field before ~10 years ago relied entirely on the use of indirect or *in vitro* methods to identify RNA and protein interaction, such as gel shift assay, mutant and knockout screening, nucleic acid-binding assay, and other classical genetic and cell biological techniques (Vermel et al., 2002; Staiger et al., 2003; Lorkovic, 2009; Lee and Lee, 2010). These techniques have contributed significantly to understanding the functions of RBPs in plant biology but have since been superseded by the development of high throughput and global methods to analyze RNA and protein interactions. These new techniques were developed first in mammalian systems and a few have been used increasingly in plants. Below, I briefly describe these methods and their limitations, especially with respect to applying them in plants.

These techniques fall into three categories: i) approaches that focus on identifying RNA targets of a candidate RBP, i.e., protein-to-RNA, ii) approaches that focus on identifying the proteins interacting with an RNA of interest, i.e., RNA-to-protein, and iii) global approaches (Fig. 4). The

vast majority of work that has been done in this field in plants has focused on the interacting partners of a single RNA or protein of interest (the bait), but recently the development of RNA-interactome capture (RIC) and its application to plants has allowed a global view of the plant RBPome.

1.6 Methods that Use a Protein Bait to Identify its RNA Targets (Protein-to-RNA) and RBPs Identified Using these Methods in Plants

Among the first techniques developed to identify direct targets of RBPs *in vivo* was RNA immunoprecipitation or RIP (He et al., 2009; Gagliardi et al., 2016) (Table 1). The basic idea of the RIP approach is simple and involves the use of an antibody against a protein of interest (Fig. 4, RIP-seq). The lysate of cells expressing the protein of interest is incubated with antibody immobilized on beads, which are then washed and the proteins on the beads digested. The pool of RNA remaining is used to identify putative RNA targets. With the development of high throughput sequencing technologies, methodologies that used such sequencing platforms became known as RIP-seq (Zambelli and Pavesi, 2015).

RIP can also involve RNA-protein crosslinking, creating covalent bonds between the protein and its RNA ligands. Reversible crosslinking is accomplished using formaldehyde and reversed via heat treatment (Niranjanakumari et al., 2002). The drawbacks of this approach are that the specificity of the results depends on the strength of the antibody-protein interaction, and that formaldehyde treatment also catalyzes DNA-protein and protein-protein crosslinking, leading to the identification of indirect as well as direct targets of an RBP.

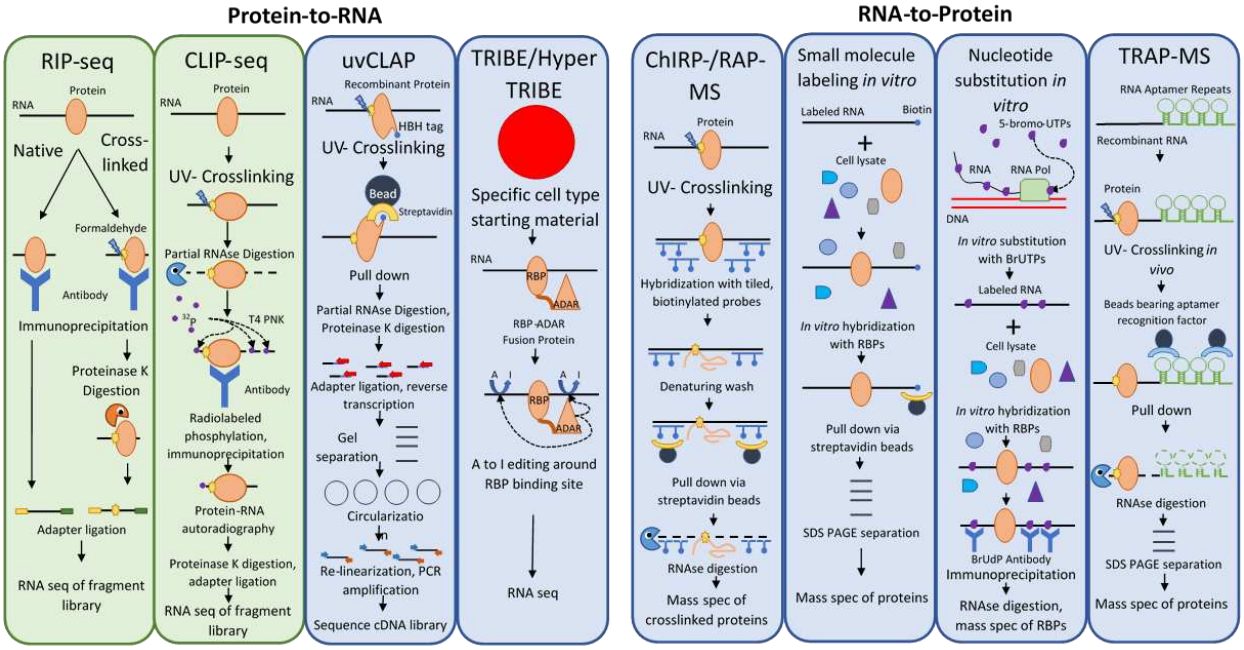

Figure 4. Methods to Detect RNA-Protein Interactions Using RNA or Protein Bait. Diagrammatic representation of the major steps in these notable methods. A green background denotes that the technique has been used in plants, whereas a blue background indicates that the technique has thus far only been used in mammals or other organisms. CLIP Crosslinking and immunoprecipitation (CLIP) derivatives are not detailed here but have been recently reviewed (Lin and Miles, 2019).

Crosslinking and immunoprecipitation (CLIP) builds on RIP by replacing formaldehyde crosslinking with UV-crosslinking to covalently link proteins with RNA molecules within several angstroms distance (i.e., bound by the protein) (Table 1). The RNA-protein complexes are selected after cell lysis using immunoprecipitation (Ule et al., 2003). Partial digestion of the bound RNA allows a rough approximation of the binding site, followed by phosphorylation of the complexes with radioisotope. The covalently bound RNA-protein complex is then rigorously washed, separated via SDS-PAGE, and transferred to a nitrocellulose membrane. The protein is then removed using proteinase K, linkers are ligated to the collected RNA fragments, and the fragment library is cloned after reverse transcription and then sequenced (Fig. 4, CLIP-seq). There are many derivative techniques based on the basic CLIP-Seq principle. High-throughput sequencing of RNA isolated by crosslinking immunoprecipitation (HITS-CLIP; Fig. 5) is the application of high throughput sequencing to CLIP fragment libraries in place of traditional sequencing, which placed a limitation on the richness of data that could be generated by a CLIP-Seq experiment, allows more data to be extracted from CLIP fragment libraries (Table 1). This allowed the identification of over 1000-fold more unique binding sites compared to CLIP with traditional sequencing techniques, although this leaves one with the opposite problem - a plethora of data to sift through and discern signal from noise (Licatalosi et al., 2008). CLIP-based methods were further improved with the advent of PAR-CLIP: CLIP experiments using photoactivatable ribonucleosides (PAR) to enhance the efficiency of crosslinking (Fig. 5). PAR-CLIP incorporates 4-thiouridine into transcripts *in vivo*, which forms covalent bonds with interacting proteins under UV far more efficiently than random UV RNA-protein crosslinking; the approach improved RNA recovery 100- to 1000-fold (Hafner et al., 2010).

Table 1. Summary of RNA-Protein Methods and their use in Plants.

Method	Pros	Cons	Plant Refs
Protein-to-RNA			
RIP-seq	No genetic trans., reversible crosslinking, well established in plants, no radiolabeling	Uses antibody-antigen interaction, non-specific crosslinking, large amounts of starting material, no info on RBP site	He et al., 2009, Streitner et al., 2012; Yin et al., 2012; Rowley et al., 2013; Bardou et al., 2014; Francisco-Mangilet et al., 2015; Xing et al., 2015; Bazin et al., 2018; Marmisolle et al., 2018; Schmid et al., 2019; Tian et al., 2019
CLIP-seq	No genetic trans., provides info. on the RBP binding site, well-established in plants	Uses antibody-antigen interaction, uses radiolabeling, large amounts of starting material	Meyer et al., 2017; Zhang et al., 2015
HITS-CLIP	Increased coverage	*As CLIP-seq*	Zhang et al., 2015
PAR-CLIP	More efficient UV-crosslinking	*As CLIP-seq,* favors certain RBP-RNA interactions	*None*
iCLIP	Increases precision of RBP site prediction	*As CLIP-seq*	Meyer et al., 2017
dCLIP	Permits comparisons across all CLIP exps.	*As CLIP-seq*	*None*
uvCLAP	Tight binding affinity, uniform pulldown efficiency, quantify background, no radiolabeling, no antibodies	Not in plants, needs genetic trans., may alter RNA-protein interactions, no info on RBP site, large amounts of starting material	*None*
TRIBE/HyperTRIBE	No pull down, small amounts of starting material, no radiolabeling, no antibodies	Not in plants, needs genetic trans., editing occurs in a wide range around the binding site, no info on RBP site	*None*
RNA-to-Protein			
ChIRP-MS/RAP-MS	High affinity interaction, no genetic trans., no radiolabeling, no antibodies	Not in plants, no info on RBP site, large amounts of starting material	*None*
RNA Small Molecule Labeling	No genetic trans., no radiolabeling, no antibodies	*In vitro* only	*None*
RNA Nucleotide Substitution	No genetic trans., no radiolabeling, no antibodies	*In vitro* only	*None*
RNA Aptamer Pulldown	High affinity interaction, many aptamers, no radiolabeling, no antibodies	Not in plants, needs genetic trans., no info on RBP site, may alter RNA-protein interactions, large amounts of starting material, may be prone to aggregation	*None*

Thus far, CLIP techniques were limited by the fact that reverse transcriptase often terminates prematurely when met with a residual amino acid covalently bound to a nucleotide at a crosslinking site causing such reads to be lost during standard CLIP library preparation. Individual-nucleotide resolution CLIP (iCLIP; Fig. 5) was developed to compensate for this problem (König et al., 2014). iCLIP captures truncated cDNAs using a cDNA self-circularization step in place of the previously used inefficient RNA ligation step in library preparation (König et al., 2014). CLIP experiments also suffered from high experimental failure rates due to their technical complexity, and enhanced CLIP (eCLIP; Fig. 5) was developed to address these issues. eCLIP decreases the amount of amplification necessary and uses random-mer barcode adapters ligated at the termination site of reverse transcriptase (the UV crosslinked nucleotide) to maintain analysis of RBP binding sites. Furthermore, the protocol omits the radiolabeling step and uses a size-matched control without immunoprecipitation to eliminate non-specific RNA interactions from the datasets (Nostrand et al., 2016).

The CLIP technique was also streamlined by the development of simplified CLIP (sCLIP; Fig. 5), which avoids radiolabeling by biotinylating the RNA for visualization, and uses polyadenylation and random-mer barcoding to uniquely identify RNAs and reduce the requirement for PCR amplification (Kargapolova et al., 2017). Another technique designed to avoid the use of radiolabeling, termed irCLIP (Fig. 5) for its use of an infrared dye, also used biotin labeling of the RNA - a biotinylated and infrared dye-conjugated 3' adapter was ligated to the RNA, allowing visualization of RNA-protein complexes without autoradiography (Zarnegar et al., 2015). irCLIP allows the use of 250 times less starting material compared to iCLIP, and

although comparisons were not performed with eCLIP or sCLIP, it seems likely that irCLIP lowers the starting material requirement most significantly.

With the advent of HITS-CLIP, many computational tools were developed to handle the large datasets produced by HITS-CLIP experiments. One of the most widely used of these is known as dCLIP, a program created to allow comparison of differential binding in different CLIP experiments (Wang et al., 2014a). dCLIP normalizes CLIP-seq data from different experiments using an application of a Bland-Altmann plot called an MA plot, then uses a Hidden Markov Model to detect shared or distinct binding sites across experiments. dCLIP has the advantage of being a universal computational tool for all types of CLIP-seq experiments; HITS-CLIP, PAR-CLIP, and iCLIP, and to allow comparison among them (Wang et al., 2014a).

CLIP-Seq and its derivatives are powerful techniques but have significant limitations. Namely, CLIP (and its derivative methodologies) are all limited by their reliance on the antibody-antigen interaction; this limits the stringency of washing conditions to those that will not disrupt the antibody-antigen interaction (Ramanathan et al., 2019). Thus, the acquisition of a high-affinity antibody is critical for such experiments, and generally cannot be guaranteed. Even meaningful CLIP experiments contain significant noise in the form of proteins that were not eluted under the weak washing conditions, or in the form of proteins that co-immunoprecipitated (Darnell et al., 2010). Furthermore, CLIP relies on radiolabeling of bound RNA, a prohibitive procedure due to its cost, difficulty, and health hazards (Maticzka et al., 2018). Finally, because of the low efficiency of CLIP techniques, they require large amounts of starting material, on the order of thousands of cells. This means that studies of RNA-

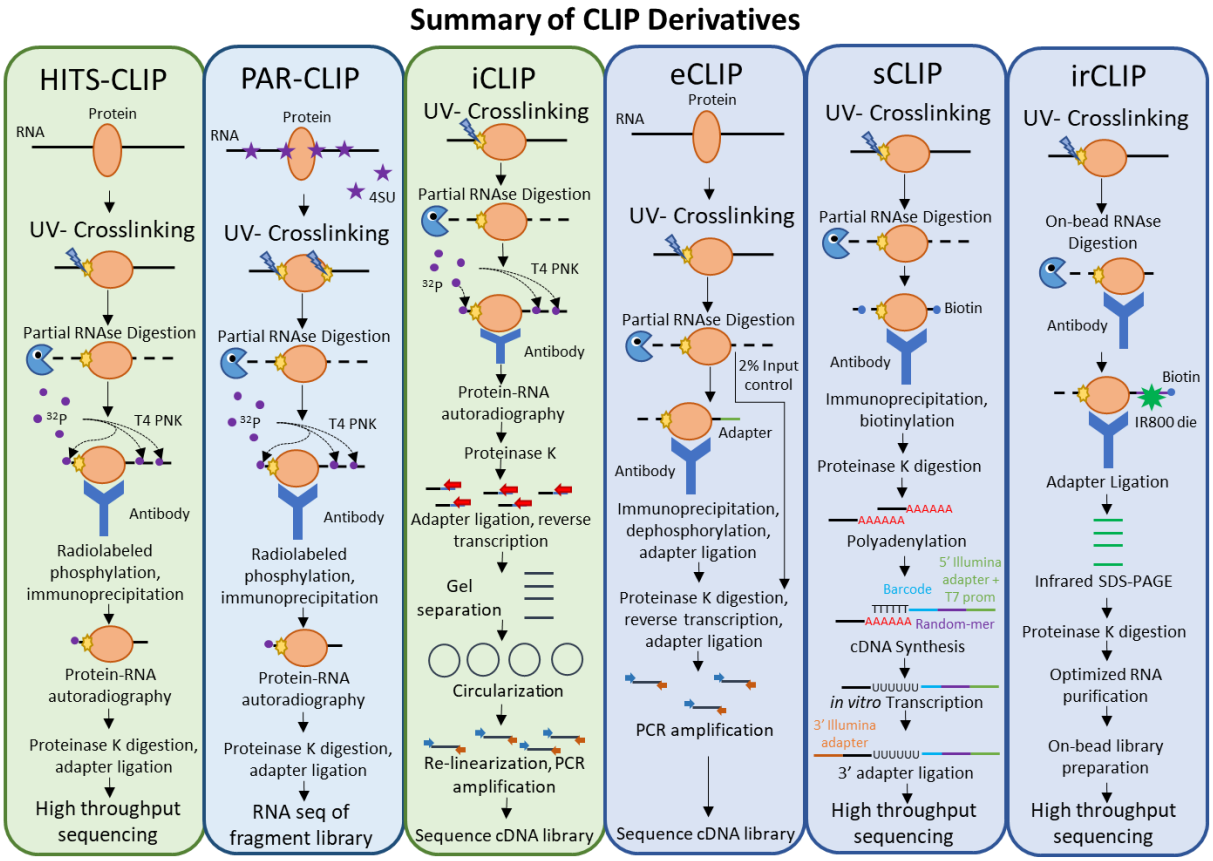

Figure 5. Diagrammatic Summary of CLIP Derivatives

Many techniques have been developed based on the basic CLIP protocol, either to simplify CLIP experiments or enhance signal to noise ratio. A blue background indicates that the method has not been used in plants, whereas a green background indicates that it has been adapted for use in plant systems.

protein complexes in specific cell types (which cannot be amassed in the thousands) are forced to use starting material of a mixed population of cell types, lowering the signal to noise ratio in their results (McMahon et al., 2016). Other techniques, discussed below, have been developed to avoid these limitations.

UV-crosslinking and affinity purification (uvCLAP) was developed as a radiolabeling- and immunoprecipitation-free alternative to CLIP methodologies (Maticzka et al., 2018) (Fig. 4, uvCLAP). Instead of using an antibody-antigen interaction, uvCLAP relies on the tight interaction of the His6-biotinylation sequence-His6 (HBH) tag with beads that bind polyhistidine-tagged proteins, and then with the even more stringent interaction with streptavidin beads. The RNA is partially digested with RNAseI and the RNA ends are repaired with T4 polynucleotide kinase. Adapters are then ligated to the RNA fragments and reverse transcribed with barcoded primers. The cDNA products are then separated on a polyacrylamide gel, circularized to capture truncated cDNA products (as in iCLIP), linearized, and amplified with PCR.

The use of tandem affinity purification in this approach allows confidence that pull-down efficiency will be similar across conditions, experiments, and laboratories, in comparison with immunoprecipitation approaches in which every antibody-antigen interaction has a unique affinity (Maticzka et al., 2018). uvCLAP also allows the quantification of nonspecific background noise, increasing its specificity. The drawback of this approach is the need for a genetic transformation with an HBH-fused construct prior to affinity purification. Although it is relatively unlikely when done carefully, such transformations could potentially alter RNA-

protein interactions from their natural state. Moreover, this introduces extra steps for each RNA-binding protein studied; the significance of this drawback will depend entirely on the ease of genetic transformation in the model system being used.

The TRIBE (targets of RNA-binding proteins identified by editing) and HyperTRIBE approaches were developed in response to the severe limitations of CLIP-based techniques in identifying cell type-specific RNA-protein interactions (McMahon et al., 2016). TRIBE was developed first; it uses the RNA-editing enzyme ADAR's (adenosine deaminase acting on RNA) to convert adenosines to guanines, leaving telltale signals in edited RNA (Fig. 4, TRIBE/HyperTRIBE). In this approach, ADAR's double-stranded RNA-binding motifs are replaced with the sequence of an RNA-binding protein of interest to create a fusion protein that targets ADAR's RNA-editing activity to the RNA targets of the fused RBP. The RNA is sequenced, and detection of editing events indicates the binding of the fusion protein, and thus the RBP of interest. The original TRIBE technique had the opposite problem as most CLIP experiments: it identified only about 25% of the target RNAs identified by CLIP techniques for the same RBP, and is thought to have had a false negative problem, rather than CLIP's false positive problem. It was found that ADAR's editing rate was low due to a sequence specificity for UAG and a double-stranded structure surrounding the edited adenosine (Xu et al., 2018).

To address these weaknesses, hyperTRIBE was developed by introducing the E448Q mutation in ADAR, which lowers ADAR's sequence and structure preferences and increases editing efficiency (Xu et al., 2018). This mutation increased the number of detected editing events by

over 20 times, while increasing the number of detected edited transcripts by 8 times. HyperTRIBE is able to identify about two-thirds of CLIP-identified target RNAs.

This approach has the advantages of avoiding the use of immunoprecipitation and radiolabeling, requiring only a small amount of starting material, and being simple. Like uvCLAP however, it also requires genetic transformation, and in comparison to both uvCLAP and CLIP techniques, has the drawback of providing no information as to the specific binding site on the RNA (as ADAR edits sites within up to 500 nucleotides of known CLIP sites). CLIP remains the method of choice if information about an RBP's binding site on an RNA is desired, whereas HyperTRIBE is desirable if interested in RNA-protein complexes in specific cell types or if only small amounts of starting material are available (Xu et al., 2018).

Among the methods described above, the only protein-to-RNA techniques that have been used in plants to-date are RIP-seq and CLIP-seq. As discussed below, the application of these techniques to several RBPs has revealed their role in several processes.

1.6.1. Regulation of RNA Processing

RIP-seq was used to demonstrate that the Arabidopsis signal responsive Serine- Arginine-rich (SR) protein SR45 directly or indirectly associates with over 4000 RNAs *in vivo*, regulating constitutive and alternative splicing, post-splicing processing of 30% of ABA signaling genes, and over 300 intron-less RNAs (Xing et al., 2015) (Table 2). This indicates that SR45 exerts multimodal influence over mRNA processing, differentially regulating intron-containing and intron-less RNAs. The action of SR45 is defined by *cis*-elements in its RNA targets; four motifs

Table 2. Summary of Plant RBPs Identified by Baited RNA-Protein Approaches.

RBP	Plant System	Method	Number of RNA targets	References
AGO4	*Arabidopsis thaliana*	RIP	2	Wierzbicki et al., 2009
AtGRP7	*Arabidopsis thaliana*	RIP-seq/iCLIP	452/858	Streitner et al., 2012; Meyer et al., 2017
AtNSRa	*Arabidopsis thaliana*	RIP-seq	>2000	Bardou et al., 2014; Bazin et al., 2018
AtNSRb	*Arabidopsis thaliana*	RIP-seq	>2000	Bardou et al., 2014; Bazin et al., 2018
CPsV 24K *(viral)*	*Nicotiana benthamiana*	RIP	2	Marmisolle et al., 2018
CPsV 24K *(viral)*	*Nicotiana benthamiana*	RIP	2	Marmisolle et al., 2018
CSP1	*Arabidopsis thaliana*	RIP-chip	>6000	Juntawong et al., 2013
IDN2	*Arabidopsis thaliana*	RIP	1	Zhu et al., 2013
FCA	*Arabidopsis thaliana*	RIP	1	Tian et al., 2019
HLP1	*Arabidopsis thaliana*	HITS-CLIP	>5000	Zhang et al., 2015
KTF1	*Arabidopsis thaliana*	RIP	1	He et al., 2009
NSF	*Oryza sativa*	RIP	?	Tian et al., 2020
PUMPKIN	*Arabidopsis thaliana*	RIP-seq	5	Schmid et al., 2019
PDM1	*Arabidopsis thaliana*	RIP	1	Yin et al., 2012
Rab5a	*Oryza sativa*	RIP	?	Tian et al., 2020
RBP-L	*Oryza sativa*	RIP	?	Tian et al., 2020
RBP-P	*Oryza sativa*	RIP	?	Tian et al., 2020
SR45	*Arabidopsis thaliana*	RIP-seq	>4000/>1800	Xing et al., 2015; Zhang et al., 2017
THO2	*Arabidopsis thaliana*	RIP	6	Francisco-Mangilet et al., 2015

were identified, two of which bear the hallmarks of exonic splicing regulators and two which showed peaks in the intronic regions of 5' and 3' splice sites. One of these motifs (M1; GAAGAA) was also found to be enriched in SR45's intron-less targets (Xing et al., 2015). Another study found 1812 RNAs associated with SR45, 81 of which were subject to alternative splicing mediated by the GGNGG motif in both activation and re-pression of splicing events (Zhang et al., 2017). These results further define SR45 as a splicing regulator whose activity cannot be easily defined as a positive or negative regulator, possibly explained by the fact that SR45 itself is alternatively spliced and its splice isoforms display differential expression. SR45 produces two splice isoforms, SR45.1 (long) and SR45.2 (short), the long isoform acting as a positive regulator in the salt stress response in Arabidopsis (Albaqami et al., 2019). In rice, SR45 is stabilized through interactions with an immunophilin (OsFKBP20-1b), which plays an essential role in a positive regulation of transcription and splicing of stress response genes during abiotic stress (Park et al., 2020). THO2, a member of the Tran-scription-Export (THO/TREX) complex, was shown via RIP to participate in the generation of microRNAs; THO2 mutants showed both a decrease of miRNA accumulation and alterations in the splicing patterns of SR proteins, suggesting that the THO/TREX complex plays a role in alternative splicing (Francisco-Mangilet et al., 2015).

RIP was used to show that the glycine-rich RBP AtGRP7 modulates alternative splicing in Arabidopsis (Streitner et al., 2008). A later study using both RIP-seq and iCLIP found 452 (RIP-seq) and 858 (iCLIP) RNA targets of AtGRP7 (Meyer et al., 2017). AtGRP7 alters the circadian regulation of its targets and seems to act in both alternative splicing and alternative polyadenylation (APA) (Meyer et al., 2017) (Table 2).

Nuclear speckle RNA binding proteins (NSRs) have also been shown via RIP-seq to regulate mRNA processing, alternative splicing, and long noncoding RNA (lncRNA) prevalence (Bardou et al., 2014) (Table 2). An NSR and an alternative splicing competitor (ASCO) lncRNA were shown to form a regulatory module of alternative splicing, in which the ASCO displaces an alternative splicing target from an NSR complex to modulate alternative splicing during development (Bardou et al., 2014). NSRs affected alternative splicing of hundreds of genes in Arabidopsis, and RIP-seq of an NSRa fusion protein showed that lncRNAs are also targets of NSRs, likely modulating their alternative polyadenylation or splicing as observed with the COOLAIR lncRNA to regulate cross-talk between auxin and immune response (Bazin et al., 2018).

HITS-CLIP was used to identify genome-wide targets of HLP1, an hnRNP A/B protein that binds preferentially to A- and U-rich elements around cleavage and polyadenylation sites of transcripts involved in RNA metabolism and flowering to target APA (Zhang et al., 2015) (Table 2). HLP1 suppresses Flowering Locus C (FLC) to release repression of flowering in Arabidopsis and control reproductive timing (Zhang et al., 2015). NSR knockout mutants showed modified APA and differential expression of the lncRNAs COOLAIR, produced from antisense transcripts generated from FLC, and function in the release of repression of flowering through suppression of FLC (Bardou et al., 2015).

Using RIP-seq, the pentatricopeptide repeat protein PDM1 was shown to mediate cleavage of a transcript from polycistronic to monocistronic fragments in chloroplasts of Arabidopsis (Yin et al., 2012) (Table 2).

1.6.2. Trafficking and Translocation

In rice, RIP-seq was used to show that RNA-binding protein-P (RBP-P) is an RNA-binding protein that plays a role in endosomal trafficking of glutelin and prolamine mRNAs, working to anchor the RBP-bound mRNAs to the endosome via the quaternary complex and transport it to the ER Subdomain for translation, coopting endosomal trafficking (Tian et al., 2019) (Table 2). RBP-L, an interacting partner of RBP-P, likely plays a coordinating role in subcellular trafficking of its mRNA targets, mediated by its 3' UTR (Tian et al., 2019) (Table 2).

1.6.3. Chaperoning

In Arabidopsis, a unique combination of RIP and microarray approaches (RIP-Chip) was used to demonstrate that the cold shock protein 1 (CSP1) acts as an RNA chaperone of polysomes to improve the translation of RNA targets at low temperatures (Juntawong et al., 2013) (Table 2).

1.6.4. Gene Silencing

The RNA-directed DNA methylation effector KTF1 was identified via RIP as an RBP that binds Pol V scaffold transcripts to recruit argonaute 4 (AGO4) and its siRNAs for chromatin remodeling-mediated gene silencing (He et al., 2009) (Table 2). AGO4 and RNA polymerase V cooperate with 24 nt siRNAs in this process; siRNAs bound to AGO4 guide AGO4 to target loci

through complementary base-pairing with nascent Pol V transcripts, where AGO4 recruits DNA modification factors such as DNA methyl-transferase DRM2 to methylate the chromatin and thus silence the affected genes (He et al., 2009; Juntawong et al., 2013). Based on RIP observations that the protein INVOLVED IN DE NOVO 2 (IDN2) is a lncRNA-binding protein that interacts with the SWItch/Sucrose Non-Fermentable (SWI/SNF) nucleosome remodeling complex, lncRNAs are thought to base-pair with siRNAs bound by AGO4 to position the SWI/SNF complex and thus target nucleosome remodeling, leading to decreased transcription by Pol II (Wierzbicki et al., 2009; Zhu et al., 2013) (Table 2). RIP was also shown to be usable in Arabidopsis for the detection of lncRNAs generated by specialized polymerases (Rowley et al., 2013).

1.6.5. Viral RNA Suppression

A modified RIP-seq assay was developed for the detection of RNAs of heterologous origin in plants and applied to transiently expressed nuclear epitope-containing proteins in *Nicotiana benthamiana*, but to-date this method has not been used for its intended purpose of detecting viral RNAs in plant cells (Marmisolle et al., 2018).

1.6.6. Other RBPs

The plastid UMP kinase (PUMPKIN) has been shown via RIP-seq to associate with several RNAs *in vivo*, altering their metabolism thereby (Schmid et al., 2019) (Table 2). This suggests that while PUMPKIN is primarily a metabolic enzyme, it may have a moonlighting function as an RBP, potentially for the purpose of coupling RNA and pyrimidine metabolism (Schmid et al., 2019).

1.6.7. Perspective on the Application of Protein-to-RNA Methods in Plants

Despite the breadth of techniques available for use in elucidating RNA-protein interactions *in vivo*, CLIP and its derivatives remain the most tenable non-global approach for use in plants. RIP has also been used extensively and is suitable for certain experimental purposes. There still remain several techniques used in other organisms to probe interactions between a protein of interest and RNAs that have yet to be successfully adapted, or even tried, in plants. These are opportunities for advancement in plant RNA biology, but if adapted into plants should be modified to include the best features and optimizations of the already-proven RIP and CLIP approaches.

Several of these techniques show particular promise; TRIBE, and particularly HyperTRIBE, have not been used in plants as yet, but if viable would overcome the signal to noise ratio problems inherent in CLIP. HyperTRIBE outperforms CLIP when using a small amount of starting material, such as a few cells of homogenous origin. Unfortunately, techniques used to select cells of a single type from a heterogeneous sample in mammalian systems, such as flow cytometry, are not tenable in plants without significantly altering the cell state (i.e., generating protoplasts by degrading the cell wall) (Libault et al., 2017). Laser microdissection of plant tissues seems the most viable route for selecting cells of a particular type in plants, and HyperTRIBE would allow the use of smaller amounts of starting material than were previously used for RNA-Seq after laser microdissection (Martin et al., 2016). Focus on single cell-types is a necessary next step for plant biology to throw off the albatross of whole-plant and tissue heterogeneity, and HyperTRIBE combined with laser microdissection would represent progress

toward that goal in the field of RBPomics (Fig. 6). However, laser microdissection requires a somewhat more extended time between sample harvesting and freezing due to the fixation step, which could result in increased RNA degradation after harvesting. Even so, transcriptional profiling has been performed successfully using cells harvested via this technique (Martin et al., 2016).

1.7. Methods that Use an RNA Bait to Identify Binding Proteins (RNA-to-Protein)

RNA antisense purification mass spectrometry (RAP-MS) is a technique used to purify long noncoding RNAs and their interacting proteins with complementary, tiled, biotinylated DNA probes bound to magnetic streptavidin beads (Engreitz et al., 2013) (Fig. 4, ChIRP-/RAP-MS). RAP-MS starts with UV crosslinking of RNA to interacting proteins *in vivo*. The cross-linked RNA-protein complexes are then extracted under denaturing conditions to disrupt non-covalent interactions, and the complexes are hybridized with ~120nt biotinylated DNA probes bound to magnetic beads. After washing, the RNA is digested, and the protein pool is analyzed using mass spectrometry (MS). This method also uses stable isotope labeling by amino acids in culture (SILAC) to label proteins, allowing quantitative comparisons to be made with mass spectrometry (McHugh et al., 2015).

Comprehensive identification of RNA-binding proteins by mass spectrometry (ChIRP-MS) is a related technique predating RAP-MS by several years (Chu et al., 2011). It also uses tiled biotinylated DNA probes bound to magnetic streptavidin beads and RNA-protein crosslinking, although the probes used were only 20nt in length and formaldehyde cross-linking was chosen instead of UV crosslinking. The use of formaldehyde crosslinking has the advantage of being

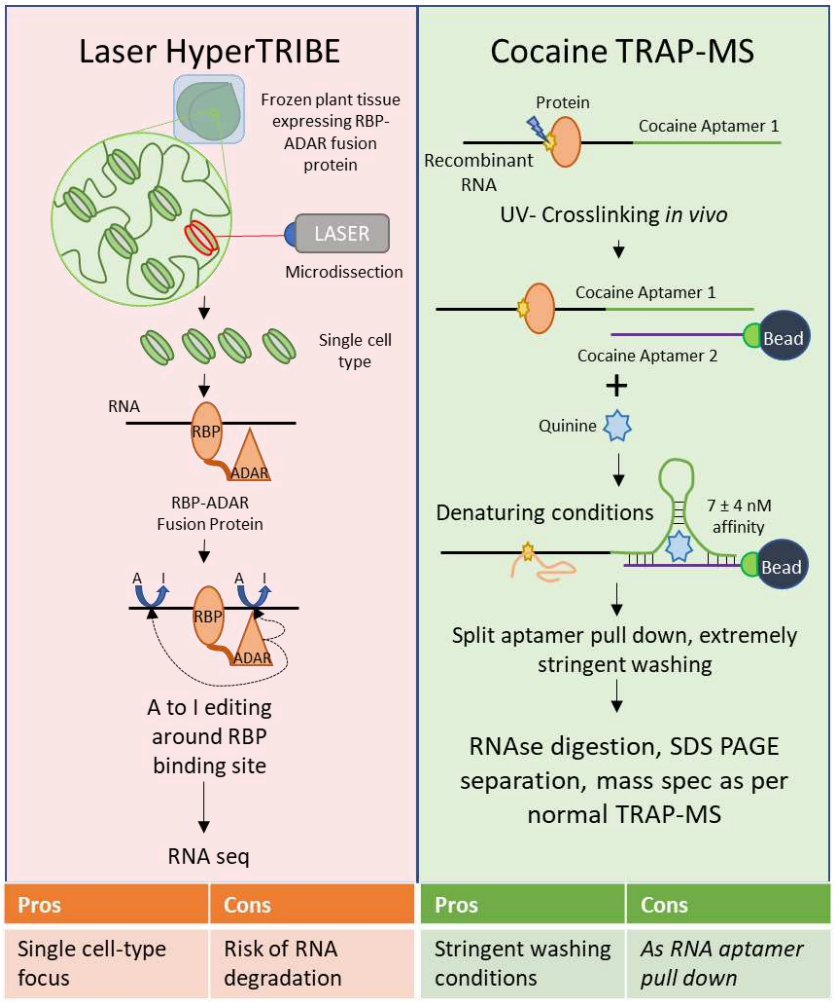

Figure 6. Proposed Modifications to Existing Techniques for Future Advancement. Laser HyperTRIBE – This is not a true modification to the HyperTRIBE approach itself, but rather a pairing of that approach with laser microdissection to enable the strengths of HyperTRIBE (capacity to accommodate small amounts of starting material) to be applied to plants. In this approach, intact plant tissue would be fixed prior to flash freezing, and then the cell types of interest selected via laser microdissection used for HyperTRIBE. Cocaine TRAP-MS – This modification suggests that rather than RNA aptamers that rely on protein binding capabilities, nucleotide-nucleotide ap-tamers should be prioritized. The split cocaine aptamer consists of two RNA fragments that interact at very high affinity in the presence of cocaine, or preferably quinine thanks to its increased affinity and ease of access. The high affinity of this interaction would permit extremely stringent washing conditions, which are critical in minimizing false positives.

reversible, and ChIRP-MS studies are able to reverse crosslinking while keeping both protein and RNA components intact and allowing further analyses on both (Chu et al., 2015). However, formaldehyde crosslinking also catalyzes the crosslinking of protein-protein and protein-DNA interactions.

The technique known as PIP-Seq has been used successfully to elucidate important RNA-protein interactions governing the differentiation of root hair cells (Foley et al., 2017). PIP-seq identifies RNA-protein interactions with precise RNA binding sites when paired with a technique capable of identifying individual interacting RBPs. PIP-seq uses formaldehyde crosslinking to covalently bond RNA to interacting proteins, followed by high-throughput sequencing. The sample is split into a matrix of four: one sample with RBPs intact treated with single-stranded RNA nuclease (ssRNAse), one without RBPs treated with ssRNAse, one with RBPs treated with double-stranded RNA nuclease (dsRNAse), and one without RBPs treated with dsRNAse. The use of ss- and dsRNAse in the presence and absence of binding RBPs allows both RNA structure and RBP protection (and thus binding) to be predicted (Foley et al., 2017).

Recently, a CRISPR-based system called CRUIS (CRISPR-based RNA-United Interaction System) was developed in mammals (Zhang et al., 2020). CRUIS uses transient expression to couple the RNA-tracking capabilities of dCas13a with a fused proximity protein, Pafa, which labels surrounding RNA-binding proteins. These labeled proteins can then be identified via mass spectrometry. CRUIS was shown to be roughly as efficient as CLIP and identified novel protein targets (Zhang et al., 2020). The advantage of this technique is that it captures truly *in vivo* interactions without the potential for spurious interactions to form during lysis and wash steps,

but it remains to be seen whether it has a false positive problem. The Pafa proximity labeling protein lacks the specificity of UV crosslinking for angstrom-level RNA-protein interactions, potentially leading to the labeling of indirectly interacting proteins.

There are a number of RNA to protein methods that are useful for *in vitro* studies but are not applicable to *in vivo* work. Among these is the labeling of RNA with small molecules (Gemmill et al., 2020). In this RNA to protein approach, small molecules are covalently bonded to an RNA of interest *in vitro,* then incubated with cell lysate and pulled down using an immobilized receptor for the small molecule ligand (Fig. 4, small molecule labeling *in vitro*). Common forms of this technique include biotin labeling, desthiobiotin labeling, and digoxigenin labeling. Unfortunately, because of the chemical reactions necessary to label an RNA of interest, small molecule RNA labeling is usually not appropriate for *in vivo* studies.

Another exclusively *in vitro* approach is nucleotide substitution in RNA (Gemmill et al., 2020). Here, RNA is transcribed *in vitro* in the presence of a heavy metal-modified dNTP, incorporating the modified nucleotide into the transcript. Immunoprecipitation can then be carried out using an antibody against the modified nucleotide (Fig. 4, nucleotide substitution *in vitro*). The drawback of this approach is that the charge of the heavy metal-modified nucleotide can strongly affect the charge distribution, structure, and protein binding of the RNA of interest.

Whereas the uvCLAP approach uses modifications to the protein primary structure, RNA aptamer pulldown (also known as tandem repeat affinity purification mass spectrometry, or TRAP-MS) uses modifications to the RNA primary and secondary structures, followed by

tandem affinity purification (Gemmill et al., 2020). RNA aptamers are short oligonucleotide sequences that reliably assume a secondary structure under physiological conditions, which tightly interacts with a target molecule - the ligand. The affinities of these interactions can be equivalent to or greater than those of antibody-antigen interactions (Johansson et al., 1997; Lim et al., 2001; Sun et al., 2016; Mallikaratchy et al., 2017). An RNA aptamer is introduced into an RNA of interest either *in vitro* or *in vivo*, the lysate is passed over a column containing immobilized ligand, washed, and ribonucleoprotein complexes are eluted. Interacting proteins are identified via mass spectrometry. This, like RAP-MS/ChIRP-MS, is one of the few *in vivo* methods to identify ribonucleoprotein complexes in the RNA-to-protein direction (Fig.4, TRAP-MS).

There are many well-studied RNA aptamers used for such studies; some of the most commonly used are the PP7, S1, D8, tobramycin, streptomycin, Csy4 (H29A), Mango, and MS2 aptamers (Johansson et al., 1997; Lim et al., 2001; Sun et al., 2016; Gemmill et al., 2020). Only the MS2 aptamer will be discussed in detail here. This aptamer exploits the tight, highly specific interaction between the coat protein (MCP) of the bacteriophage MS2 and a 19nt RNA hairpin structure from the bacteriophage's genome, which the virus presents on the surface of its genome to assemble its coat protein (Johansson et al., 1997). Repeats of the MS2 hairpin structure are inserted at the 3' end of an RNA of interest, while a fusion protein of MCP and maltose-binding protein (MBP) is immobilized on amylose beads. After pulldown, the protein-RNA-MCP-MBP complex is eluted using excess maltose, which MBP binds preferentially (Fig 4., TRAP-MS). RNA aptamer pulldown has the disadvantage of requiring genetic transformation, which may

alter the structure of the RNA of interest and thus distort the pool of RNA binding proteins associated with it. Furthermore, the presence of the RNA aptamer may risk aggregation.

Two other RNA-to-protein techniques were developed in the last year in non-plant systems. One of these methods targets engineered peroxidase (APEX) with MS2 or Cas13 to a specific RNA. APEX targeting uses either the MS2-MCP interaction or an engineered CRISPR-Cas13 interaction to target the biotinylation activity of APEX2 to proteins proximal to target RNAs *in vivo* (Han et al., 2020). After rapid, one-minute biotin labeling, cells are lysed and pulled down using streptavidin beads. Isolated proteins are identified using liquid chromatography-mass spectrometry (LC-MS). This method was based on the RNA proximity biotinylation (RNA-BioID) and APEX RNA immunoprecipitation (APEX-RIP) approaches. RNA-BioID uses MCP to target a biotin ligase (BirA*) to an MS2-tagged RNA of interest (Mukherjee et al., 2019). APEX-RIP uses the promiscuous engineered peroxidase APEX2 expressed by live cells to target cellular components of interest and biotinylate proximal proteins during a short pulse of treatment with hydrogen peroxide and biotin-phenol (Kaewsapsak et al., 2017). Following biotinylation, labeled proteins are crosslinked to proximal RNAs using formaldehyde and pulled down using streptavidin beads, along with co-eluting RNAs. APEX targeting improves on BioID by decreasing the amount of time necessary for biotin labeling (Kaewsapsak et al., 2017). Although it is claimed (Kaewsapsak et al., 2017) that APEX2 does not label distal proteins due to the short half-life of the biotin-phenoxyl radical it generates, it is unknown whether APEX2 may label proteins interacting indirectly with the target RNA. Compared to crosslinking, which establishes a hard limit on the distance of RNA–protein interaction, this may raise a concern of false positives when using APEX targeting.

The second method is called CRISPR-assisted RNA–protein interaction detection (CARPID). This method was also inspired by APEX-based approaches but uses the engineered biotin ligase BASU instead of APEX2 (Yi et al., 2020). Using a nuclease-activity-free RNA targeting dCasRx to tether BASU to RNAs of interest, CARPID labels interacting proteins via biotinylation, followed by pull-down with streptavidin beads (Yi et al., 2020). This method was able to identify RBPs interacting with lncRNAs but requires a longer labeling period as compared to APEX targeting.

1.7.1. Perspective on the use of RNA-to-Protein Methods in Plants

There is much room for improvement in the RNA-to-protein direction, particularly considering that none of these techniques have been used in plants to-date. ChIRP-MS in particular would be an attractive technique to attempt in plants for the following reasons: it avoids the need for antibody generation used in RIP and CLIP, it does not use radio-labeling, it permits denaturing conditions and stringent washes, and it does not require genetic transformation. However, as previously described it cannot provide any information regarding the binding site of an RBP.

RNA aptamer-mediated pull-down techniques could also be an area for advancement. These approaches do require genetic transformation and could potentially result in altered RNA secondary structure (depending on the aptamer used), but their potential to exceed the antibody-antigen affinity limitations and avoid the antibody generation variabilities of CLIP makes them attractive nevertheless. However, because most of the annotated RNA aptamers in use rely on the binding capabilities of partner proteins (such as the MS2 stem loop's binding by the MS2 viral coat protein MCP), their use limits the stringency of washing conditions; denaturing conditions

cannot be used during incubation and washing to prevent the formation of post-lysis ribonucleoprotein complexes without de-naturing the aptamer's binding partner and thereby compromising pull down. Of those that do not rely on protein partners, few match the affinity granted by the polyA-oligo(dT) interactions used in other techniques, such as RNA-interactome capture.

It might be advantageous to develop nucleotide-nucleotide RNA aptamers to increase the binding affinity, such as by applying a split RNA aptamer. Split aptamer approaches involve separating out an existing aptamer, such as an RNA that forms a tight stem-loop secondary structure, into two fragments that tightly interact in the presence of a ligand; thus, one fragment of the aptamer is appended to a transcript of interest, and the second is immobilized on a nonreactive bead. For example, the cocaine aptamer has successfully been split and used as a biosensor (Slavkovic et al., 2018). Although its target as a biosensor is cocaine, the split aptamer actually shows 30- to 50-fold greater affinity for quinine over cocaine, binding at an affinity of 7 ± 4 nM (Slavkovic et al., 2018; Debiais et al., 2020). Use of the cocaine aptamer in the presence of quinine during pull-down could potentially tolerate extremely stringent washing conditions. For a summary of these suggested techniques, see Figure 6.

Proximity biotinylation-based methods, such as APEX targeting and CARPID could theoretically be used in plants and would be of interest due to their status as RNA-to-protein methods with some modifications.

1.8. Global RNA-Protein Interactome

Until very recently, there was only one currently available global approach to capturing the plant RBPome, called RNA-interactome capture (RIC). RIC uses techniques common to directed RNA-protein interaction studies, beginning with the UV-crosslinking of interacting proteins to their partner RNAs as in CLIP and PAR-CLIP. The cell lysate is then passed over oligo(dT)-magnetic beads under denaturing conditions to pull down polyA RNAs and the denatured proteins covalently bonded to them. After stringent washes to elute any non-covalently interacting proteins, the RNA is enzymatically digested and the protein sample is subjected for proteomics via mass spectrometry (Bach-Pages et al., 2017) (Fig. 7). This technique is powerful but limited by its restriction to polyA RNA.

The RIC technique was used in plants several years ago by a trio of studies using cell suspension cultures, seedling leaves, leaf mesophyll protoplasts, and etiolated whole seedlings (Marondedze et al., 2016; Reichel et al., 2016; Zhang et al., 2016). These studies identified between 300 and 1200 RBPs, all showing enrichment of proteins containing canonical RNA-binding domains. They also all identified a significant proportion of proteins lacking a canonical RNA-binding domain and playing no known role in RNA biology, underscoring how poorly described RNA-protein interactions are in plants. Finally, all three studies found significant proportions of enzymes involved in intermediate metabolism making up the RBPome, suggesting that the RNA-enzyme-metabolite hypothesis may be a valid consideration in plants as well as mammals.

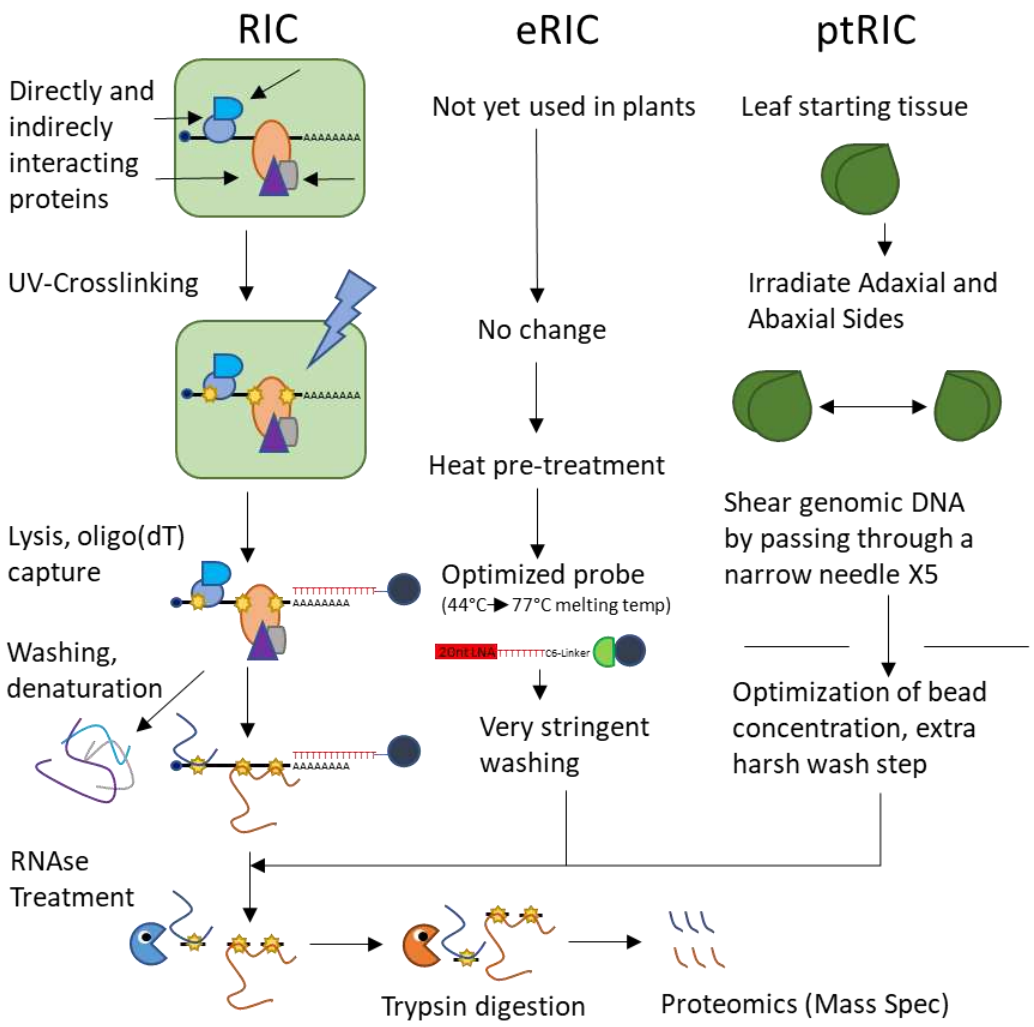

Figure 7. RNA Interactome Approaches for RBPome Investigation.

The basic RNA interactome approach involves UV-crosslinking (either traditional or using photoactivatable nucleoside 4SU) to covalently bond RNA to interacting proteins, cell lysis, pulldown of polyA RNA using oligo(dT) conjugated beads, followed by stringent washing, denaturation of proteins to eliminate non-crosslinked interactions, and then RNAse treatment to remove RNA, trypsin digestion, and mass spectrometry proteomics to identify the crosslinked protein cohort. Enhanced RIC (eRIC, not yet used in plants) uses a heat pre-treatment to dissociate non-crosslinked proteins and an optimized DNA probe conjugated to beads instead of standard oligo(dT) beads. The optimized probe permits very stringent washing conditions, which eliminates background. ptRIC was developed specifically for plants and optimizes irradiation conditions by repeatedly irradiating both sides of the leaves, removing genomic DNA by shearing, and optimizing bead concentration. There is no apparent barrier to combining the eRIC and ptRIC approaches to generate a super-optimized RIC protocol for plants.

These studies provide us with a perspective on heterogenous plant samples grown under normal conditions and provide a baseline against which future studies may com-pare the results of experiments using the array of sample types described. Since their publication, the RIC method has been applied to Arabidopsis cell cultures grown under drought stress (using PEG to simulate drought conditions in culture) to identify 150 RBPs responsive to drought stress (Marondedze et al., 2019). Similarly, RIC was used to probe modifications of the spliceosome and its RBPs in response to drought, identifying 44 spliceosomal proteins and 32 proteins associated with stress granules (Marondedze et al., 2020). Like the previous studies, this work identified many metabolic enzymes interacting with RNA, comprising proteins involved in carbohydrate metabolism and the glycolytic and citric acid pathways. Recently, several optimizations of the RIC protocol - deemed enhanced RNA interactome capture or eRIC - were described, but these modifications have yet to be applied to plants (Perez-Perri et al., 2018) (Fig. 7). Separately, RIC has been optimized for leaf tissue (termed plant RNA interactome capture or ptRIC) by adjusting UV conditions, irradiating both adaxial and abaxial surfaces of leaves, increasing the stringency of washing conditions, and shearing genomic DNA by passing the RNA-loaded beads through a narrow needle (Bach-Pages et al., 2020) (Fig. 7). It remains now for RIC or its derivatives to be used to view the changes of the RBPome in response to biotic and abiotic stresses beyond drought.

Very recently, a new method for the identification of RNA-protein interactions has been adapted from bacterial and mammalian systems, known as orthogonal Organic Phase Separation, or OOPS. This method uses UV-crosslinking, similar to other techniques, and acidic guanidiniumthiocyanate-phenol-chloroform (AGPC) phase separation to collect RBPs at the

interface between the aqueous and organic phases (Queiroz et al., 2019). OOPs has the advantage of being simpler than many other techniques and of not requiring mRNA pulldown, thus capturing RBP interactions with all types of RNA rather than solely coding RNAs. OOPS was applied in Arabidopsis to identify 468 RBPs, 232 of which were enzymatic putative RBPs (Liu et al., 2020b).

1.9. RNA-Protein Interactions in Plants as Unearthed by Classical Methods

The study of RNA-protein interactions predates the use of the methods discussed above. Before the advent of techniques capable of directly establishing RNA-protein interaction *in vivo*, classical genetics and cell biological methods were used to compile evidence supporting the interaction of RNA and protein. To provide a comprehensive understanding of plant RBPs role in diverse cellular processes, I reviewed the literature using classical methods to probe RNA-protein interactions in plants (Table 3). The totality of our current understanding of RNA-protein interactions in plants, derived from both modern and classical methods, is summarized in Figure 8.

In all eukaryotes, RNAs are processed with a 5' methylguanosine cap shortly after RNA polymerase synthesizes the first 25-30 nucleotides; capping is accomplished by the catalytic activities of RBPs, and the cap subsequently increases stability and participates in pre-mRNA splicing via cap binding proteins (Hocine et al., 2010). Next, exons are spliced together by the spliceosome complex, which is composed of a small nuclear ribonucleoprotein (snRNP) complex containing multiple RBPs; the U2 snRNP auxiliary factors U2AF35 and U2AF65 subunits bind to the intron/exon borders to mediate cleavage at both splice sites and then ligation (Meyer et al.,

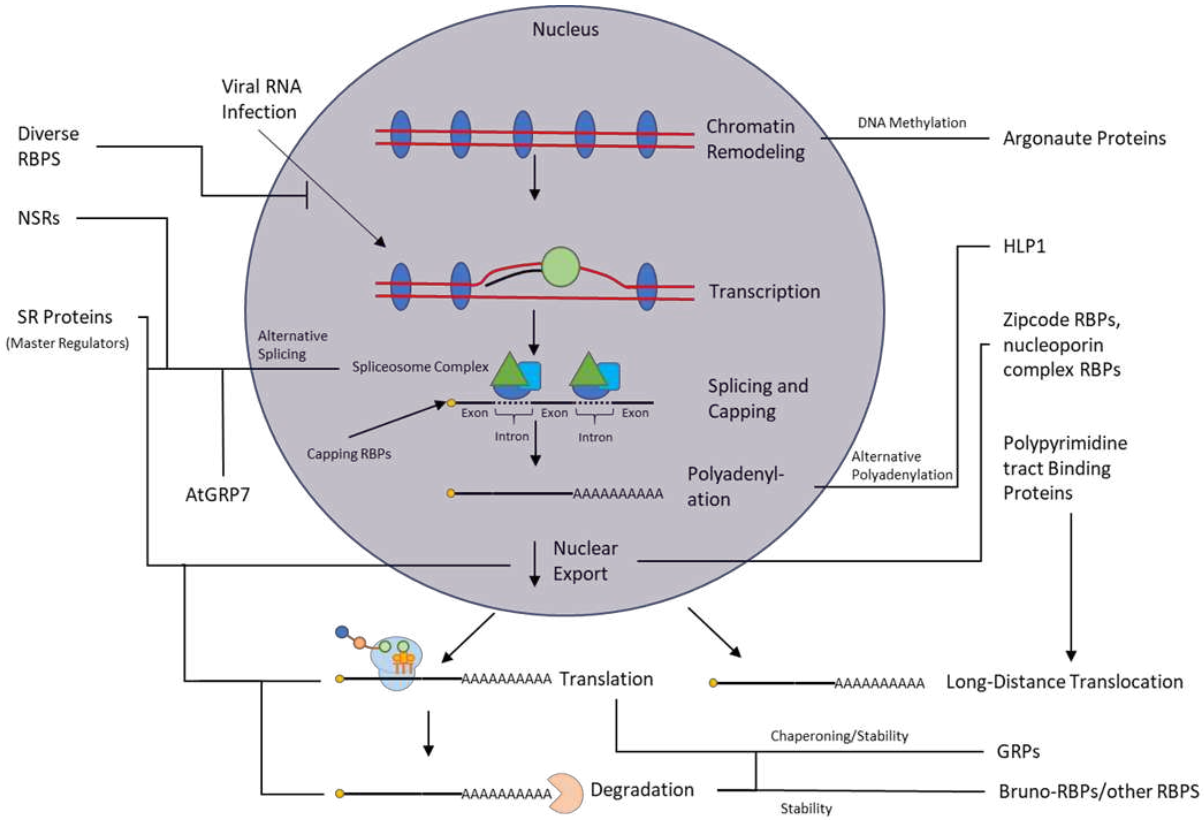

Figure 8. Summary of Known RNA-Protein Interactions in Plants.

RNA-Binding Proteins play significant roles in carrying out and regulating every step and stage of the existence of RNAs. This diagram illustrates currently known RBPs and their RNA-binding roles, highlighting their ubiquity. Most of these RBP classes are capable of both positive and negative regulation, and as such lines indicating their activity have been left without arrows or bars.

2015). Alternative splicing of exons can regulate transcript abundance by generating premature termination codons or unstable mRNA isoforms targeted for nonsense-mediated degradation, and novel protein isoforms may be produced in response to stress to alter protein localization or function (Reddy et al., 2013; Shang et al., 2017).

Fully transcribed and spliced mRNAs are polyadenylated at the end of the 3' UTR (although alternative polyadenylation sites with significance in transcript stability, ex-pression, and regulation have been observed), by the polyadenylation complex which is composed of a large number of proteins, some of which are RBPs (Hunt, 2012; Hunt et al., 2012). Finally, the ribosome itself is a ribonucleoprotein complex containing at least 80 ribosomal proteins, many of which are RBPs (Saéz-Vásquez and Delseny, 2019).

1.9.1 RNA Processing

Regulation of RNA processing is mediated by RBPs at multiple levels. As discussed in section 1.6, SRs and NSRs participate in the regulation of alternative splicing and polyadenylation. In *Medicago truncatula*, NSRs are known to partner with the lncRNA early nodulin 40 (ENOD40) involved with root nodulation (Campalans et al., 2004). NSRs are quite ancient, pre-dating the rise of true vascular plants, and have shown a reductive evolutionary trend in eudicots compared to other angiosperms, sometimes limited to as few as one or two genes (Lucero et al., 2020). This phylogenetic analysis showed that there are three motifs conserved across NSRs in plants: a nuclear localization signal, a motif of unknown function, and the C-terminal RRM. It has been suggested that alternative splicing of NSRs may help compensate for their reduction in eudicots (Lucero et al., 2020).

Splicing of plant resistance genes is controlled by modifier of snc1,12 (MOS12), a cyclin L homolog, and the MOS4-associated complex (MAC), localized to the nucleus (Xu et al., 2012). The MAC is a nuclear complex that also comprises the Arabidopsis homolog of cell cycle serine/threonine-protein kinase (AtCDC5) transcription factor and protein pleiotropic regulatory locus (1PRL1), a beta-transducin repeat (WD-40) protein (Palma et al., 2007). Immuno-affinity purification of the MAC followed by proteomics identified 24 MAC-interacting proteins, most of which are predicted to participate in RNA processing, including U2 and U5 sub-units and several other RBPs (Monaghan et al., 2009). The splicing modulator AtGRP7, shown by RIP to modulate alternative splicing (section 1.6), is regulated by the circadian clock and downregulates FLC, as indicated by At-GRP7 knockout and overexpression lines, to control flowering time (Schoning et al., 2007; Streitner et al., 2008; Staiger et al., 2003). At-GRP7 also controls alternative splicing of the flowering locus M (FLM) floral repressor to act in the thermosensory control of flowering time (Steffen et al., 2019). A paralog of AtGRP7, AtGRP8, coordinates with AtGRP7 in

the alternative splicing of FLM, potentially playing a stronger role in that process that AtGRP7 (Steffen et al., 2019). The circadian-clock functions of AtGRP7 are controlled by its RNA binding domain as determined by transcriptional profiling of lines ex-pressing AtGRP7 with a point mutation in the RNA binding domain (Staiger, 2001; Streitner et al., 2008; Streitner et al., 2010). At-GRP7 is a target of a bacterial type III-secreted effector, HopU1, to suppress plant immunity via ADP-ribosylation of AtGRP7's RNA binding site and thus interfering with its ability to bind RNA (Fu et al., 2007).

In maize, the nuclear-localized RRM protein defective kernels 42 (Dek42) impacts alternative splicing through its interaction with spliceosome components, including splicing factor 3a subunit 1 (SF3a1) and U1 small nuclear ribonucleoprotein 70 kDa (U1-70k) (Zuo et al., 2019).

Alternative polyadenylation (APA) forms another mechanism of regulation by RBPs, which produces mRNAs with distinct 3' ends by modifying cleavage and polyadenylation sites in the 3' UTR (Tian and Manley, 2017). Over 70% of mammalian transcripts have APA isoforms, and over 50% of plant transcripts (Tian and Manley, 2017; Xing and Li, 2011). The RBP known as flowering time control protein (FPA) is involved in FLC regulation repression to enable flowering, involved in 3' end processing and alternative polyadenylation redundantly with flowering time control protein (FCA), another RBP (Hornyik et al., 2010). FPA and FCA were further shown to be involved in transcription termination limiting intergenic transcription for a wide array of genes (Sonmez et al., 2011). FPA controls cleavage and polyadenylation of ETHYLENE RESPONSE FACTOR 4 (ERF4) during exposure to the bacterial flagellin peptide elicitor flg22 to limit the defense response to bacterial infection (Lyons et al., 2013).

Table 3. Summary of Plant RBPs Identified by Classical Methods

RBP	**Role**	**References**
AlSRG1	*Abiotic stress response*	Ben Saad et al., 2018
APUM5	*Repress viral replication*	Huh and Paek, 2013b
ARP1	*Modulation of transcript levels*	Jung et al., 2013
AtBRN1	*Control flowering time*	Kim et al., 2013
AtBRN2	*Control flowering time*	Kim et al., 2013
AtGRP7	*Modulation of alternative splicing*	Schoning et al., 2007
AtGRP8	*Modulation of alternative splicing*	Steffen et al., 2019
AtRBP45b	*RNA stability*	Muthuramalingam et al., 2016
AtRZ-1a	*Cold stress defense*	Kim et al., 2005
AtUSP	*RNA chaperoning*	Melencion et al., 2017
BTR1	*Repress viral replication*	Fujisaki et al., 2008
CaPR-10	*Cleavage of viral RNAs*	Park et al., 2004
CaRBP	*Delay flowering*	Kim et al., 2016
CmRBP50	*Long distance RNA translocation*	Li et al., 2011
Dek42	*Modulation of alternative splicing*	Zuo et al., 2019
DRB4	*Repress viral protein accumulation*	Jakubiec et al., 2012
FCA	*Alternative polyadenylation, transcription termination*	Hornyik et al., 2010; Sonmez et al., 2011
FPA	*Alternative polyadenylation, release of flowering repression, limit defense response*	Hornyik et al., 2010; Lyons et al., 2013
GR-RBP3	*RNA chaperoning, cold resistance*	Wang et al., 2018
GRP8	*Root hair cell determination*	Foley et al., 2017
HEN1	*RNA stability*	Ren et al., 2012
HESO1	*RNA stability*	Zhao et al., 2012
HPR1	*mRNA nuclear export, defense signaling*	Pan et al., 2012
MCT1	*Modulation of gene expression*	Gu et al., 2016
MOS2	*Nucleoporin trafficking of RNAs, plant innate immunity*	Zhang et al., 2005; Monaghan et al., 2010
MOS3	*Nucleoporin trafficking of RNAs*	Zhang et al., 2005; Monaghan et al., 2010
MOS11	*Nucleoporin trafficking of RNAs*	Germain et al., 2010; Monaghan et al., 2010
MOS12	*Splicing of resistance genes*	Xu et al., 2012
MpGR-RBP1	*Germination, salt stress resistance*	Tan et al., 2014
MtNSR1	*Modulation of splicing*	Campalans et al., 2004
PPR10	*RNA stability*	Pfalz et al., 2009

RBP50	*Long distance RNA translocation*	Ham et al., 2009
RBP-L	*Subcellular trafficking of mRNAs*	Tian et al., 2018; Tian et al., 2020
RBP-P	*Subcellular trafficking of mRNAs*	Tian et al., 2018; Tian et al., 2020
SARs	*Nucleoporin trafficking of RNAs*	Parry et al., 2006
SDP	*RNA chaperoning, stress resistance*	Han et al., 2015
SERRATE (SE)	*Inhibition of root hair cell determination, RNA stability*	Foley et al., 2017
UIP1	*Mediation of RNA decay, abiotic stress resistance*	Park et al., 2013

1.9.2 Trafficking and Translocation

RBPs ensure that mature RNAs are transported to the correct cellular locale. In rice endosperm, it was shown that two zipcode RBPs binding glutelin mRNA form a quaternary structure with two membrane fusion factors (Crofts et al., 2010). RBP-P and RBP-L, as discussed in Section 1.6, participate in the coopting of endosomal trafficking for mRNA translocation (Crofts et al., 2010; Tian et al., 2020). Mutant lines of RBP-P proteins in rice showed mis-localized glutelin and prolamine mRNAs (coding for the two most prominent seed storage proteins), as well as altered regulation of biological processes during seed development (Tian et al., 2018).

The nucleoporin complex participates in the proper apportioning of mRNAs between the nucleus and cytoplasm in response to stresses, mediated by the RBPs MOS2, MOS3, and MOS11. These MOS factors were originally identified as modifiers of snc1 (suppressor of NPR1-1, constitutive1), which encodes a resistance gene involved in basal plant immunity (Monaghan et al., 2010). MOS2 contains a G-patch motif and Kyprides, Ouzounis, Woese (KOW) domains, indicating that it binds RNA. Mutant lines showed suppressed constitutive defense responses, and MOS2 has been predicted to play a role in RNA processing (Zhang et al., 2005; Zhang and Li, 2005). MOS3 is localized to the nuclear envelope, where it is involved in nuclear mRNA export with a role in innate immunity (Zhang et al., 2005). MOS11 has homology to a human RNA binding protein (cytokine-inducible protein 29, or CIP29) and is localized to the nucleus, where it acts in mRNA nuclear export (Germain et al., 2010). A plant homolog of a component of the transcription export complex in yeast and humans, heparanase 1 or HPR1, is further involved in mRNA export and defense signaling (Pan et al., 2012). The SARs (suppressor of

auxin resistance) are localized to the nuclear membrane, acting as nucleoporins and mediating export of polyadenylated RNA (Parry et al., 2006).

In angiosperms, certain mRNAs involved in organ development are translocated through the phloem as long-distance signaling agents in the form of ribonucleoprotein complexes mediated by RBPs (Lucas et al., 2001). CmRBP50, a polypyrimidine tract binding protein, is essential for the assembly of one such complex based on the phosphorylation of phosphoserine residues at the C terminus (Li et al., 2011). Three proteins bind directly with phosphorylated CbRBP50 to assemble a complex that binds mRNA containing polypyrimidine tract binding motifs for transport through the phloem sieve tube system (Li et al., 2011). In pumpkin, another polypyrimidine tract binding protein, RBP50, forms ribonucleoprotein complexes with phloem-mobile mRNAs (Ham et al., 2009).

1.9.3. Chaperoning

RNA chaperones play a significant role in cold acclimation by binding RNAs non-specifically and modulating their secondary structure during chilling conditions (Czolpinska and Rurek, 2018). These proteins are typically from the glycine-rich RNA-binding protein (GRP) family, a group of developmentally regulated RBPs that possess N-terminal RNA recognition motifs (RRMs) and often exhibit induction by low temperatures. A family of such genes was identified in plant mitochondria via affinity chromatography, diverging in their C-terminal sequence; this indicates that while they may recognize RNA through the same mechanism, they target diverse areas of RNA biology for regulation (Vermel et al., 2002). One of these mitochondrially-located proteins, GR-RBP3, was found in cucumber to be highly expressed during chilling and to

minimize the effects of stress such as slowed growth speed, electrolyte leakage, and reactive oxygen species (Wang et al., 2018). Overexpression of GR-RBP3 also up-regulated nine Arabidopsis genes involved in stress defense; together, these results imply that GR-RBP3 plays a role in maintaining mitochondrial function during low temperature and thereby increasing cold stress resistance (Wang et al., 2018). Another GRP, termed AtRZ-1a, showed remarkably similar patterns of expression to GR-RBP3 under stress, and knockout and overexpression lines showed that AtRZ-1a plays a key role in cold stress defense (Kim et al., 2005). The GRPs are heavily regulated by stress conditions, including cold, salt, and de-hydration (Kwak et al., 2005).

In cotton, between 32 and 37 GRPs have been identified and subdivided into four families based on the arrangement of glycine repeats and the presence of other motifs (Yang et al., 2019). Gene expression analysis in cotton and Chinese cabbage (*Brassica rapa*) showed that these GRPs participate in response to various abiotic stresses in different tissues according to developmental stage (Yang et al., 2019; Lu et al., 2020). A member of this protein family, GRP8, has also been shown to participate in root hair cell determination in a phosphate starvation-dependent manner by binding to and promoting the abundance of WRKY DNA-BINDING PROTEIN 75 (WRKY75) (Foley et al., 2017). GRP8 binds to a TG-rich motif and promotes the abundance of the mRNAs of phosphate transporters.

In *Arabidopsis thaliana*, the universal stress protein UDP-Sugar pyrophosphorylase (AtUSP) acts as an RNA chaperone to bind nucleic acids nonspecifically, showing high nucleic acid-melting activity, to help maintain the RNA secondary structure during cold temperatures and maintain gene expression (Melencion et al., 2017).

1.9.4. Stability and Decay

Bruno-RBPs AtBRN1 and AtBRN2 in Arabidopsis bind the 3' UTR of the flowering pathway integrator SUPPRESSOR OF OVEREXPRESSION OF CONSTANS1 (SOC1), which is regulated by FLC, to repress SOC1 via mRNA decay pathways to control flowering time (Lee and Lee, 2010; Kim et al., 2013). Overexpression lines of these Bruno-RBPs showed delayed flowering time even when crossed with SOC1 overexpression lines provided the 3' UTR was included, whereas an AtBRN1 AtBRN2 double mutant line showed early flowering (Kim et al., 2013b).

In chloroplasts and mitochondria, transcripts are protected against degradation by exonucleases by RBPs at their 5'- and 3'-termini (Pfalz et al., 2009; Barkan and Small, 2014). Such protection leaves behind a small RNA footprint after RNA degradation, which has been used to probe the organellar RBP binding using the sRNA miner software and reveal differential protective patterns in mitochondria compared to chloroplasts (Ruwe et al., 2016). Mitochondrial transcripts showed a bias for protection at the 3' end, whereas chloroplast transcripts showed no such bias (Ruwe et al., 2016). The nuclear-encoded chloroplast-targeted RBP pentatricopeptide re-peat-containing protein 10 (PPR10) protects two intergenic RNA regions overlapping by 25 nucleotides to protect the RNA against degradation (Pfalz et al., 2009).

The nuclear-encoded protein termed S1 domain containing RBP (SDP), which is chloroplast-targeted, binds the chloroplast ribosomal RNAs 23S, 16S, 5S, and 4.5S and possesses RNA chaperone activity, indicating that SDP may play a role in ribosomal RNA processing in chloroplasts (Han et al., 2015). SDP knockout mutants show decreased survival rate during salt,

heat, UV, and cold stress as well as altered expression of nuclear stress-responsive genes, indicating that SDP plays a role in abiotic stress response (Dinh et al., 2019). These SDP mutants also showed slowed germination, dwarfism, chlorophyll a deficiency, and abnormal chloroplast structures (Han et al., 2015).

The protein SERRATE (SE) was identified by PIP-seq and RNA-chromatography as an inhibitor of root hair cell determination via miRNA biogenesis (Foley et al., 2017). SE binds to a GGN repeat motif, and independently of its inhibitory role promotes the stability of several mRNAs involved in root hair cell length (Foley et al., 2017). The RRM-containing protein AtRBP45b may play a role in RNA metabolism, specifically RNA stability, through interaction with cap-binding protein CBP20 and polyA binding protein PAB8 (Muthurumalingam et al., 2016). AtRBP45b is found in the nucleus and cytoplasm and has auxiliary domains related to protein-protein interaction, likely mediating its interaction with CBP20 and PAB8 (Muthurumalingam et al., 2016).

In rice, 3′-UTR-interacting protein 1 (UIP1) was identified as an RBP through yeast three-hybrid screening (Park et al., 2013). UIP1 interacts with the 3' UTR of the RuBisCo small subunit (rbcS) mRNA to mediate its stress-induced mRNA decay under drought and salt stress conditions. Rice overexpression lines showed increased resistance to salt, drought, and chilling stress (Park et al., 2013).

1.9.5. Gene Silencing

RBPs partner with small RNAs to silence retrotransposons and repetitive DNA elements through the formation of heterochromatin (Brodersen et al., 2008). This silencing involves AGO1, AGO10 (Argonaute proteins), katanin (microtubule severing enzyme), and VCS (decapping component) (Brodersen et al., 2008). Small RNAs involved in this process are stabilized in plants by 3' termini methylation, protecting them uridylation-targeted degradation mediated by the nucleotidyl transferases HESO1 and HEN1 (Ren et al., 2012; Zhao et al., 2012).

1.9.6. Viral RNA Suppression

Viral genomes rely on many RBPs of host origin for their replication and dissemination (Marmisolle et al., 2018). Consequently, host RBPs play a role in defense against viral pathogens; the Arabidopsis pumilio RNA binding protein 5 (APUM5) provides protection against cucumber mosaic virus (CMV) by directly binding to the 3' UTR of CMV RNAs to repress CMV replication (Huh and Paek, 2013; Huh and Paek, 2013b). Another RBP, binding to ToMV RNA 1 (BTR1), binds RNA around the initiation codons of the replication genes for tomato mosaic virus (ToMV) to inhibit ToMV replication, as demonstrated by BTR1 knockout and overexpression lines (Fujisaki and Ishikawa, 2008). Antiviral RNA silencing in plants occurs via the production of small RNAs from viral RNAs by dicer-like protein 4 (DCL4), as targeted by the interacting partner of DCL4, double-stranded RNA-binding protein 4 (DRB4), which binds double-stranded RNA of turnip yellow mosaic virus (TYMV) (Jakubiec et al., 2012). DRB4 is induced during viral infection and exported from the nucleus to the cytoplasm, where it associates not only with viral RNA but with a viral translational enhancer to repress viral protein accumulation (Jakubiec et al., 2012). In *Capsicum annuum*, pathogenesis-related protein 10

(CaPR-10) functions as a ribonuclease targeting tobacco mosaic virus (TMV) RNA; CaPR-10 is induced upon TMV infection, after which it is phosphorylated to increase its ribonucleolytic activity and increase its cleavage of viral RNAs (Park et al., 2004). Thus, RBPs are critically involved in multiple mechanisms of plant defense against viral infection: translational repression, ribonucleolytic cleavage, and RNA interference.

1.9.7. Other Plant RBPs

Other plant RBPs or putative RBPs have been identified, from a variety of species, whose impact on the life of their RNA targets has not yet been elucidated. Those discussed briefly hereafter demonstrate the importance of RBPs in regulation of stress response and development, particularly in germination and flowering.

In Arabidopsis, the ABA-regulated RNA-binding protein ARP1 was identified as an ABA-responsive protein localized to the nucleus (Jung et al., 2013). ARP1 is downregulated by ABA, seems to modulate the transcript levels of several genes involved in gene regulation, and both overexpression and knockout lines showed delayed germination during ABA, salt, and dehydration conditions, indicating that ARP1 plays a role in posttranscriptional RNA regulation during germination (Jung et al., 2013). Similarly, the mei2 C-terminal RRM only protein MCT1 is localized to the nucleus to impact the expression of several ABA-related genes (Gu et al., 2016). Overexpression and knockout lines for this protein demonstrated that, conversely to ARP1, it is upregulated under ABA treatment and inhibits germination and greening, suggesting that it plays an inhibitory role in germination and seedling growth, likely mediated by its RNA

binding domain. However, no such binding activity has been directly observed as yet (Gu et al., 2016).

Another putative RBP involved in seed germination was identified in *Malus prunifolia*. The glycine-rich protein MpGR-RBP1 was predicted as an RBP that is upregulated during salt, oxidative, or ABA stress (Tan et al., 2014). An Arabidopsis overexpression line demonstrated that MpGR-RBP1 is involved in seed germination; this line showed accelerated germination under salt and oxidative stress, and enhanced salt tolerance as measured by electrolyte leakage, chlorophyll concentration, ROS accumulation, and stomatal closure (Tan et al., 2014). Similarly, the *Aeluropus littoralis* Stress-Related Gene 1 (AlSRG1) gene encodes a protein involved in abiotic stress response that contains an RRM motif (Ben Saad et al., 2018). In tobacco overexpression lines, AlSRG1 improved resistance to several abiotic stresses and reproduced successfully under conditions that killed the control plants before flowering, and showed higher levels of the transcripts of genes related to ROS-scavenging and stress-related transcription factors, indicating that AlSRG1 plays a positive role in abiotic stress response (Ben Saad et al., 2018).

A putative RBP isolated from hot pepper (*Capsicum annuum* cv. *Bukwang*) termed CaRBP is also localized to the nucleus - specifically to the nucleolus - and functions in transgenic tomato to delay flowering and alter the expression of various genes related to flowering (Kim et al., 2016). Given its nucleolar localization and predicted RNA binding capacity, CaRBP may be involved in ribosome biogenesis or RNA metabolism.

These putative RBPs represent a rich potential for the characterization of the roles of RBPs in RNA biogenesis, processing, and degradation in plants. Techniques like those discussed in section 2 are key for tying these RBPs and others like them to the processes they regulate in their target RNAs.

1.10. Manipulation of RBPs Confers Desirable Traits in Plants

Because of their widespread nature and the role they play in abiotic stress response, RBPs and their RNA partners are key targets for biotechnological development in plants. Furthermore, understanding RNA-protein regulatory networks will facilitate successful application of plant biotechnology in general, because of the significant genotype to phenotype barrier that can be presented by highly redundant and interlinked endogenous networks (Moshelion and Altman, 2015). All genes and their mRNAs are part of these networks, regulated at every level by RBPs. A deeper understanding of those networks will allow judicious selection of the smallest number of key intervention points necessary to produce desired phenotypes.

Several RBPs have already been identified as important biotechnological targets in various plant species. The glycine-rich proteins, in particular, seem of great interest; At-GRP2 and AtGRP7 were expressed in rice, showing similar phenotype during salt or cold stress, but faster recovery and higher grain yields compared to controls during drought stress (Yang et al., 2013). GRP8 is a target for biotechnological advancement in engineering stress-resistant plants due to its role in upregulating phosphate uptake and biomass ac-cumulation and the fact that overexpression lines do not exhibit negative aerial phenotypes (Foley et al., 2017). The GRP MhGR-RBP1 was identified as a putative RBP in *Malus hupehensis*, where its transcript levels are highly regulated

by various abiotic stresses, indicating that it may be involved in abiotic stress response and a potential target for biotechnological development (Wang et al., 2012).

RNA chaperones are also targets of interest. A bacterial cold shock protein expressed in plants conferred improved growth in Arabidopsis and improved grain yield under drought stress in Maize (Castiglioni et al., 2008). Field trials of maize expressing this heterologous cold shock protein showed a 6% yield increase across trials due to increased drought resistance (Nemali et al., 2015).

In sugar beet, six genes coding for RBPs were identified as being able to increase salt tolerance in yeast (Téllez et al., 2020). Two of these genes participate in splicing, and the other four have only been putatively assigned as being involved in RNA metabolism. One of these salt-tolerance genes, BvSATO1 (which is involved in splicing), was verified in sugar beet and Arabidopsis, which showed that BvSATO1 increased salt tolerance in Arabidopsis (Téllez et al., 2020).

In Arabidopsis, the RBP AtRGGA is involved in the proper response to osmotic stress (Ambrosone et al., 2015). Overexpression of AtRGGA conferred increased resistance to ABA and salt stress in Arabidopsis due to modification of the transcriptome (Ambrosone et al., 2015). In apple, overexpression of the RBP MhYTP1 improved drought resistance as measured by photosynthesis and water use efficiency (Guo et al., 2019). Further discovery of such RBPs will play an important role in biotechnological advancement in plants.

1.11 Furthering the SR1 Story

The work described here follows up on work recently completed in our lab, which was described earlier in this introduction. Namely, the observation that SR1 mRNA accumulates several-fold under salt stress, and that this accumulation is dependent on a 500nt segment at the 3' end of the mRNA (Abdel-Hameed, 2020). We hypothesized that this accumulation may be due to an RNA modification in the critical region, and thus that one or more reader proteins of such modifications would preferentially bind to the RNA under salt stress conditions. Alternatively, we proposed that a protein factor may be binding SR1 mRNA at the poly-A tail and preventing deadenylation, thus increasing stability (Abdel-Hameed et al., 2020) (Fig. 9). To investigate both these hypotheses simultaneously, I used an RNA aptamer pulldown approach I call MS2-TRAP-MS to elucidate the protein interactome of SR1 during salt stress.

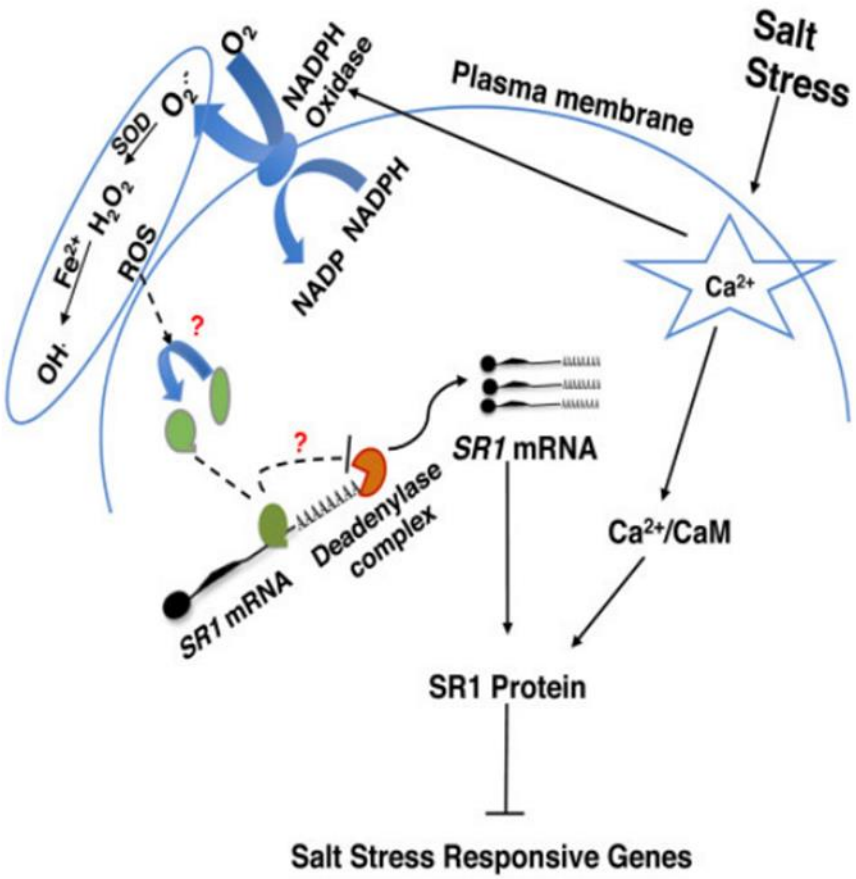

Figure 9. Current Model of AtSR1 Regulation During Salt Stress

Upon incidence of salt stress, primary stress sensors trigger calcium flux, which activates NADPH oxidase to release reactive oxygen species and binds with calmodulin. Ca^{2+}/calmodulin binds the SR1 protein to repress salt responsive genes. As reactive oxygen species increase in response to salt stress, conformational changes in RBPs are triggered that cause them to bind the SR1 mRNA and protect it from degradation by the deadenylase complex, leading to accumulation of the SR1 mRNA. Reproduced from Abdel-Hameed et al., 2020.

I transformed *Arabidopsis thaliana* with a construct expressing SR1 with two tags: an N-terminal 3X FLAG tag, and a 24x MS2 tag in the 3' UTR. The FLAG tag allowed identification of the SR1 fusion protein, whereas the MS2 RNA aptamer tag allowed pulldown of *SR1* mRNA using MS2 Coat Protein (MCP). I transformed this construct into two genetic backgrounds: wild type Arabidopsis, and a mutant background in which endogenous SR1 expression has been eliminated (SR1-KO, also referred to as *sr1-2*). Seedlings expressing this construct were grown in liquid culture containing 4-thiouridine and UV-crosslinked at 7 days after germination, then flash-frozen in liquid nitrogen. I passed cell lysate from UV-crosslinked seedlings over amylose beads loaded with a maltose binding protein-MCP fusion protein (MBP-MCP), allowing *SR1-MS2* mRNA to bind MCP. After washing, I eluted the MBP-MCP-RNA complexes using excess maltose. I digested the RNA component of the complexes using RNAse A, then submitted the samples for proteomics analysis via liquid chromatography-mass spectrometry (Fig. 9).

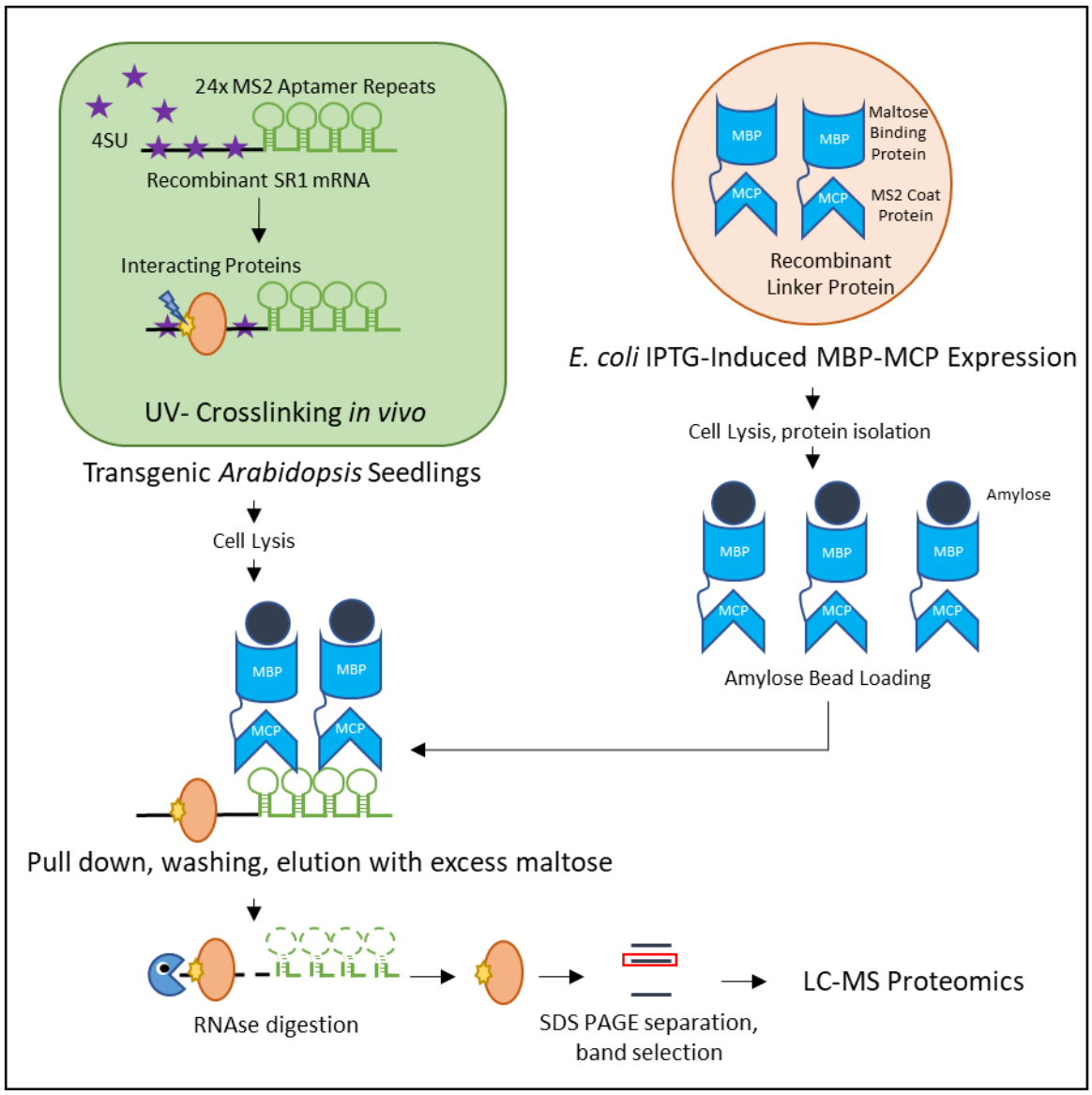

Figure 10: MS2-TRAP-MS

Diagrammatic representation of my use of MS2-TRAP-MS in *Arabidopsis thaliana*.

2. Methods

To generate reagents for analysis of protein interactors of *SR1* mRNA via the MS2-TRAP-MS method, I began by cloning an expression construct for plants containing 3x FLAG fused to the *SR1* coding sequence and a 24x repeat of the MS2 aptamer. Then, I transformed this expression construct into *Arabidopsis thaliana,* selected for positive transformants and lines expressing *3x-FLAG-SR1-MS2*. The verified transformed lines were grown in liquid culture for 14 days to perform MS2-TRAP-MS. To prepare for MS2-TRAP-MS, I grew and harvested the MBP-MCP linker protein from *E. coli* and loaded this protein on amylose beads. Cell lysate from the UV crosslinked liquid seedling cultures was passed over the beads, washed, and then eluted using excess maltose. The eluted proteins were run into SDS gels for separation and bands or entire lanes were submitted for liquid chromatography mass spectrometry. Proteomics results were obtained in the form of Scaffold files with protein IDs rated by the prevalence of peptides mapped to each ID.

2.1. Cloning the SR1 Expression Construct

I cloned *3xFLAG-SR1-24xMS2* using two vectors as my starting material: *3xFLAG-SR1*, which was previously developed in our lab and expressed *3xFLAG-SR1* using the PFGC 5941 plant expression vector backbone, and *SM-KDM5B-MS2*, which was graciously donated to us by Dr. Tim Stasevich's lab. *SM-KDM5B-MS2* contained 30x MS2 repeats. PFGC 5941 contains an expression cassette consisting of the Cauliflower mosaic virus (CaMV) 35S promoter, the tobacco mosaic virus translational enhancer omega (TMV Ω) and the octopine synthase transcriptional terminator (OCS). PFGC 5941 expresses a kanamycin resistance gene for selection in *E. coli,* and a glufosinate resistance gene for selecting transgenic plants.

To generate a directional cloning site in 3xFLAG-SR1, I selected *Xba*I and *Pac*I sites located between the termination codon of *SR1* and the *OCS* terminator. Because these enzymes required different buffers, I performed a sequential digest of *3x-FLAG-SR1*, first with *Pac*I, then with *Xba*I. After each digestion, the reaction was run on an agarose gel and the backbone purified from the gel using a plasmid purification kit. To release my desired 24x MS2 fragment from *SM-KDM5B-MS2*, I performed a double digestion of the vector using *Nhe*I and *Pac*I. After the digestion, the 2.7 kb 24xMS2 fragment was purified from an agarose gel using a fragment purification kit (Fig. 11).

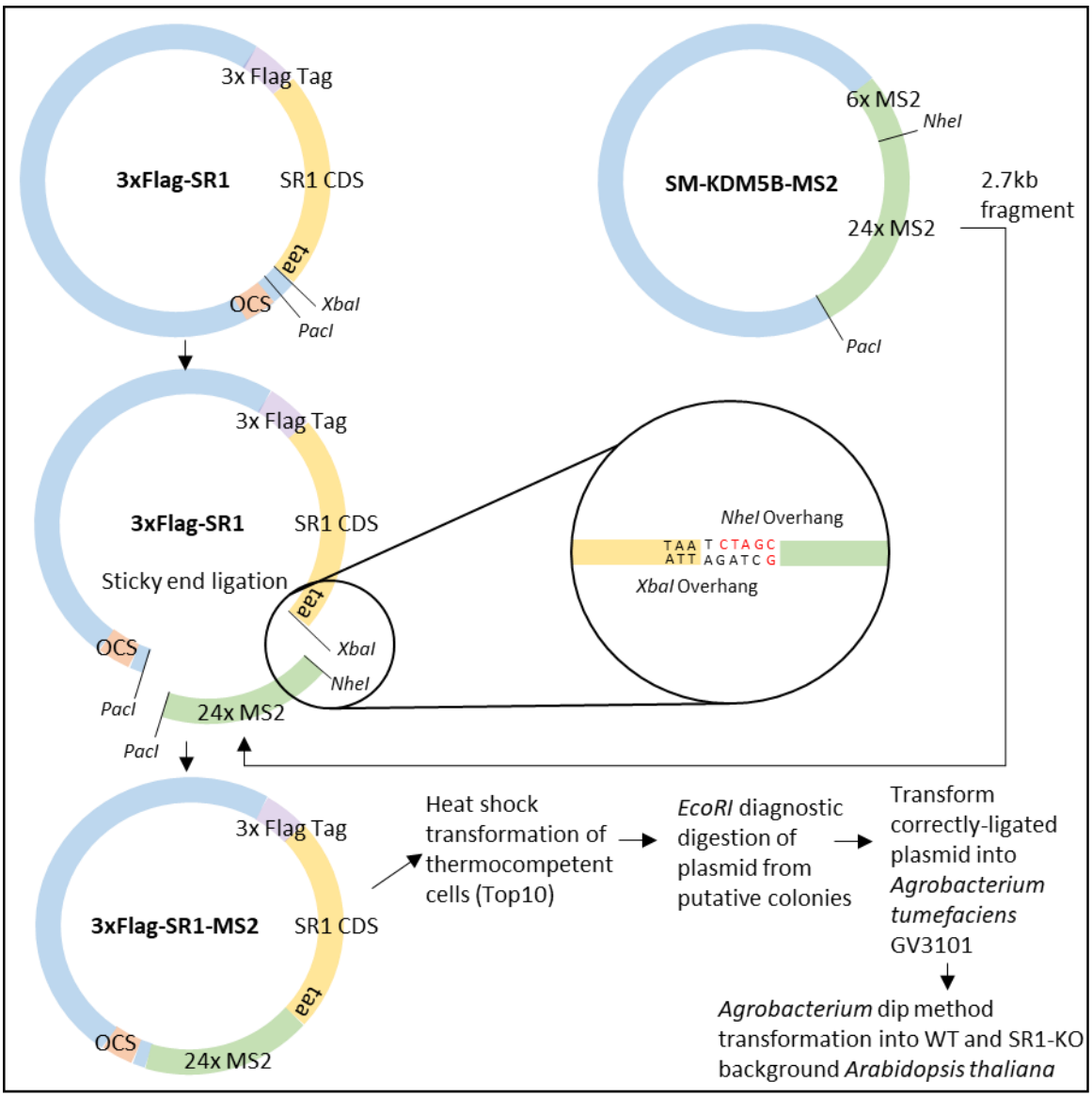

Figure 11. *3xFLAG-SR1-MS2* Cloning

Diagrammatic representation of my cloning of *3xFLAG-SR1-MS2*.

I then ligated the cut 3xFLAG-SR1 backbone containing *Xba*I and *Pac*I overhangs with the 24xMS2 fragment containing *Nhe*I and *Pac*I overhangs. *Xba*I and *Nhe*I generate compatible overhangs (CTAG), allowing the backbone *Xba*I overhang to ligate to the MS2 *Nhe*I overhang. I performed the ligation using a 1:3 vector: insert ratio, using T4 DNA ligase and incubating overnight at 16 ^{o}C. Six microliters of the ten-microliter ligation mixture was transformed into Top10 thermocompetent cells using heat shock for 1 minute at 42 ^{o}C in a water bath, followed by 2 minutes on ice and 1 hour recovering at 37 ^{o}C with 250 rpm shaking in 1 ml LB medium. After recovery, I spread the full contents of the transformation reaction onto LB plates containing 50 micromolar kanamycin (the selection present in the PFGC backbone) and allowed them to grow overnight at 37 ^{o}C. Twenty hours after transformation, I observed the presence of approximately 50 colonies and selected 8 for further analysis. These colonies were inoculated into liquid LB containing 50 micromolar kanamycin and cultured overnight at 37 ^{o}C with 250 rpm shaking.

To determine the identity of the putative clones, I purified plasmid from the cell cultures and then performed a diagnostic digestion using *Eco*RI. I expected *Eco*RI to produce 10 kb and 4 kb fragments from *3xFLAG-SR1*, and 10 kb, 4 kb, and 2.2 kb fragments from *3xFLAG-CAMTA-MS2*; the 2.2 kb fragment being distinguishing. Of the eight colonies selected for analysis, two showed the correct digestion pattern, and one was selected for verification by sequencing and preservation as a glycerol stock (in 80% glycerol kept at -80 °C for future work (Fig. 12).

2.2. Plant Transformation

I transformed Arabidopsis plants using the *Agrobacterium tumefaciens* dip method. I first generated an Agrobacterium GV3101 line containing my *3xFLAG-SR1-MS2* plant expression vector; GV3101 thermocompetent cells were transformed as previously described. DNA isolated from colonies, and screened using *Hind*III: I expected 12.1 kb, 3.2 kb, 0.9 kb, and 0.6 kb bands, and I observed the correct digestion pattern. I cultured approximately half a liter of this GV3101 cell line, pelleted the cells, then resuspended them into a solution containing 5% sucrose and 0.05% Silwet L-77. Wild type (WT) and *SR1*-KO (*sr1-2)* Arabidopsis plants at the flowering stage were dipped for 15 seconds into the Agrobacterium suspension, then allowed to set seed. Seeds were collected, sterilized (see Seed Sterilization), and germinated on 1/2 MS plates containing 1% sucrose, 200 mg/L cefotaxime (to inhibit the growth of Agrobacterium possibly still present on the seeds), and 10 micromolar glufosinate (*3xFLAG-SR1-MS2* contains glufosinate (Basta) resistance gene).

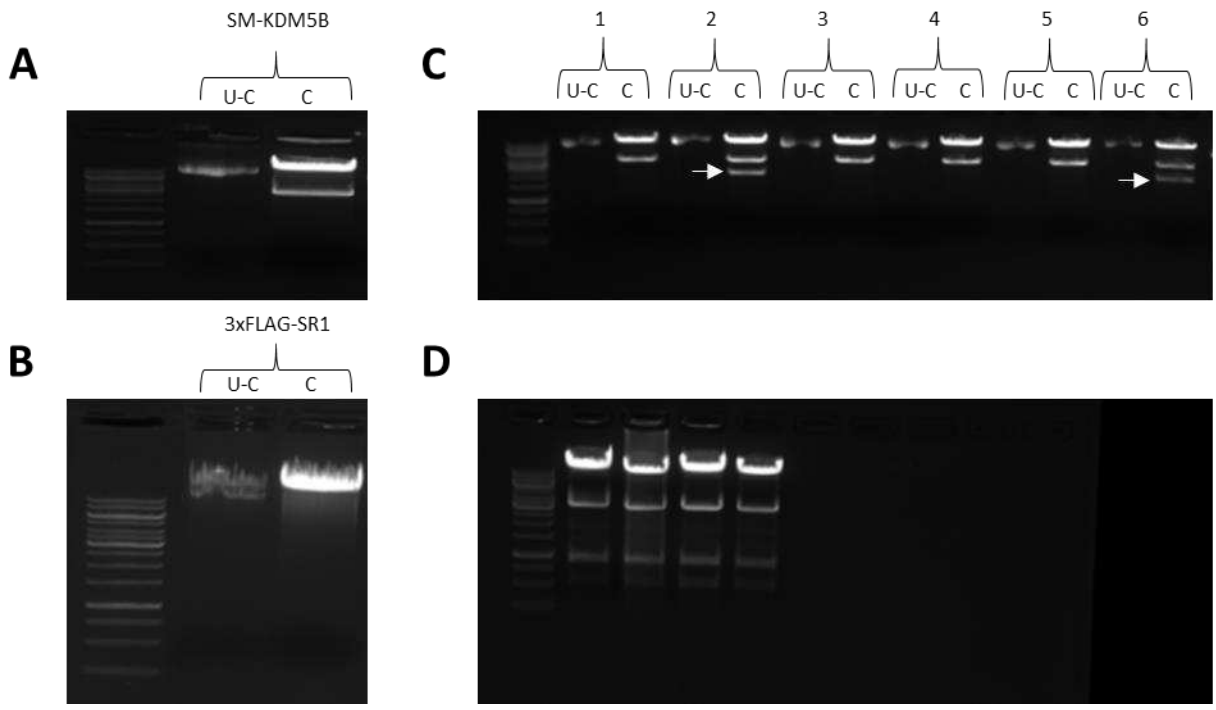

Figure 12. *3xFLAG-SR1-MS2* Cloning

Cloning steps and verification of putative colonies; U-C = uncut, C = cut. A) Digestion of SM-KDM5B with *Nhe*I and *Pac*I to release a 2.7kb fragment containing 24x MS2 repeats. B) Digestion of *3x-FLAG-SR1* with *Xba*I and *Pac*I to linearize the 14kb backbone (only 10 bp between the *Xba*I and *Pac*I sites). C) Verification of *3x-Flag-SR1-MS2* colonies after ligation of 2.7kb 24x MS2 fragment with 14kb *3xFLAG-SR1* backbone via diagnostic digest with *Eco*RI; ligated backbone produces ~10kb and ~4kb bands, whereas backbone ligated with the insert produces an additional ~2.4 kb band, indicated with white arrows. Colonies 2 and 6 contained the insert and plasmid from colony 2 was used to transform Agrobacterium tumefaciens GV3101. D) Verification of *Agrobacterium tumefaciens* colonies via diagnostic digest with *Hind*III; correct colonies produce four bands. All selected colonies contained the correct insert.

At 10 days after germination, I selected seedlings at the 2-4 leaf stage that demonstrated glufosinate-resistance (dark leaf color and normal size vs. leaf chlorosis and growth inhibition of seedlings affected by glufosinate) and transferred them to Sunshine potting media for collection of T1 seeds. T1 seeds were subjected to a second round of selection following the same protocol, transferred to soil, and T2 seeds were collected. During the soil stage, all plants were grown on Sunshine potting media in growth chambers set at 16 hours light/8 dark, 24 °C. Seedlings were grown under plastic covers for ~3-4 days after transfer to pots.

2.3. Seed Surface Sterilization

Arabidopsis seeds were surface sterilized according to the following protocol: incubation with 100% ethanol for 1 minute, followed by 20 minutes in 20% bleach, then 5 washes in sterilized double-distilled water performed in a laminar flow hood. After the fifth wash, the sterilized seeds were placed at 4 °C for 3-5 days for stratification. Surface-sterilized seeds were used in all experiments.

2.4. qRT-PCR Verification of Construct Expression

Leaf tissue was harvested from 3-week-old WT, KO, WT-MS2, and KO-MS2 plants and flash-frozen in liquid nitrogen. After grinding in liquid nitrogen in a mortar and pestle, RNA was isolated from powdered leaf tissue using TRIzol-chloroform extraction. cDNA was synthesized from this RNA using Superscript II reverse transcriptase and used for qPCR analysis of the *SR1-MS2* fusion RNA. I used Sybr Green I and qPCR primers (F: TGCCTATGTCCTCATCTTTGTG; R: GACTGTTACTGAGCTGCGTT) designed to overlap the 3' end of the *SR1* coding sequence and the 5' end of the *MS2* repeats tag to analyze the

prevalence of *SR1-MS2* cDNA in the cDNA samples. Primers against the housekeeping gene ubiquitin were used as control, and data was analyzed according to the delta-delta-CT method (Livak and Schmittgen, 2001) (Fig. 13).

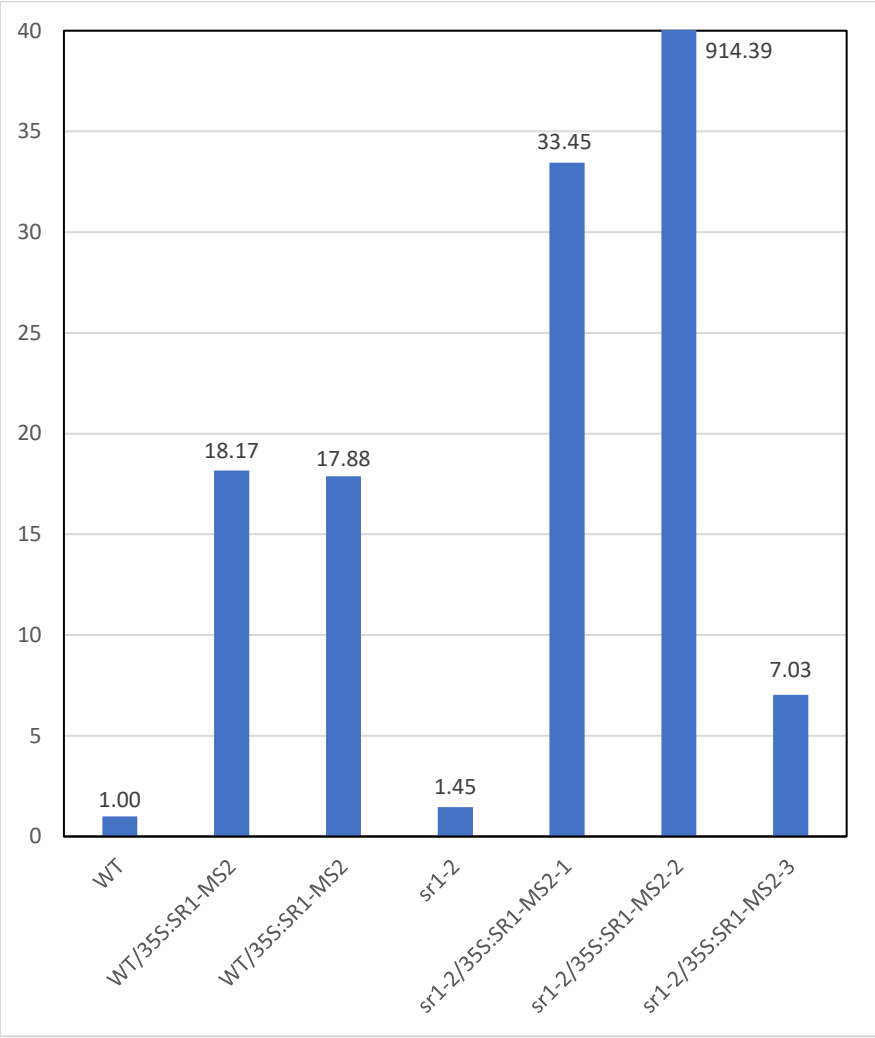

Figure 13. qRT-PCR Verification of *3x-FLAG-SR1-MS2* Expression in Transgenic Lines

As calculated by the delta-delta-CT method with reference to the ubiquitin housekeeping gene, fold changes of the *SR1-MS2* qRT-PCR product in cDNA samples are shown for WT, *sr1-2*, WT-MS2, and *sr1-2*/MS2 lines.

2.5. Phenotypic Verification of Transgene Expression

To verify the expression of my 3x-FLAG-SR1-MS2 construct, I grew seedlings of WT, *sr1-2* (*AtSR1* knockout line), *sr1-2:35s:SR1-YFP* (complemented line), and my *sr1-2*-background (knockout background) lines expressing *3x-FLAG-SR1-MS2* as determined by qPCR. Seedlings were treated as described below and grown in a growth chamber at 19-21 °C, which causes a dwarf phenotype in the knockout line (Du et al., 2009). No stunting was expected in the WT-background transgenic line regardless of proper expression of the construct due to the presence of endogenous SR1. In the knockout-background lines, complementation of the dwarf phenotype was observed (Fig. 14).

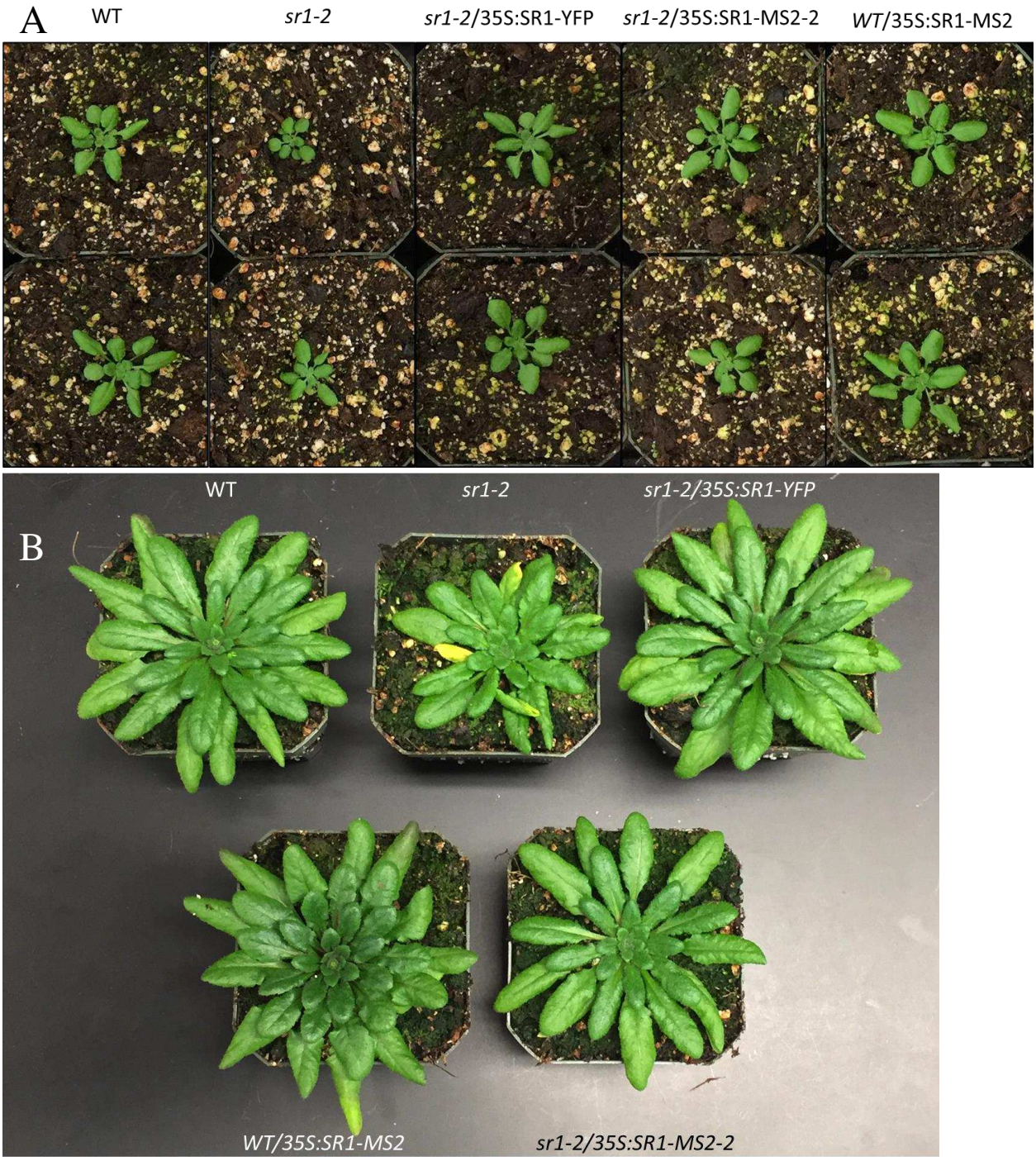

Figure 14. Dwarf Phenotype and Complementation in Transgenic Lines

A. Arabidopsis seedlings grown in Sunshine media at 19-21 °C to 14 days old. Knockout-background *3x-FLAG-SR1-MS2* lines fully complemented the dwarf phenotype, indicating that the *SR1-MS2* fusion construct is biologically functional. B. Arabidopsis plants grown in Sunshine media at 19-21 °C to approximately 30 days old, demonstrating complementation of the *SR1* knockout phenotype by *3X-FLAG-SR1-MS2* at later stages of development.

2.6. Experimental Design

Three experiments were performed: a pilot experiment including only WT and WT-MS2 lines without salt treatment (noted hereafter as C), an initial salt-treatment experiment including WT and WT-MS2 lines (noted hereafter as 1), and a secondary salt-treatment experiment using WT, KO, WT-MS2, and KO-MS2 seeds (noted hereafter as 2). For a diagrammatic representation of the processes involved for each of these experiments, see Figure 15.

2.7. Plant Growth, Treatment, UV-Crosslinking

Sterilized Arabidopsis seeds from wild type and transgenic lines were grown in liquid Murashige and Skoog (MS) media (1/2 concentration MS basal salts, 5% sucrose) in a growth chamber at 22 °C with 16 hours light and 120 rpm shaking (Murashige and Skoog, 1962). At 7 days after germination, treatment groups were subjected to salt stress (250 mM NaCl) for 6 hours. One day prior to treatment, seedlings were incubated with 200 μM of 4-thiouridine (4SU). After treatment, seedlings were collected, washed, and spread into a single seedling layer on plates. Plates were irradiated on ice with 365 nm UV light (0.2 J/cm2) in a Stratalinker 2400 (Stratagene). Following UV-crosslinking, seedlings were harvested in liquid nitrogen and stored at -80 °C. Frozen seedlings were ground to fine powder in liquid nitrogen using a mortar and pestle and resuspended in Column Buffer (200 mM NaCl; 20 mM Tris HCl pH 7.4; 1 mM EDTA) plus 1 mM PMSF, plant protease inhibitor cocktail at 1:200 (P9599 Sigma Aldrich), and RiboLock 3 μl/10 mL (EO0381 Thermo Scientific). After 1 hour of slow inversion at 4 °C, I pelleted cell debris by centrifugation at 8,000 rpm for 15 minutes at 4 °C.

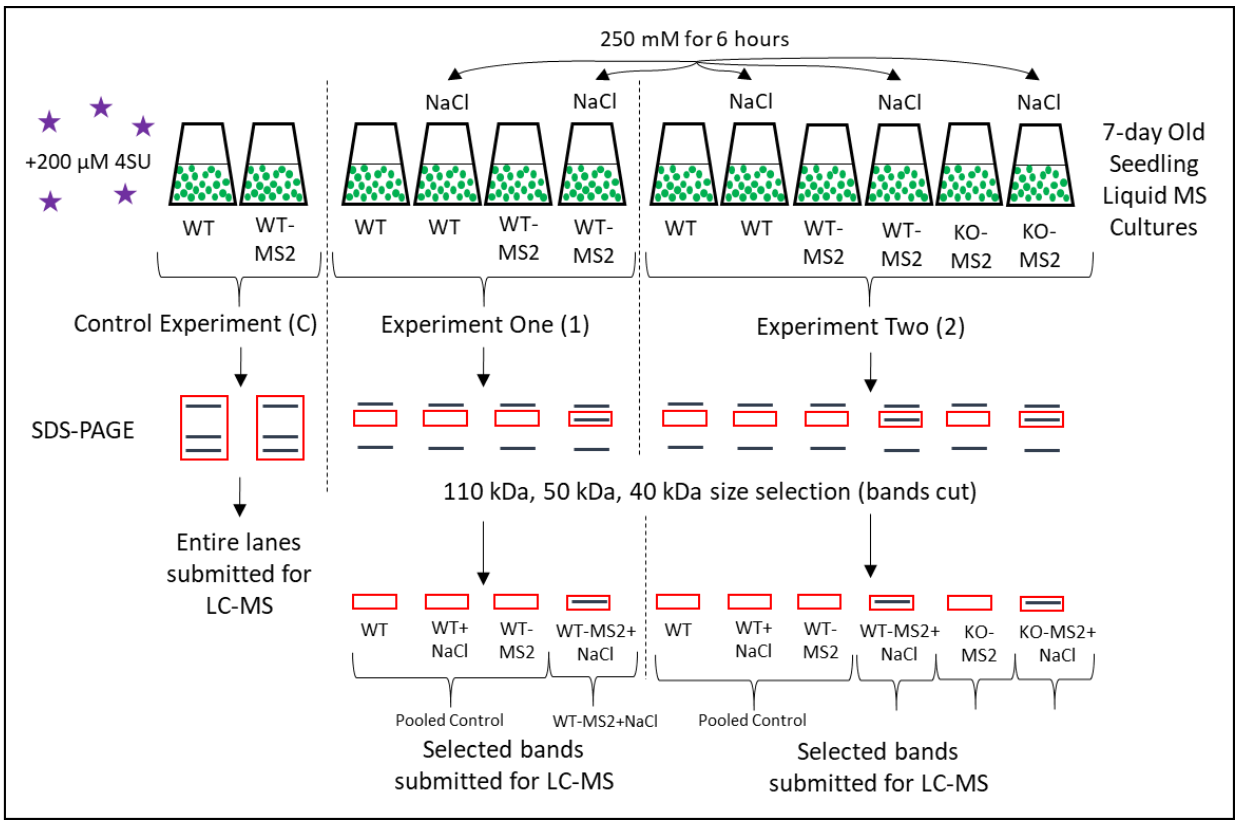

Figure 15. Experimental Design

I performed three experiments: a control experiment (C) comprised of WT and WT-MS2 and submitted the entire lane from SDS-PAGE for LC-MS proteomics; experiment one (1), comprised of WT and WT-MS2 with and without treatment by 250 mM NaCl for 6 hours, submitted 110 kDa, 50 kDa, and 40 kDa bands from SDS-PAGE for LC-MS proteomics; and experiment two (2), comprising WT, WT-MS2, and KO-MS2 with and without salt treatment and the same bands cut from SDS-PAGE for LC-MS proteomics. In all experiments, seedlings were grown in liquid culture with 200 µM 4SU for one day before harvesting.

2.8. Bead Loading

Amylose beads (E8021L New England Biolabs) were loaded with MBP-MCP fusion protein prior to use in TRAP. *Escherichia coli* containing an expression vector for this fusion protein was grown at 37 °C with 250 rpm shaking in LB media for 24 hours. I induced expression of the fusion protein using 1 mM IPTG for 4 hours, then pelleted cells via centrifugation at 10,000 rpm for 20 minutes. I removed the supernatant and resuspended the cell pellet in column buffer + 1 mM PMSF, 1 tablet/15 mL protease inhibitor cocktail (S8830 Sigma Aldrich), RiboLock 3 µl/10 mL (EO0381 Thermo Scientific), and 1mg/mL lysozyme, serving as bacterial lysis buffer. Cells were incubated in lysis buffer at 4 °C for 10 minutes, then sonicated 3 times for 10 seconds on ice. When lysed (solution is translucent and viscous), the lysate was pelleted via centrifugation at 10,000 rpm for 20 minutes at 4 °C and the supernatant removed.

Amylose beads were equilibrated with two washes in sterilized distilled water followed by two washes with column buffer. After equilibration, supernatant from MBP-MCP lysate was added to the beads and incubated for 24 hours at 4 C with slow inversion. I then pelleted the loaded beads via centrifugation at 10,000 rpm for 15 minutes, removed the supernatant and washed 5 times with column buffer via centrifugation as above.

MBP-MCP Protein Sequence:

MKTEEGKLVIWINGDKGYNGLAEVGKKFEKDTGIKVTVEHPDKLEEKFPQVAATGDGP
DIIFWAHDRFGGYAQSGLLAEITPDKAFQDKLYPFTWDAVRYNGKLIAYPIAVEALSLIY
NKDLLPNPPKTWEEIPALDKELKAKGKSALMFNLQEPYFTWPLIAADGGYAFKYENGK
YDIKDVGVDNAGAKAGLTFLVDLIKNKHMNADTDYSIAEAAFNKGETAMTINGPWAW

SNIDTSKVNYGVTVLPTFKGQPSKPFVGVLSAGINAASPNKELAKEFLENYLLTDEGLEA
VNKDKPLGAVALKSYEEELAKDPRIAATMENAQKGEIMPNIPQMSAFWYAVRTAVINA
ASGRQTVDEALKDAQTNSSSVPGRGSIEGRASNFTQFVLVDNGGTGDVTVAPSNFANGI
AEWISSNSRSQAYKVTCSVRQSSAQNRKYTIKVEVPKGAWRSYLNMELTIPIFATNSDCE
LIVKAMQGLLKDGNPIPSAIAANSGIYZ

2.9. MS2-TRAP

Supernatant of seedling cell lysate was removed and then incubated with amylose beads loaded with MBP-MCP fusion protein for 24 hours with slow inversion at 4 °C. Afterward, beads were pelleted as above, the supernatant was removed, and the beads were washed 5 times with Column Buffer via sequential centrifugation at 4 °C. I eluted the *MBP-MCP-SR1 mRNA* complexes from the beads using elution buffer containing excess maltose (column buffer + 10 mM maltose), performing 3 sequential elutions and collecting the supernatants separately. RNA was removed from the elutions via treatment with 1 U/100 μL RNAse A (BP2539100 Fisher Scientific) for 1 hour on ice.

2.10. Mass Spectrometry

RNAse-treated elutions were run with SDS-PAGE containing 10% polyacrylamide, then stained using Coomassie Blue to visualize protein bands. After destaining overnight with destaining solution (10% v/v Glacial Acetic Acid, 20% methanol, 80% water), the gel was preserved via drying between cellophane sheets in a plastic frame. I identified protein bands of interest showing differential between control and treated conditions by visual analysis of the dried gels,

then cut gel slices at identified protein weights (110 kDa, 50 kDa, and 40 kDa) from all samples for LC-MS.

Gel fragments were subjected to in-gel trypsin digestion and LC-MS/MS as previously described (Saveliev et al., 2013). Briefly, the gel pieces were washed with 200 µL of LC-MS Grade Water (Optima LC-MS, Fisher Scientific) for 30s and destained with 2 x 200 µL of 50% Acetonitrile (ACN; Optima LC-MS Grade)/50 mM Ammonium bicarbonate at 60° C, with intermittent mixing. The pieces were dehydrated with 100% ACN and allowed to air dry. Proteins were reduced and alkylated, in-gel with 25 mM DTT in 50 mM Ammonium bicarbonate (60 °C for 20 min) and 55 mM IAA or IAH in 50 mM Ammonium bicarbonate at room temperature in the dark for 20 min. Gel pieces were then washed with Optima water and dried. The dried gel pieces were rehydrated in 20 µL 12 ng/µL MS-grade Trypsin (ThermoPierce, San Jose, CA) /0.01% ProteaseMAX surfactant/50 mM ammonium bicarbonate mixture for 10 min. at room temperature, overlaid with 30 µL 0.01% ProteaseMAX surfactant/50 mM ammonium bicarbonate and incubated at 50 °C for 1 h. Extracted peptides were transferred and the digestion halted by addition of 10% trifluoro-acetic acid to a final concentration of 0.5%. Peptide extracts were dehydrated then resuspended in 5% ACN/0.1% formic acid. Once resolubilized, absorbance at 205nm was measured on a NanoDrop (ThermoScientific) and total peptide concentration was subsequently calculated using an extinction coefficient of 31 (Scopes, 1974).

Reverse phase chromatography was performed using water with 0.1% formic acid (A) and acetonitrile with 0.1% formic acid (B). A total of 0.75 µg of peptides were purified and concentrated using an on-line enrichment column (Waters Symmetry Trap C18 100Å, 5µm, 180

µm ID x 20mm column). Subsequent chromatographic separation was performed on a reverse phase nanospray column (Waters, Peptide BEH C18; 1.7µm, 75 µm ID x 150mm column, 45 °C) using a 30 minute gradient: 3%-8% B over 3 minutes followed by 8%-35% B over 27 minutes (0.1% formic acid in ACN) at a flow rate of 350 nanoliters/min. Peptides were eluted directly into the mass spectrometer (Orbitrap Velos Pro, Thermo Scientific) equipped with a Nanospray Flex ion source (Thermo Scientific) and spectra were collected over a m/z range of 400–2000, positive mode ionization. Ions with charge state +2 or +3 were accepted for MS/MS using a dynamic exclusion limit of 2 MS/MS spectra of a given m/z value for 30 s (exclusion duration of 90 s). The instrument was operated in FT mode for MS detection (resolution of 60,000) and ion trap mode for MS/MS detection with a normalized collision energy set to 35%. Compound lists of the resulting spectra were generated using Xcalibur 3.0 software (Thermo Scientific) with a S/N threshold of 1.5 and 1 scan/group.Tandem mass spectra were extracted, charge state deconvoluted and deisotoped by ProteoWizard MsConvert (version 3.0). Spectra from all samples were searched using Mascot (Matrix Science, London, UK; version 2.6.0) against reverse concatenated Uniport_Arabidopsis_thaliana_rev_051319, Uniprot_Ecoli_rev_022218 and cRAP_rev_100518 databases (92083 total entries) assuming the digestion enzyme trypsin. Mascot was searched with a fragment ion mass tolerance of 0.80 Da and a parent ion tolerance of 20 PPM. Carboxymethylation of cysteine was specified in Mascot as a fixed modification. Deamidation of asparagine and glutamine and oxidation of methionine were specified in Mascot as variable modifications. Search results from all samples were imported and combined using the probabilistic protein identification algorithms (Keller et al., 2002) implemented in the Scaffold software (version Scaffold_4.11.0, Proteome Software Inc., Portland, OR) (Searle et al., 2008). Peptide thresholds were set (90%) such that a peptide FDR of 0.0% was achieved based on hits

to the reverse database (Kall et al., 2008). Protein identifications were accepted if they could be established at greater than 95.0% probability and contained at least 2 identified peptides. Protein probabilities were assigned by the Protein Prophet algorithm (Nesvizhskii et al., 2003). Proteins that contained similar peptides and could not be differentiated based on MS/MS analysis alone were grouped to satisfy the principles of parsimony.

3. Results

3.1 Amylose bead Loading and Protein Eluates from Experiments 1 and 2

To demonstrate that I can purify MBP-MCP using amylose beads l, I performed a bead loading with bacterially expressed MBP-MCP and elution in the absence of plant lysate. Samples of supernatant were collected from the initial MBP-MCP protein extract from *E. coli* and during each stage of bead loading, washing, and elution. These samples were then seprated on an SDS-gel and stained with Coomassie blue. As shown in Fig. 16, extraction, bead loading, and elution of MBP-MCP with maltose were all successful.

Additionally, proteins eluted after TRAP of plant lysates in experiments 1 and 2 were run via SDS-PAGE and analyzed with Coomassie staining (Fig. 17). Visual analysis of the stained and dried gel in experiment 1 revealed that WT-MS2 and salt-treated WT-MS2 showed bands unique from the WT samples at 110, 50, and 40 kDa. Bands corresponding to these molecular weights were cut from all lanes in both experiments 1 and 2 and submitted for LC-MS. Although the bands in question were not visible in experiment 2 due to lower overall protein concentration (as indicated by the intensity of the MBP-MCP band), I did cut bands of the sizes corresponding to those in experiment 1 in order to attempt to reproduce the results, as it could be possible that there might be proteins detectable by LC-MS that I could not detect visually (Fig. 17). In experiment C, the lanes were submitted in their entirety.

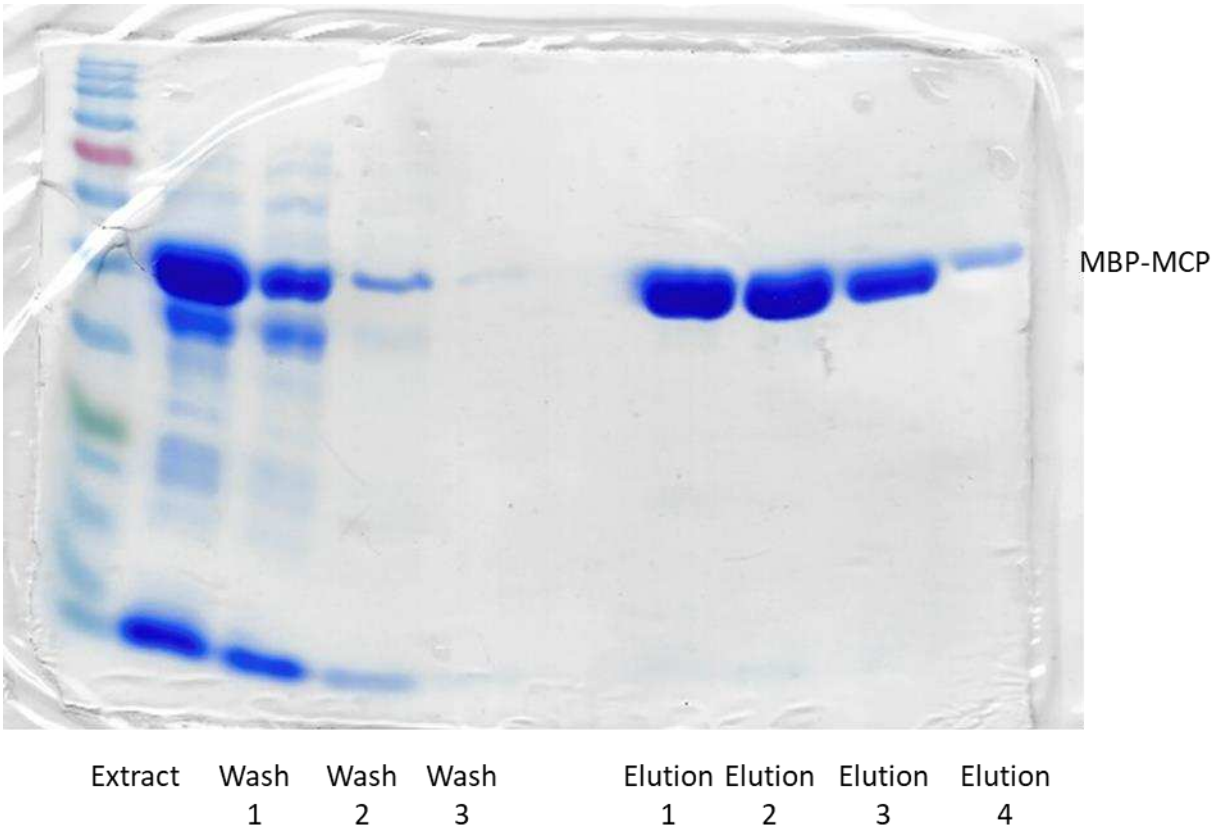

Figure 16. Amylose Bead Loading with MBP-MCP and its Elution with Maltose.

Protein extract and different fractions of wash and elution were separated on a 10% SDS gel and stained with Coomassie blue. **Extract** –*E. coli* protein extract was prepared after 4 hours induction of maltose binding protein-MS2 coat protein fusion protein (MBP-MCP) expression with 1 mM IPTG. **Washes** – After loading amylose beads for 24 hours at 4 °C, excess proteins were washed three times with 5 mL Column Buffer. **Elutions** – After washing, MBP-MCP was eluted four times with 300 µL Elution Buffer, releasing MBP-MCP from the amylose beads.

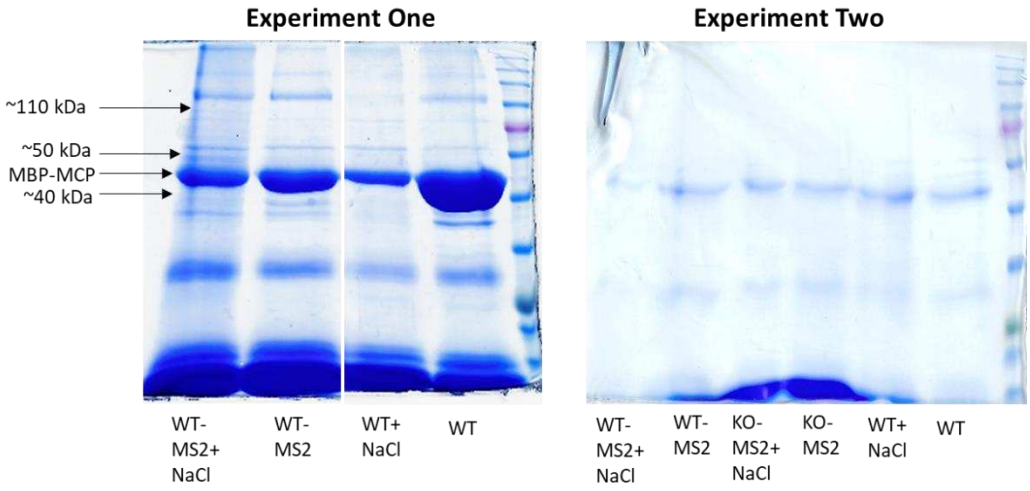

Figure 17. *A. thaliana* Protein Eluates from Experiments 1 and 2

10% SDS-PAGE with Coomassie staining. Experiment one identified three bands distinct in WT-MS2 samples compared to WT samples, at 110 kDa, 50 kDa, and 40 kDa. These bands were cut from all samples for submission to proteomics LC-MS. Eluates from experiment two contained much less concentrated protein precluding visual detection of bands, but gel slices were cut at the same positions as experiment one.

3.2 *SR1* mRNA Interacting proteins

I obtained the results from the three MS2-TRAP-MS experiments I conducted (C, 1, and 2) in the form of Scaffold files containing the accession numbers of the proteins identified and the number of peptides sequenced from each protein. The data was sorted according to normalized total spectra at 95% protein identification threshold (a measure of the confidence of protein identification using the protein prophet algorithm; higher values impose more rigorous requirements for proteins to be listed), a minimum of 1 peptide detected, and 95% peptide identification threshold (a measure of the confidence of peptide identification using a naïve Bayesian qualifier; higher values impose more rigorous requirements for peptides to be listed). The accession numbers were scored for biological origin, and proteins originating from Arabidopsis were selected for further analysis. In total across all samples and treatments, I identified 395 *Arabidopsis thaliana* proteins, 19 of which were found in at least one sample in all experiments (Fig. 18).

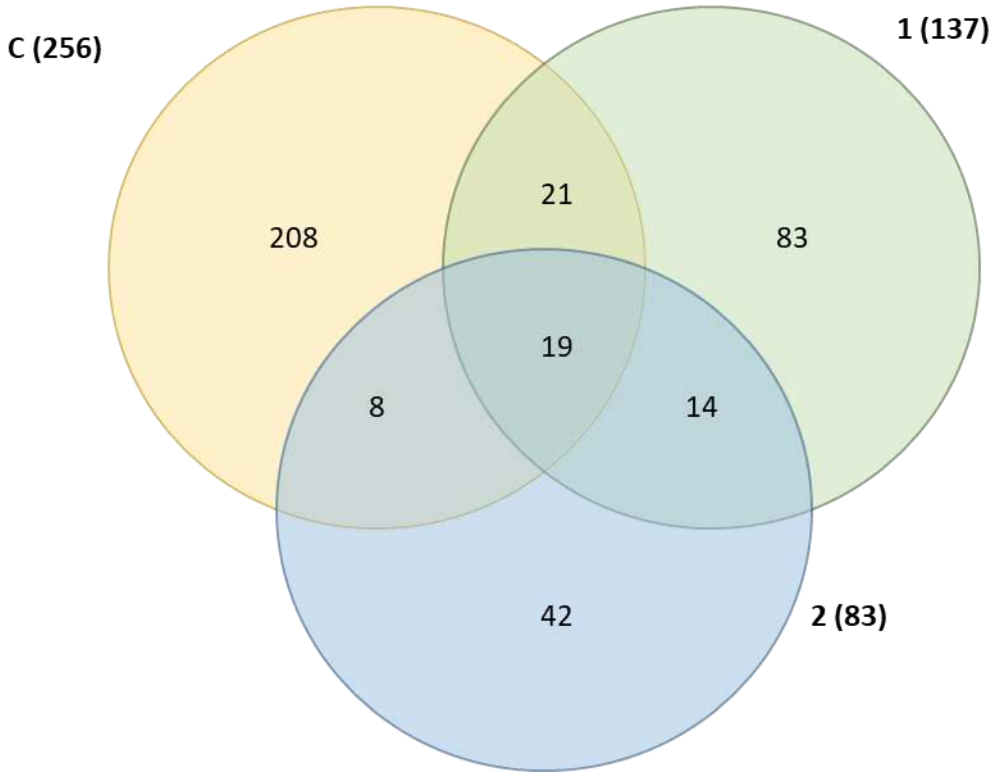

Figure 18. Overlap of Proteins Identified by MS2-TRAP-MS

395 individual proteins were identified over all three experiments (C-Pilot experiment, 1-experiment one, 2-experiment two).

3.3 Enrichment in Gene Ontology Categories

I performed GO analysis using TAIR (https://www.arabidopsis.org/) to classify proteins according to cellular component, biological process, and molecular function. In the control samples, the highest enrichments were for the terms “reductive pentose-phosphate cycle” at 40-fold enrichment over the term’s prevalence in the background set, “proteasome regulatory particle” (30-fold), and “glyceraldehyde-3-phosphate metabolic process” (40-fold). In the salt-treated samples, I saw much more significant enrichment of GO-terms. The highest enrichments were “regulation of oxidative-phosphorylation” (>100-fold), “positive regulation of oxidative-phosphorylation” (>100-fold), “positive regulation of ATP metabolic process” (>100-fold), “regulation of ATP metabolic process” (>100-fold), “photosynthetic electron transport in photosystem II” (>100-fold), “stromule” (70-fold), “phosphoglycerate kinase activity” (>100-fold), “transferring electrons within the cyclic electron transport pathway of photosynthesis activity” (>100-fold), glyceraldehyde-3-phosphate dehydrogenase (NAD^+) (phosphorylating) activity (>100-fold), and “glyceraldehyde-3-phosphate dehydrogenase ($NAD(P)^+$) (phosphorylating) activity” (>100-fold) (Fig. 19).

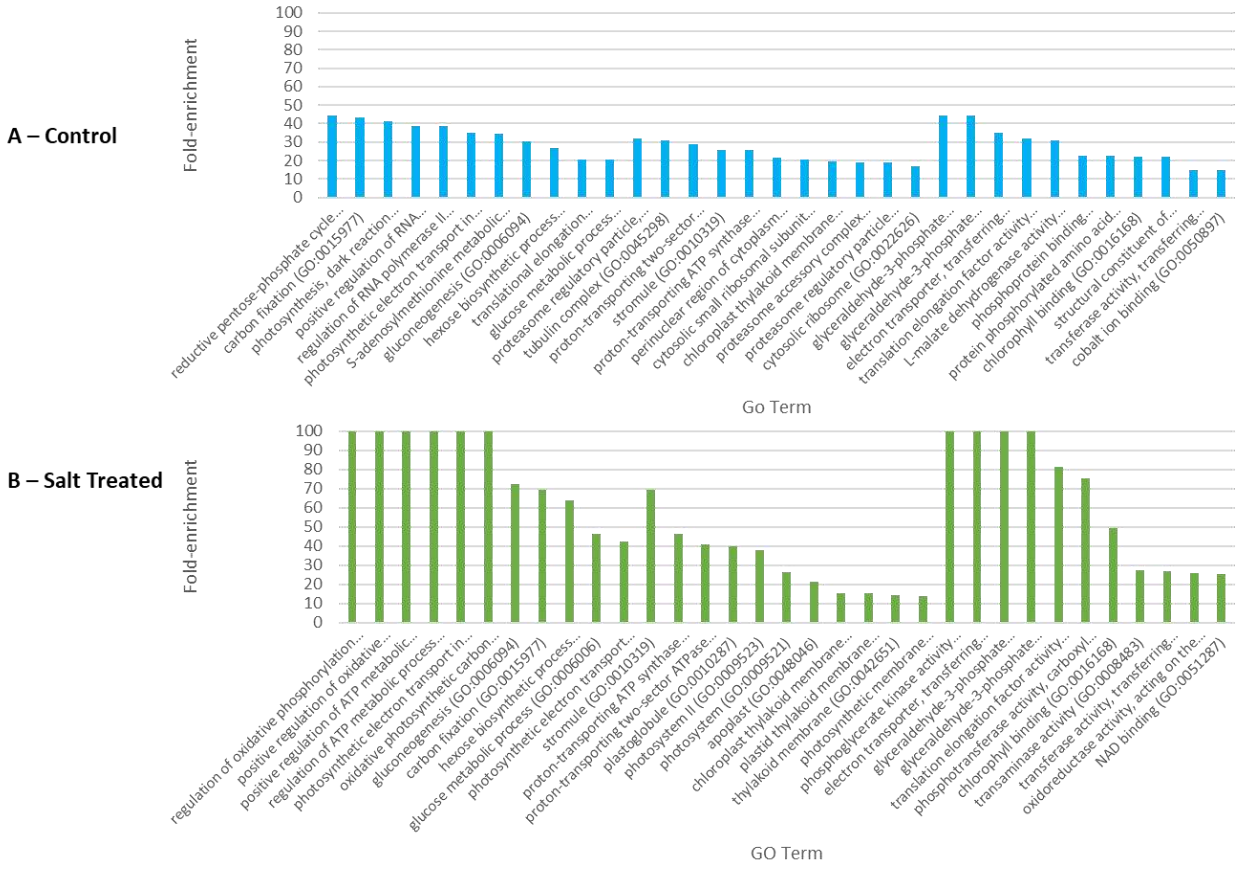

Figure 19. GO Term Enrichment

GO Term enrichment analysis was performed using TAIR (https://www.arabidopsis.org/) on proteins identified from the salt-treated samples and those identified from the control samples using biological process, molecular function, and cellular component analyses for each. The top 10 enrichment categories were selected from the results of all three analyses for both control and salt-treated. Salt treatment caused 100-fold enrichment of the following GO terms: regulation of oxidative phosphorylation (GO:0002082), positive regulation of oxidative phosphorylation (GO:1903862), positive regulation of ATP metabolic process (GO:1903580), regulation of ATP metabolic process (GO:1903578), photosynthetic electron transport in photosystem II (GO:0009772), oxidative photosynthetic carbon pathway (GO:0009854), phosphoglycerate kinase activity (GO:0004618), electron transporter, transferring electrons within the cyclic electron transport pathway of photosynthesis activity (GO:0045156), glyceraldehyde-3-phosphate dehydrogenase (NAD^+) (phosphorylating) activity (GO:0004365), and glyceraldehyde-3-phosphate dehydrogenase ($NAD(P)^+$) (phosphorylating) activity (GO:0043891).

3.4 Relative Prevalence of Candidate RBPs Under Salt Stress

Enrichment of proteins in each of the treated samples over the control was calculated as a ratio of the protein prevalence (calculated as the percentage of peptides identified from that protein out of the total number of Arabidopsis peptides in the sample) in the treated sample by the protein prevalence in the control sample. The enrichment ratios of the replicate samples (Control and WT-MS2-Na) were then averaged and the standard deviations calculated using Microsoft Excel's StDev function. These criteria identified 72 proteins, with a maximum enrichment ratio of 215, but the majority of these proteins were not identified reproducibly. To determine reproducibility, proteins were scored according to their standard deviation and enrichment ratio; proteins were selected according to the following formula:

$$Reproducible\ if\ (average\ enrichment\ ratio - standard\ deviation) > 0$$

This formula identified 17 proteins as reproducibly enriched either in the control or treated samples. Within this group, 15 were enriched in the control over the salt treated samples and 2 were enriched in the WT-MS2-Na sample over the control: GDH2 (2.1 enrichment ratio) and rbcL (3.3 enrichment ratio) (Fig. 20). Between the exclusive and enriched datasets, three members of the PYK10 complex (which is highly expressed in seeds and seedlings), including PYK10/BGLU23, were identified in the control sample. The rest of the control-enriched cohort was made up of metabolic enzymes.

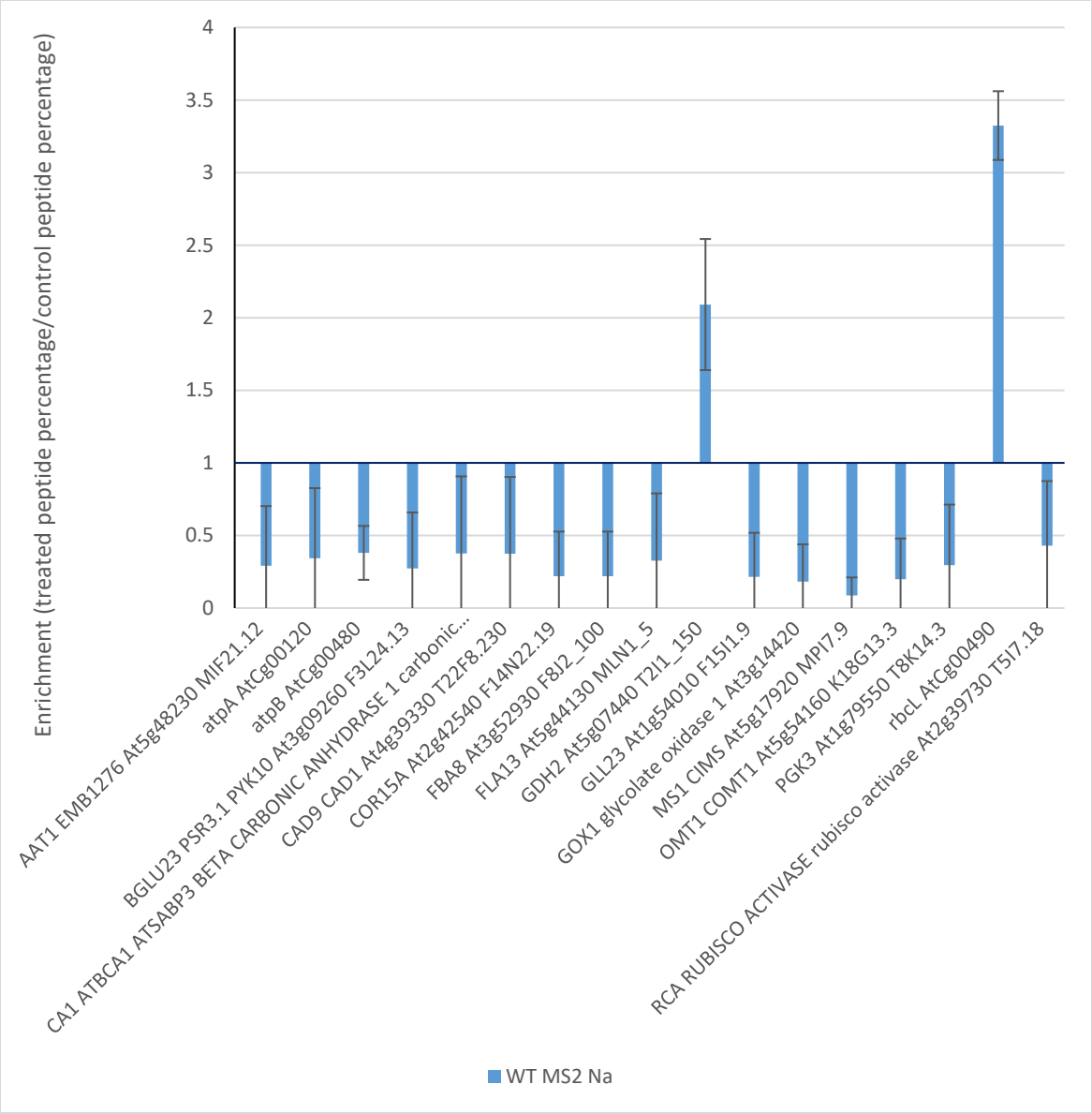

Figure 20. Reproducible Protein Enrichment

Reproducibly enriched proteins from the control and WT-MS2-Na samples. Proteins were selected based on the standard deviation of enrichment in the WT-MS2-Na sample; if the standard deviation was less than the absolute value of the enrichment ratio, protein enrichment as considered to be reproducible. 15 proteins were identified as reproducibly enriched in the control samples, whereas only 2 proteins (GDH2 and rbcL) were identified as reproducibly enriched in the WT-MS2-Na samples.

The two proteins found enriched in the WT-MS2-Na sample were glutamate dehydrogenase 2 and RuBisCo large chain, both multimeric organellar (mitochondrial and plastid) metabolic enzymes. GDH2 is a nuclear-encoded protein that oligomerizes with other GDHs to form a mixture of hexameric isoenzymes that function in nitrogen metabolism, catalyzing the reversible deamination of glutamate that yields 2-oxoglutarate (Fontaine et al., 2006; Grzechowiak et al., 2020). I also identified GDH1 under salt stress in the exclusive dataset, but it was only detected in one experiment and thus was not considered for detailed analysis. The GDH isoform 1was downloaded from RCSB Protein Data Bank (https://www.rcsb.org/structure/6YEH) and analyzed in PyMol as a scaffold for the GDH2 primary sequence for visualization (see Figure 21), and motifs were identified using Motif Finder (https://www.genome.jp/tools/motif/). GDH2 is composed of an NAD-binding catalytic domain (green) that contains a Rossmann fold and an oligomerization domain (yellow) (Fig. 21).. Within the NAD-binding catalytic domain is an EF-hand motif known to bind calcium and modulate the enzyme's activity in response (Grzechowiak et al., 2020). There are 6 cysteines in the primary structure of GDH2 and their positions were probed in PyMol for the possibility of disulfide bonds, but although two pairs are closely positioned to potentially form a disulfide bond, the hypothetically-paired sulfur atoms of both sets are more distant (4 A and 8 A) than the standard for disulfide bond length (2.05 A).

RbcL is one of the components of the well-known and ubiquitous chloroplast enzyme ribulose bisphosphate carboxylase (RuBisCo), which plays the key role in photosynthesis carbon fixation. In Arabidposis, RuBisCo is made up of eight large subunits (rbcL) encoded in the chloroplast genome and eight small subunits (rbcS) encoded in the nuclear genome (Yosef et al., 2004).

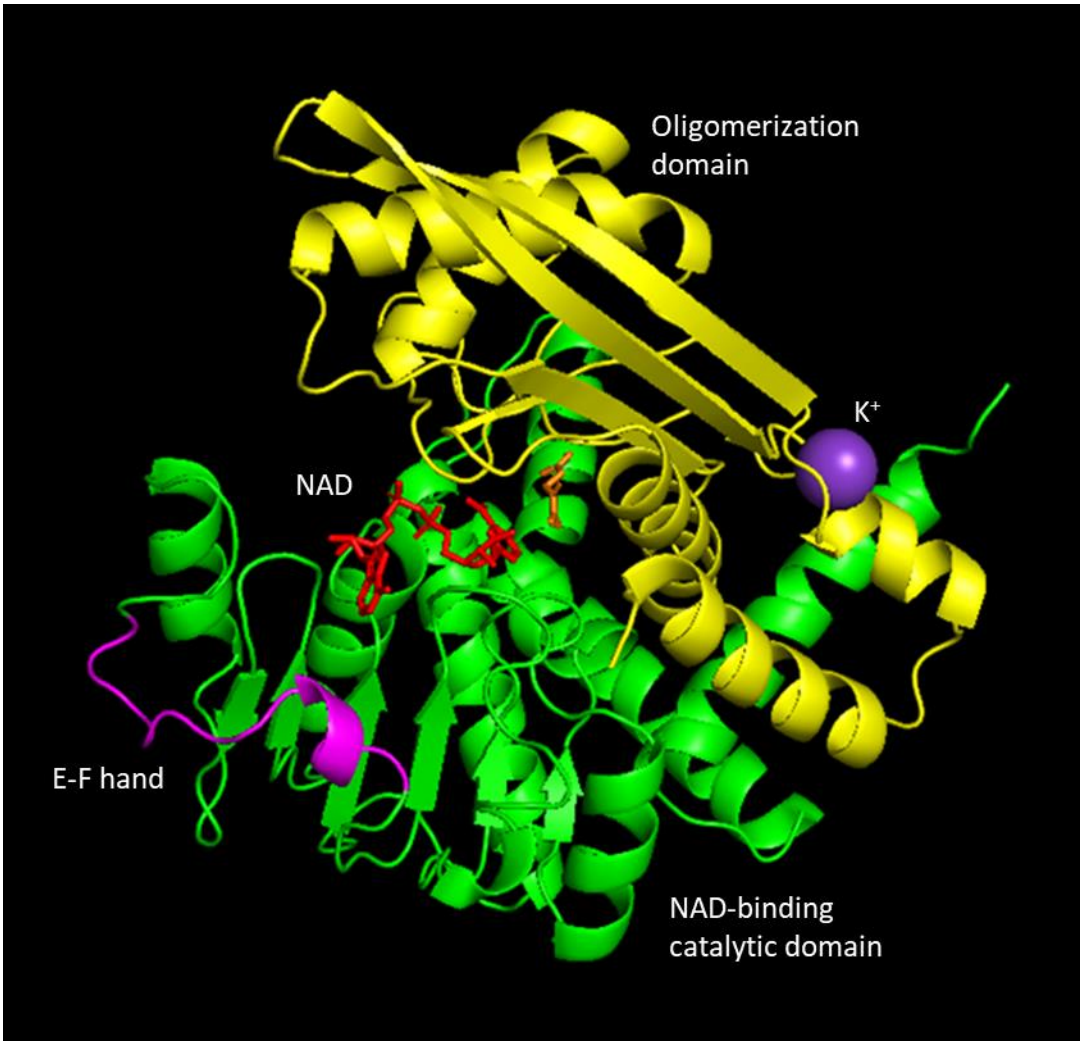

Figure 21. Secondary Structure of GDH2 in Complex with NAD^+ and 2-oxoglutarate

The secondary structure of GDH2 was downloaded from the RCSB Protein Database and color annotated in PyMol. Yellow – oligomerization domain; green – NAD-binding catalytic domain; magenta – calcium-responsive EF-hand motif; purple – K^+; red – NAD^+; orange – 2-oxoglutarate.

RuBisCo is one of the most highly expressed proteins in plants (up to 50% of total proteins). I also identified RuBisCo Small chain (rbcS) in both the exclusive dataset and the enriched dataset, and RuBisCo Activase in the enriched dataset. The primary sequence of rbcL is about 2.6 times longer than rbcS, and I identified rbcL peptides in my salt-treated samples at an average prevalence of 13 times those of peptides of rbcS. RuBisCo Activase was reproducibly enriched in the control samples over the salt-treated samples.

3.5 Subcellular Localizations of All Identified Proteins

Having noticed that my samples included some proteins of interest that are typically localized to the organelles rather than the cytoplasm, I performed a prediction of the subcellular localizations of my identified proteins using LocTree3 (https://rostlab.org/services/loctree3/). Comparing the predicted subcellular localizations for the whole *Arabidopsis* proteome to the predicted localizations for all proteins I identified, those enriched in the control samples, and those enriched in the salt-treated samples, I observed that cytoplasmic proteins were underrepresented in the salt-treated samples, and that organellar (mitochondrial and plastid-localized) proteins were overrepresented (Fig. 22). This is true with respect to the control-enriched subset, all proteins identified by my experiments, and to the whole proteome prevalence for cytoplasmic, mitochondrial, and chloroplastic proteins.

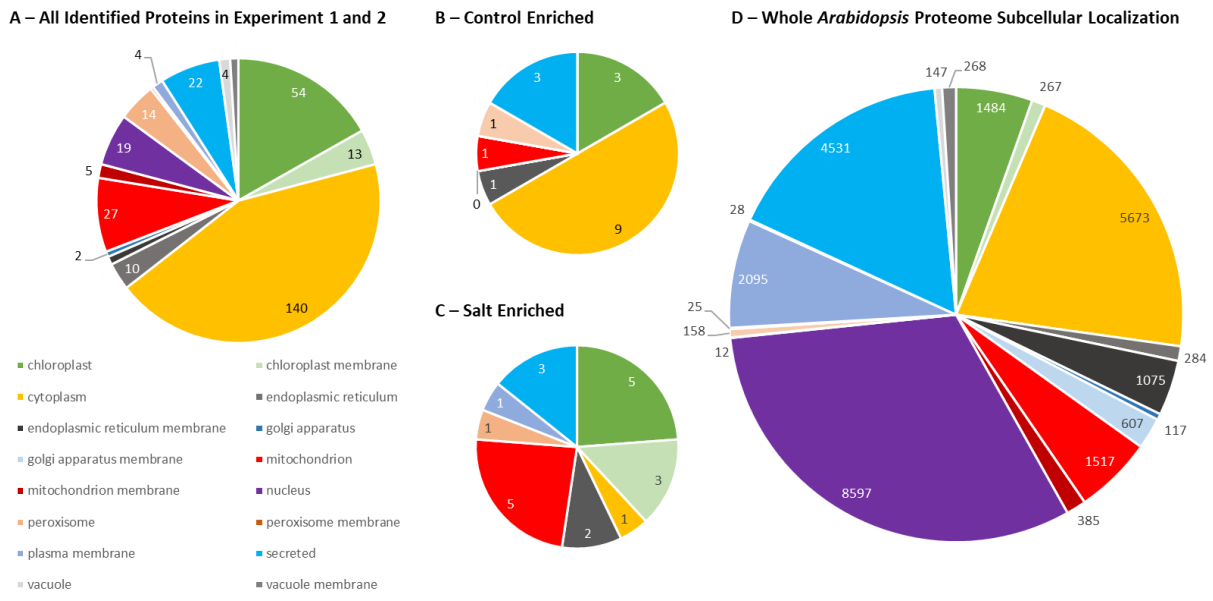

Figure 22. Predicted Subcellular Localizations of Identified Proteins

Proteins subcellular localization was predicted using LocTree3 (https://rostlab.org/services/loctree3/). **A)** Localization of proteins identified in any sample with a reviewed UniProt entry (322 proteins out of 370). **B)** Localization of proteins enriched reproducibly in control samples. **C)** Localization of proteins enriched under salt stress. D) Localization of the entire Arabidopsis proteome.

4. Discussion

4.1 GDH2 and rbcL May Bind *SR1* mRNA Under Salt Stress

My data show that out of 72 proteins identified in the enriched dataset, only GDH2 and rbcL are reproducibly enriched in the WT-MS2-Na sample, at rates of ~2 times over the control (GDH2) and ~3.5 times over the control (rbcL). I also detected other proteins known to interact with GDH2 or rbcL: GDH1, which forms an isoenzyme with GDH2, rbcS, the other subunit of the RuBisCo holoenzyme, and RuBisCo Activase, which functions to maintain the holoenzyme's activity (Grzechowiak et al., 2020; Yosef et al., 2004). Of these interacting proteins, only RuBisCo Activase was found reproducibly, and it was enriched in the control sample rather than WT-MS2-Na: these results are consistent with the interpretation that these proteins are co-purified at low rates with GDH2 and rbcL because of their interactions with those proteins, rather than because they are UV-crosslinked to SR1 mRNA. Even in the case of rbcL, which is so highly expressed that it is to be expected as a contaminant in plant proteomics, my data may not support an interpretation of its presence as background noise; if that were the case, I would expect to see rbcL appear at rates of ~2.6 times those of rbcS to reflect the two subunits' equal stoichiometry in the holoenzyme and rbcL's greater amino acid length, I would expect to see rbcL enriched in the control sample rather than the salt-treated, as I observed RuBisCo Activase to be, and I would expect its prevalence to be more variable (Fig. 23). Another possible explanation for the overrepresentation of the rbcL subunit compared to rbcS could be that the structural conformation of the holoenzyme hides rbcS while exposing rbcL during *in vivo* UV crosslinking. However, examination of the holoenzyme structure in Arabidopsis reveals that this is not the case; rbcS is superficially located on the holoenzyme, although rbcL is exposed to the surface as well (Fig. 24). These data lead me to tentatively conclude that the enrichment of

GDH2 and rbcL in my data might represent real *in vivo* binding of *SR1* mRNA but are insufficient to definitively establish such binding. More work is needed to increase confidence in this result; see section 4.2 for details on potential next steps for experimental validation of these results.

Although I cannot conclude based on my data that GDH2 and rbcL are binding *SR1* mRNA *in vivo*, a role for both proteins in RNA-binding is supported by the literature. GDH2 has long been known to have RNA-binding capabilities in humans, where it binds to the 3' UTR of liver isopeptides and may play a role in modulating mRNA expression (Preiss et al., 1995). GDH2 was also shown to play a role in RNA editing in cauliflower mitochondria *in vitro*, binding to RNA to inhibit the editing reaction, where it was hypothesized that the NAD-binding domain is likely in contact with the RNA (Takenaka et al., 2009). Takenaka et al. used competition with GDH2 cofactors NADH, NADP, NAD, and NADPH to demonstrate that GDH2 inhibits the editing reaction *in vitro* (Takenaka et al., 2009). Although these experiments used mitochondrial extracts, there is evidence that GDH2 can also be found in the cytosol under certain conditions: it was found there in senescing flowers and tissues and in companion cells of vascular tissues depending on mineral availability (Fontaine et al., 2006; Tercé-Laforgue et al., 2004). The expression and enzymatic activity of GDH2 in overexpression lines of tobacco is increased under salt stress, suggesting that GDH plays a role in salt stress response in plants (Tercé-Laforgue et al., 2015).

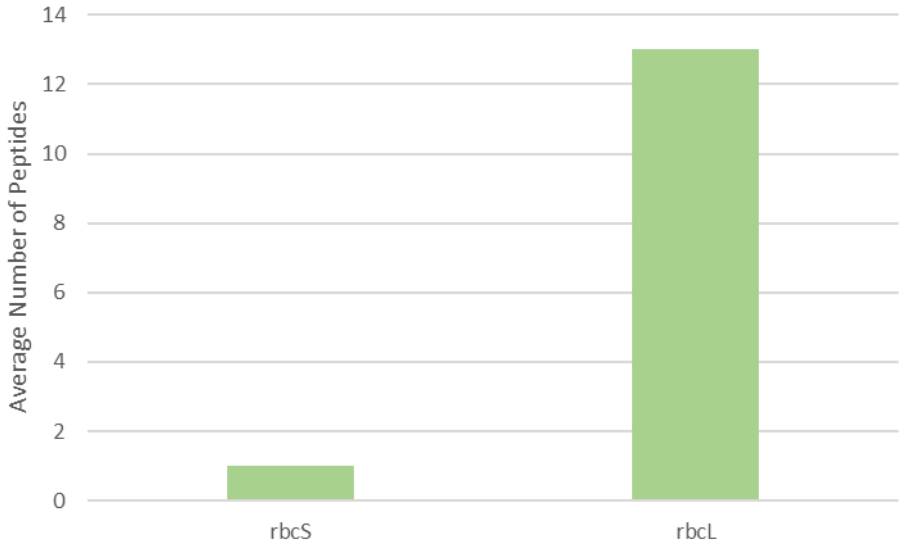

Figure 23. Average Number of RuBisCo Peptides Identified in WT-MS2-Na Samples

The average number of peptides of each of the subunits of RuBisCo (rbcS – small chain; rbcL – large chain) was calculated between experiments 1 and 2. RbcL is ~2.6 times amino acids longer than rbcS, and the two subunits exist in equal stoichiometries in the holoenzyme. The small subunit is almost entirely exposed on the surface, whereas the large subunit is partially exposed. Based on this data, I could expect a ratio of rbcL/rbcS of ~2.6. My observed ratio of rbcL/rbcS peptides was 13.

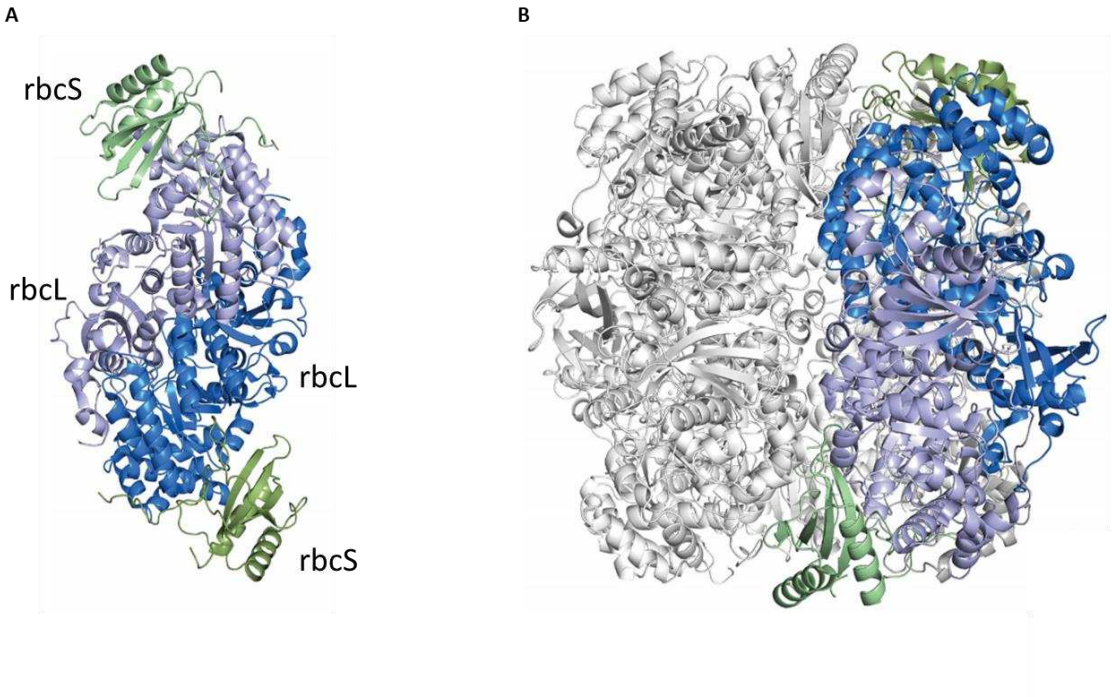

Figure 24. Crystal Structure of *Arabidopsis thaliana* RuBisCo Holoenzyme

A) Crystal structure of a RuBisCo tetramer composed of two rbcS subunits and two rbcL subunits. Tetramers form a barrel-like structure made up by the rbcL head-to-tail oriented homodimer 'capped' by the rbcS subunits. B) The holoenzyme is made up of four rbcS/rbcL tetramers. Both rbcS and rbCL are exposed on the surface of the 16-mer holoenzyme. rbcS – small subunit, green shading; rbcL – large subunit, blue shading.

RuBisCo is predominantly localized to the chloroplast where it plays a key role in photosynthesis. RbcL was shown to bind RNA nonspecifically in *Chlamydomonas reinhardtii*, where it binds its own mRNA non-specifically, possibly forming an autoregulatory loop (Yosef et al., 2004) (Fig. 25). I performed an amino acid sequence alignment between rbcL of *Arabidopsis thaliana* and *Chlamydomonas reinhardtii* (see Figure 26), which showed that despite the two species' evolutionary distance they share almost 90% sequence amino acid identity (Fig. 26). Yosef et al. also found that the amino terminal domain of rbcL had high structural similarities to RNA Binding Domains (RBDs), containing a ferredoxin-like domain, and that its RNA-binding capacity is modulated by the redox status of the cell, which induces structural changes in RuBisCo (likely mediated by the formation of disulfide bridges within the holoenzyme) that expose the amino terminal domain and allow it contact RNA (Yosef et al., 2004).

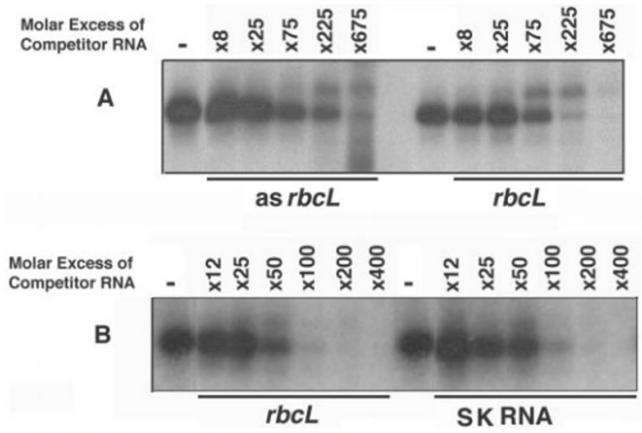

FIG. 5. **Rubisco LSU binds RNA in a sequence-independent manner.** *A*, competition with unlabeled sense and antisense *rbcL* RNAs. Purified Rubisco (25 ng) was pretreated with 2 mM GSSG and incubated with increasing amounts of competing non-labeled RNA fragments comprising sense (*rbcL*) or antisense (as-*rbcL*) RNAs before the addition of the radiolabeled *rbcL* 5′-UTR. The samples were UV-cross-linked, treated with RNase A, and resolved on 15% SDS-PAGE. *B*, competition with SK RNA and with the sense *rbcL* RNA. Purified Rubisco (25 ng) was pretreated with 2 mM GSSG and incubated with increasing amounts of competing non-labeled RNA fragments comprising the sense (*rbcL*) or SK RNA before the addition of radiolabeled *rbcL* 5′-UTR. The samples were treated as described in *A*.

Figure 25. Non-specific RNA Binding of RuBisCo Large Subunit

Reproduced from Yosef et al., 2004.

Figure 26. Alignment of rbcL Amino Acid Sequences from *Chlamydomonas reinhardtii* and *Arabidopsis thaliana*

I performed sequence alignment between the rbcL amino acid sequences from *C. reinhardtii* and *A. thaliana* using CLUSTALW multiple sequence alignment. This revealed 88.42% sequence identity between the two rbcLs' amino acid sequences. Amino acid sequences were downloaded from UniProt (www.uniprot.org/). Per Yosef et al., 2004, the 150 amino acids at the N-terminal are responsible for non-specific RNA binding by *Chlamydomonas reinhardtii* rbcL.

4.2 Models of Possible Biological Significance of *SR1* mRNA Binding to GDH2 and/or rbcL

I propose that if these interactions are real, then under salt stress-induced redox fluctuations, new disulfide bonds or other protein modifications triggered by ROS are created in both RuBisCo and GDH2. These modifications result in binding of *SR1* mRNA at the 3' end, thereby protecting the mRNA from deadenylation-mediated degradation and resulting in increased stability (Fig. 9). In the case of rbcL, these conformational changes likely result in the exposure of the amino terminal, allowing it to bind RNA nonspecifically, as was previously proposed (Yosef et al., 2004). In GDH2, the nature of the conformational changes is unknown, although I did observe that it has two pairs of cysteine residues that - although apparently not part of disulfides in the structure found in the Protein Database - are seemingly poised to form disulfides under redox conditions. It was shown that *SR1* mRNA accumulation was mediated by redox status, and that NADPH oxidase responded to Ca^{2+} fluctuations induced by salt stress to generate ROS but that SR1 protein levels do not show a corresponding increase (Abdel-Hameed et al., 2020). In this model, I postulate that rbcL and GDH2 bind to the 3' end of *SR1* because it was shown that 500 nucleotides at the 3' end were necessary for salt-induced stability (Abdel-Hameed et al., 2020). Many metabolic enzymes have been observed to 'moonlight' as RBPs under certain conditions, and a broad link between metabolism and RNA status has been hypothesized. RbcL was identified as an RBP in two RBPome study using the RIC and ptRIC methods, along with other components of photosynthesis (Zhang et al., 2016; Bach-Pages et al., 2020). Although it is possible that this finding is indeed artifactual, the authors of this study were able to perform in-depth statistical analysis, and their experimental design included a larger number of biological replicates than ours. Furthermore, the ptRIC approach uses stringent washing conditions, including protein denaturation, which preclude the post-lysis formation of ribonucleoprotein

complexes (Bach-Pages et al., 2020). Even so, their classification of rbcL as an RBP does not necessarily mean that *SR1* mRNA is one of its targets; RIC is a global approach, so rbcL in their data could have been interacting with any RNA due to its non-specific binding, as was shown previously in algae (Yosef et al., 2004). GDH2 was not previously identified as an RBP in RIC studies (Castello et al., 2015; Reichel et al., 2015; Marondedze et al., 2016).

If my data does represent real *in vivo* binding of *SR1* by rbcL and GDH2, it raises significant questions regarding the localization of the *SR1* mRNA under salt stress. Both GDH2 and rbcL are organellar proteins, localized to the mitochondria and plastid respectively, and in the case of rbcL this localization is almost exclusive except during autophagy-mediated degradation; I could find nothing in the literature showing that RuBisCo is localized to the cytoplasm under any conditions. The localization of *SR1* mRNA has not been tested, but because the SR1 protein is localized to the nucleus under most circumstances, I would expect *SR1* mRNA to be cytosolic. Certainly, an organellar localization for *SR1* mRNA, as suggested if *in vivo* interactions with rbcL and GDH2 were to be proven, and to have any physiological significance, would be a surprising result.

I have constructed three theories that provide theoretically plausible biological explanations of the observed rise in *SR1* mRNA level in response to salt stress and binding of these unexpected metabolic enzymes. All three posit that changes occur in response to a flux of reactive oxygen species in response to salt stress (Fig. 27). First, it is possible that the interaction occurs in the vacuole: under ROS, autophagy targets mitochondria, chloroplast, and stress granules (of which *SR1* mRNA has been posited to be a component) to the vacuole for degradation. Non-specific

RNA binding on the part of GDH2 and rbcL, taking place after ROS-triggered conformational changes in those proteins, could provide temporary protection against RNA degradation while in the vacuole, leading to a spike in *SR1* mRNA levels under salt stress that lasts until the proteins protecting it by happenstance are degraded themselves. This explanation would suggest that the accumulation of *SR1* mRNA under salt stress is not of physiological significance.

Second, *SR1* mRNA could be localized to the mitochondria and chloroplast under salt stress and binding by GDH2 and rbcL take place there. Although not well-studied, it has been demonstrated that nuclear mRNA can be transported into the plastid, as with the translation initiation factor 4e in four different species (Nicolai et al., 2007). If this were to be the case for *SR1* mRNA, there are possible explanations for such behavior and binding with GDH2 and rbcL. First, as there is limited evidence to suggest that GDH2 may play a role in the regulation of mitochondrial RNA editing via RNA binding, *SR1* mRNA could act as a competitor for GDH2 binding and thereby impact editing in the mitochondria. Second, rbcL is known to bind RNA nonspecifically, including its own transcript, and it has been hypothesized that it may form an autoregulatory loop. *SR1* mRNA in the chloroplast could compete with other rbcL targets and impact chloroplastic gene regulation. This would provide a physiological role for *SR1* mRNA that explains its accumulation under salt stress despite the fact that I observe no concomitant accumulation of the SR1 protein.

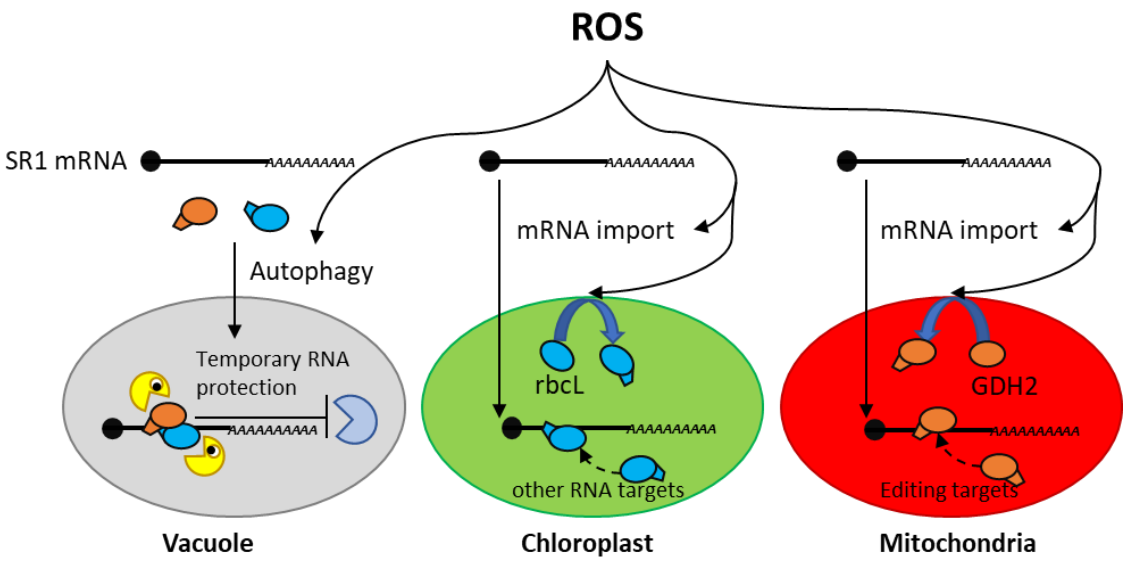

Figure 27. Autophagy and RNA-Target Competition Model of *AtSR1* mRNA Regulation Under Salt Stress Mediated by Reactive Oxygen Species

Possible explanations of observed *SR1* mRNA binding by GDH2 and rbcL under salt stress. In response to ROS, autophagy could target mitochondria, chloroplasts, and stress granules containing *SR1* mRNA to the vacuole for degradation, wherein *SR1* mRNA could be temporarily protected from degradation by non-specific binding by GDH2 and rbcL. Alternatively, *SR1* mRNA could be imported into the organelles in response to ROS, impacting gene regulation via RNA editing (in mitochondria, regulated partially by GDH2) and RNA-binding regulation (in chloroplast) by competing for rbcL and GDH2 binding (Yosef et al., 2004; Takenaka et al., 2009).

Third, *SR1* mRNA could play a role in stabilizing organellar liquid-liquid phase separation (LLPS). LLPS involves condensation of molecular components into phase-separated droplets within cellular compartments for the purpose of locally concentrating components of a cellular process. There are several reasons why this could be a viable explanation for my results. First, LLPS is known to concentrate mRNA during translation in response to stress, as in the case of stress granules and p-bodies (Feng et al., 2019). Although this concentration of mRNA is often thought of as being for the purpose of translational repression, in neuronal cells translation has been observed to occur within RNP granules (Tatavarty et al., 2012; Yasuda et al., 2013; Shi and Barna, 2015). Second, RNA and RBPs participate in LLPS in multiple systems, including in RuBisCo condensates in algal chloroplasts (Feng et al., 2019). In *Chlamydomonas reinhardtii,* rbcL assembles into chloroplastic stress granules during oxidative stress (Uniacke and Zerges, 2008). Third, RuBisCo translation is stymied by oxidative stress, which is a secondary signal of salt stress (Xiong et al., 2017). Fourth, LLPS has been demonstrated to be affected by conformational changes induced by ROS, such as those that may induce exposure of rbcL's RNA binding domain (Reed and Hammer, 2018; Yosef et al., 2004; Cohen et al., 2005). Fifth, one of the means by which salt causes stress in plants is via ionic imbalance; although the mechanistic pathway of this stress is poorly understood, it is likely that electrostatic interactions in the cell are disrupted by changes in the ionic strength of the solution, and it has been hypothesized that salt stress may cause the dissolution of cellular condensates such as those involved in translation (Emenecker et al., 2020; Zhao et al., 2020).

With these facts in mind, I propose the following model (Fig. 28). Upon salt stress, ionic imbalance impedes translation in the chloroplast and other organelles by interfering with electrostatic interactions and dissolving translational condensates. In response, cytosolic RNAs such as *SR1* are imported into the organelles as partners for metabolic enzymes with moonlighting RBP properties, such as rbcL and GDH2, in stabilizing translational condensates. These moonlighting RBPs undergo conformational changes due to ROS which augment their RNA-binding capabilities; in the case of rbcL, conformational changes expose the amino terminal for RNA binding. For the example of *SR1* mRNA, binding likely occurs at the 3' end of the mRNA, due to that region's significance in *SR1* accumulation and increased stability under salt stress. The newly formed ribonucleoproteins stabilize the translational condensates and thus facilitate translation within the droplet. By this means, the repression imposed by salt stress on translation of key metabolic enzymes is alleviated.

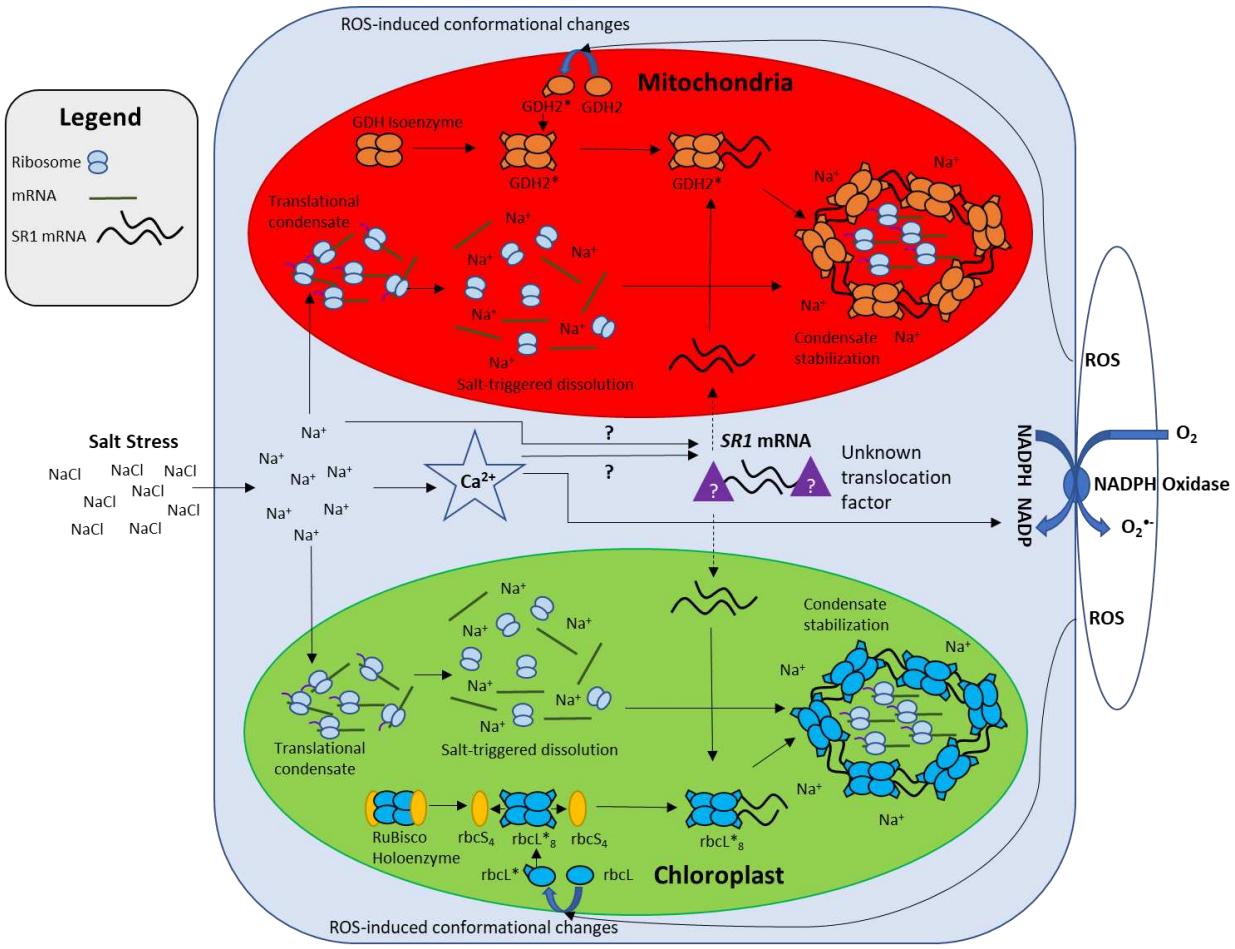

Figure 28. Liquid-liquid Phase Separation Model of *AtSR1* mRNA Regulation Under Salt Stress

Ionic imbalance induced by salt stress may dissolve translational condensates in organelles such as chloroplasts and mitochondria, impeding organellar translation and thus metabolism. In my proposed model, calcium-triggered ROS generation induces conformational changes in metabolic enzymes such as those I identified, rbcL and GDH2, which expose RNA-binding domains. Simultaneously, salt stress triggers translocation of RNA from the cytosol to the organelles, such as SR1 mRNA, via unknown translocation factors and possibly mediated by calcium signaling. In the organelles, these imported RNAs become bound by the newly exposed RNA-binding domains of moonlighting metabolic enzymes such as rbcL and GDH2, helping to stabilize translational condensates destabilized by ionic imbalance and thus to maintain organellar translation necessary for metabolism. Thus, LLPS mediated by *SR1* mRNA and the moonlighting metabolic enzymes rbcL and GDH2 help maintain cellular homeostasis during abiotic stress.

This model fits my observations and those from the literature in many respects. First, it explains why *SR1* mRNA accumulates under salt stress, even though I see no concomitant accumulation of *SR1* protein (Abdel-Hameed et al., 2020). Second, it explains the role of ROS in mediating this accumulation of *SR1* mRNA. Third, it fits the observation of nonspecific RNA binding by rbcL in algae; in this model, *SR1* would be just one of many RNAs being imported into the organelles for binding by plastid and mitochondrial moonlighting RBPs. Fourth, it was already suggested that *SR1* mRNA is localized to stress granules, which are a form of cytosolic translational condensate; this model only alters that suggestion in the subcellular localization of the droplets to which *SR1* is targeted (Abdel-Hameed et al., 2020). Fifth, multivalent proteins and ions play roles in stabilizing cellular condensates, and both GDH2 and rbcL exist as multimeric metabolic enzymes (Feng et al., 2019). Data in contradiction of this model would be anything showing that *SR1* mRNA does not localize to the chloroplast and mitochondria during salt stress, but this data does not yet exist and nothing is known about the localization of *SR1* mRNA.

4.3 Possible Experimental Follow-up to Validate GDH2/rbcL Binding of SR1 mRNA

Because of the surprising nature of the two possible RBPs identified by my data, validation of these results by at least two other experimental approaches is required before I could confidently conclude that they are true RBPs binding *SR1* mRNA. One approach of interest would be yeast-three-hybrid; because this method uses MS2-tagged RNA, it would be easy to carry out using my existing *3x-FLAG-SR1-MS2* construct. In such an experiment, I would test interaction of *SR1* full length mRNA and the *SR1* 3' ~500 bp fragment shown to be sufficient for RNA accumulation

with GDH2 full length, rbcL full length, and rbcL putative RNA binding domain (amino acids 1-150) in the presence and absence of ROS (Fig. 29). This would demonstrate three things: first, whether any binding between *SR1* mRNA and GDH2/rbcL occurs; second, whether the 3' end of *SR1* mRNA is the target of mRNA binding or if its significance comes from some other role, such as targeting the mRNA for organellar import; and third, whether RNA binding by GDH2/rbcL is activated by ROS. This would provide evidence for or against many aspects of the models I have suggested. However, it should be noted that because of RuBisCo's extensive list of chaperones and other partners required for its proper folding, care would need to be given in the design of the experiment to ensure that the yeast expression construct could generate properly folded rbcL.

Another technique of interest would be to perform a gel-shift assay with *SR1* full-length and *SR1* 3' ~500 bp mRNA and GDH2/rbcL. This has the advantage of not requiring expression of rbcL in a heterologous system that risks improper folding; rbcL extracted from WT Arabidopsis plants could be used instead. Similarly to the aforementioned experiment, GDH2/rbcL could be treated with ROS prior to gel shift assay to test the role of ROS-induced conformational changes in RNA binding. Indeed, GDH2 and rbcL isolated from salt-treated plants could also be used. This experiment would provide evidence for or against the binding of *SR1* mRNA by GDH2/rbcL, and for or against ROS-activation of this binding, if it exists.

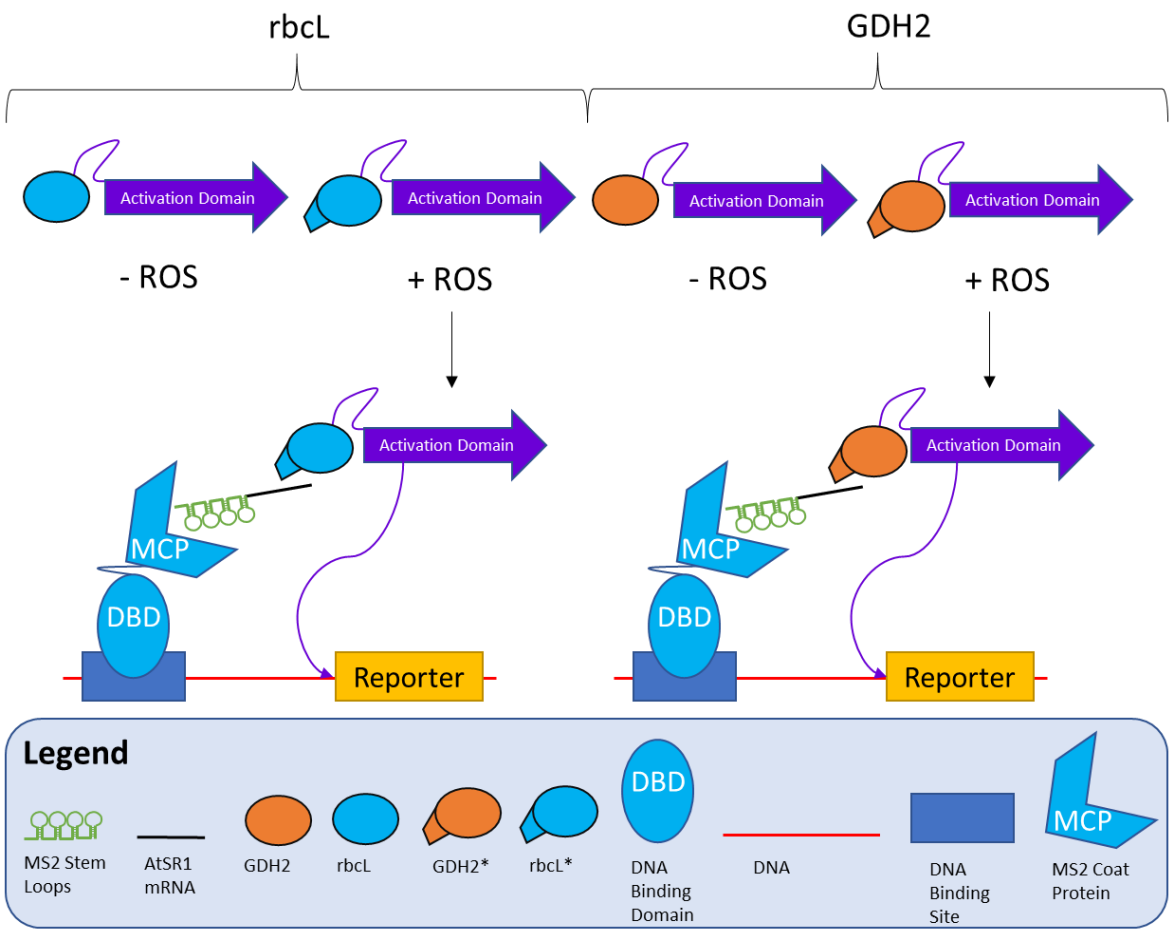

Figure 29. Yeast Three-Hybrid Experimental Design

Diagrammatic representation of a potential design of a yeast three-hybrid experiment to test the interactions of GDH2/rbcL with *SR1*. Two fusion proteins (MCP fused to a DNA binding domain, and our protein of interested fused to a reporter activation domain) would be expressed in yeast, along with *SR1-MS2*, in the presence and absence of ROS to test the role of ROS-induced conformational changes in the proteins of interest in RNA binding. Activation of the reporter gene would indicate binding of *SR1-MS2* by our protein of interest.

In addition to these experiments, it is of great interest to explore the subcellular localization of *SR1* mRNA with and without salt stress (Fig. 30). The transgenic lines that I generated express SR1 tagged with both FLAG (at the amino terminal of the SR1 protein) and MS2 (in the 3' UTR of the *SR1* mRNA). This would allow us to simultaneously probe the localizations of SR1 protein and *SR1* mRNA under salt stress. By transiently expressing a fusion construct of MCP-GFP in leaves treated also with anti-FLAG conjugated to a fluorophore, I could use fluorescence microscopy to visualize the dynamics of SR1 protein and mRNA localization upon treatment with salt. If I observed localization of SR1 mRNA to the chloroplast and mitochondria upon salt treatment, this would be strong evidence that GDH2/rbcL can act as RBPs for SR1 and would corroborate some aspects of my models. Furthermore, I could visualize these localizations in the presence and absence of agents that interfere with RNA gelation to test the possibility that *SR1* mRNA bound by GDH2/rbcL plays a role in LLPS.

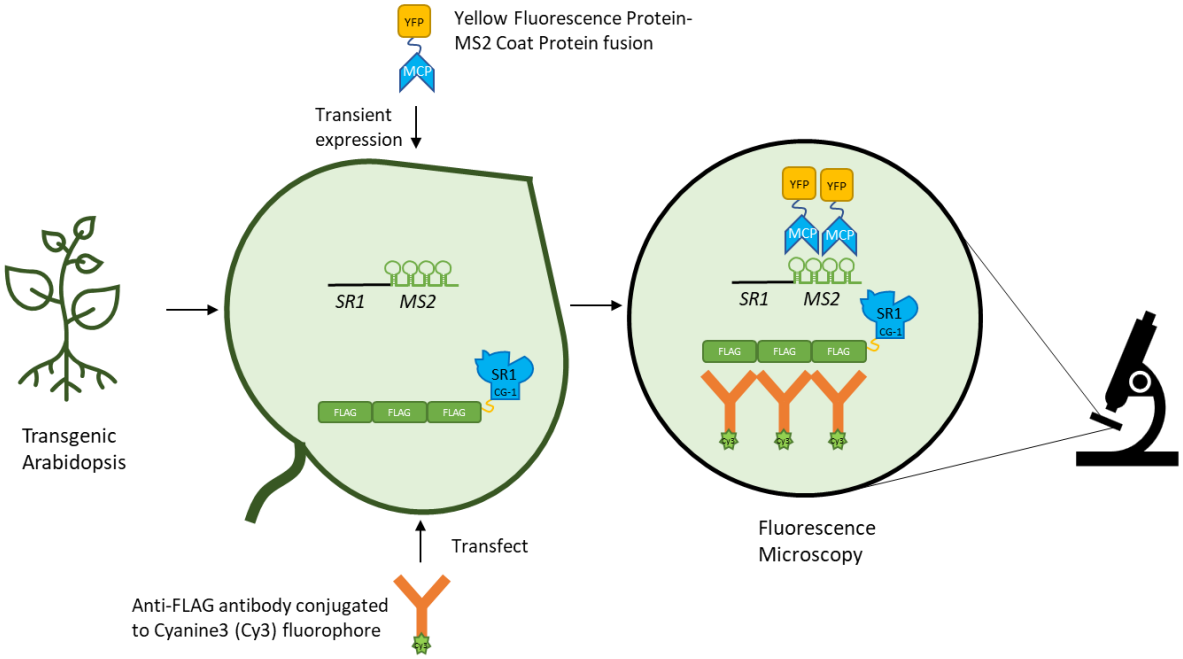

Figure 30. Visualization of *SR1* Localization via Transient Expression.

Transgenic Arabidopsis expressing *3x-FLAG-SR1-MS2* would be transfected with anti-FLAG antibody conjugated to the Cyanine3 (Cy3) fluorophore and a vector encoding yellow fluorescence protein (YFP) fused to MCP. Anti-FLAG would colocalize the Cy3 fluorophore signal with the FLAG repeats at the N-terminal of my SR1 fusion protein, and MCP would colocalize YFP with the MS2 repeats of my *SR1-MS2* mRNA. Via fluorescence microscopy, I would determine the subcellular localization of 3xFLAG-SR1 and *SR1-MS2* in the presence and absence of salt, and the presence and absence of ROS.

BIBLIOGRAPHY

Abdel-Hameed, A., Prasad, K., Jiang, Q., Reddy, A., 2020. Salt-Induced Stability of SR1/SR1 mRNA Is Mediated by Reactive Oxygen Species and Requires the 3' End of Its Open Reading Frame. Plant Cell Physiol. 61: 748-760.

Acqaah, G., 2009 Principles of Plant Genetics and Breeding. Wiley.

Albaqami, M., Laluk, K., Reddy, A., 2019. The Arabidopsis splicing regulator SR45 confers salt tolerance in a splice isoform-dependent manner. Plant Mol. Biol.. 100: 379-390.

Allis, C., Jenuwein, T., 2016 The molecular hallmarks of epigenetic control. Nature Reviews. 17: 487-500.

Ambrosone, A., Batelli, G., Nurcato, R., Aurilia, V., Punzo, P., Bangarusamy, D., Ruberti, I., Sassi, M., Leone, A., Costa, A., Grillo, S., 2015. The Arabidopsis RNA-Binding Protein AtRGGA Regulates Tolerance to Salt and Drought Stress. Plant Physiol.. 168: 292-306.

Arribas-Hernández, L., Bressendorff, S., Hansen, M., Poulsen, C., Erdmann, S., Brodersen, P., 2018. An m6A-YTH Module Controls Developmental Timing and Morphogenesis in Arabidopsis. The Plant Cell. 30: 952-967.

Babu, Y., Bugg, C., Cook, W., 1988. Structure of calmodulin refined at 2.2 Å resolution. J. Mol. Biol. 204: 191-204.

Bach-Pages, M., Castello, A., Preston, G., 2017. Plant RNA Interactome Capture: Revealing the Plant RBPome. Trends Plant Sci.. 22(6): 449-451.

Bach-Pages, M., Homma, F., Kourelis, J., Kaschani, F., Mohammed, S., Kaiser, M., van der Hoorn, R., Castello, A., Preston, G., 2020. Discovering the RNA-Binding Proteome of Plant Leaves with an Improved RNA Interactome Capture Method. Biomolecules. 10: 661.

Bardou, F., Ariel, F., Simpson, C., Romero-Barrios, N., Laporte, P., Balzergue, S., Brown, J., Crespi, M., 2014. Long Noncoding RNA Modulates Alternative Splicing Regulators in Arabidopsis. Developmental Cell. 30: 166-176.

Barkan, A., Small, I., 2014. Pentatricopeptide Repeat Proteins in Plants. Annu. Rev. Plant Biol.. 65: 415-442.

Bazin, J., Romero, N., Rigo, R., Charon, C., Blein, T., Ariel, F., Crespi, M., 2018. Nuclear Speckle RNA Binding Proteins Remodel Alternative Splicing and the Non-coding Arabidopsis Transcriptome to Regulate a Cross-Talk Between Auxin and Immune Responses. Frontiers of Plant Science. 9: 1209.

Ben Saad, R., Ben Halima, N., Ghorbel, M., Zouari, N., Ben Romdhane, W., Guiderdoni, E., Al-Doss, A., Hassairi, A., 2018. AlSRG1, a novel gene encoding an RRM-type RNA-binding protein (RBP) from Aeluropus littoralis, confers salt and drought tolerance in transgenic tobacco. Environmental and Experimental Botany. 150: 25-36.

Benn, G., Wang, C., Hicks, D., Stein, J., Guthrie, C., Dehesh, K., 2014. A key general stress response motif is regulated non-uniformly by CAMTA transcription factors. The Plant Journal. 80: 82-92.

Berridge, M., Bootman, M., Roderick, H., 2003. Nature Reviews. 4: 517-529.

Berridge, M., Lipp, P., Bootman, M., 2000. The Versatility and Universality of Calcium Signaling. Nature Reviews. 1: 11-21.

Bird, J., Basu, U., Kuster, D., Ramachandran, A., Grudzien-Nogalska, E., Towheed, A., Wallace, D., Kiledjian, M., Temiakov, D., Patel, S., Ebright, R., Nickels, B., 2018. Highly efficient 5' capping of mitochondrial RNA with NAD^+ and NADH by yeast and human mitochondrial RNA polymerase. eLife. 7: 42179.

Bird, J., Zhang, Y., Tian, Y., Panova, N., Barvik, I., Greene, L., Liu, M., Buckley, B., Krásny, L., Lee, J., Kaplan, C., Ebright, R., Nickels, B., 2016. The mechanism of RNA 5′ capping with NAD^+, NADH and desphospho-CoA. Nature. 535: 444-447.

Bjornson, M., Benn, G., Song, X., Comai, L., Franz, A., Dandekar, A., Drakakaki, G., Dehesh, K., 2014. Distinct Roles for Mitogen-Activated Protein Kinase Signaling and CALMODULIN-BINDING TRANSCRIPTIONAL ACTIVATOR3 in Regulating the Peak Time and Amplitude of the Plant GeneralStress Response. Plant Physiology. 166: 988-996.

Boccaletto, P., Machnicka, M., Purta, E., Piatkowski, P., Bagínski, B., Wirecki, T., de Crécy-Lagard, V., Ross, R., Limbach, P., Kotter, A., Helm, M., Bujnicki, J., 2017. MODOMICS: a database of RNA modification pathways. 2017 update. Nucleic Acids Research. 46: D303-D307.

Boeynaems S., Alberti, S., Fawzi N., Mittag, T., Polymenidou, M., Rousseau, F., Schymkowitz, J., Shorter, J., Wolozin, B., Van Den Bosch, L., Tompa, P., Fuxreiter, M., 2018. Protein Phase Separation: A New Phase in Cell Biology. Trends in Cell Biology. 28: 420-435.

Boo, S., Kim, Y., 2020. The emerging role of RNA modifications in the regulation of mRNA stability. 52: 400-408.

Borkhsenious, O., Mason, C., Moroney, J., 1998. The Intracellular Localization of Ribulose-1,5-Bisphosphate Carboxylase/Oxygenase in Chlamydomonas reinhardtii. Plant Physiology. 116: 1585-1591.

Bouché, N., Yellin, A., Snedden, W., Fromm, H., 2005. Plant-Specific Calmodulin-Binding Proteins. Annual Review of Plant Biology. 56: 435-466.

Bouché, N.. Scharlat, A., Snedden, W., Bouchez, D., Fromm, H., 2002. A novel family of calmodulin-binding transcription activators in multicellular organisms. Journal of Biological Chemistry. 277: 21851-21861.

Bouvier, M., Carpousis, A., 2011. A tale of two mRNA degradation pathways mediated by RNase E. Molecular Microbiology. 82: 1305-1310.

Brodersen, P., Sakvarelidze-Achard, L., Bruun-Rasmussen, M., Dunoyer, P., Yamamoto, Y., Sieburth, L., Voinnet, O., 2008. Widespread Translational Inhibition by Plant miRNAs and siRNAs. 320: 1185-1189.

Cahová, H., Winz, M., Hofer, K., Nubel, G., Jaschke, A., 2015. NAD captureSeq indicates NAD as a bacterial cap for a subset of regulatory RNAs. Nature. 519: 374-376.

Campalans, A., Kondorosi, A., Crespi, M. Enod40, a Short Open Reading Frame–Containing mRNA, Induces Cytoplasmic Localization of a Nuclear RNA Binding Protein in Medicago truncatula. The Plant Cell 2004, 16:1047-1059.

Castello, A., Hentze, M., Preiss, T., 2015. Metabolic Enzymes Enjoying New Partnerships as RNA-Binding Proteins. Trends in Endocrinology and Metabolism. 26: 746-757.

Castiglioni, P., Warner, D., Bensen, R., Anstrom, D., Harrison, J., Stoecker, M., Abad, M., Kumar, G., Salvador, S., D'Ordine, R., Navarro, S., Back, S., Fernandes, M., Targolli, J., Dasgupta, S., Bonin, C., Luethy, M., Heard, J., 2008. Bacterial RNA Chaperones Confer Abiotic Stress Tolerance in Plants and Improved Grain Yield in Maize under Water-Limited Conditions. Plant Physiology. 147: 445-455.

Chen, X., Zhang, J., Zhu, J., 2019. The role of m(6)A RNA methylation in human cancer. Molecular Cancer. 18: 103.

Chu, C., Qu, K., Zhong, F., Artandi, S., Chang, H., 2011. Genomic Maps of Long Noncoding RNA Occupancy Reveal Principles of RNA-Chromatin Interactions. Molecular Cell. 44: 667-678.

Chu, C., Zhang, Q., Heard, E., Chang, H., 2015. Systematic Discovery of Xist RNA Binding Proteins. Cell. 161: 404-416.

Clapham, D., 1995. Calcium Signaling. Cell. 80: 259-268.

Cohen, I., Knopf, J., Irihimovitch, V., Shapira, M., 2005. A proposed mechanism for the inhibitory effects of oxidative stress on Rubisco assembly and its subunit expression. Plant Physiol. 137(2):738-746.

Crofts, A., Crofts, N., Whitelegge, J., Okita, T., 2010. Isolation and identification of cytoskeleton-associated prolamine mRNA binding proteins from developing rice seeds. Planta. 231: 1261-1276.

Cui P., Xiong, L., 2015. Environmental Stress and Pre-mRNA Splicing. Molecular Plant. 8: 1302-1303.

Cutler, S., Rodriguez, P., Finkelstein, R., Abrams, S., 2010. Abscisic Acid: Emergence of a Core Signaling Network. Annu. Rev. Plant Biol. 61: 651-79.

Czolpinska, M., Rurek, M., 2018. Plant Glycine-Rich Proteins in Stress Response: An Emerging, Still Prospective Story. Frontiers in Plant Science. 9: 302.

Dai, W., Chen, M., Myers, C., Ludtke, S., Pettitt, B., King, J., Schmid, M., Chiu, W., 2018. Visualizing Individual RuBisCO and its Assembly into Carboxysomes in Marine Cyanobacteria by Cryo-Electron Tomography. Journal of Molecular Biology. 430(21): 4156-4167.

Darnell, R., 2010. HITS-CLIP: panoramic views of protein-RNA regulation in living cells. Wiley Interdisciplinary Reviews of RNA. 1: 266-286.

Day, I., Reddy., V., Ali, G., Reddy., A., 2002. Analysis of EF-hand-containing proteins in Arabidopsis. Genome Biology. 3: 0056.1-0056.24.

Debiais, M., Lelievre, A., Smietana, M., Muller, S., 2020. Splitting aptamers and nucleic acid enzymes for the development of advanced biosensors. Nucleic Acids Research. 48(7): 3400-3422.

Dinh, S., Park, S., Han, J., Kang, H., 2019. A Chloroplast-targeted S1 RNA-binding Domain Protein Plays a Role in Arabidopsis Response to Diverse Abiotic Stresses. Journal of Plant Biology. 62: 74-81.

Doherty, C., Van Buskirk, H., Myers, S., Thomashow, M., 2009. Roles for Arabidopsis CAMTA Transcription Factors in Cold-Regulated Gene Expression and Freezing Tolerance. The Plant Cell. 21: 972-984.

Du, L., Ali, G., Simons, K., Hou, J., Yang, T., Reddy, A., Poovaiah, B., 2009. Ca^{2+}/calmodulin regulates salicylic-acid-mediated plant immunity. Nature. 457: 1154-1159.

Dubrovina, A., Aleynova, O., Ogneva, Z., Suprun, A., Ananev, A., Kiselev, K., 2019. The effect of Calmodulin (CaM) and Calmodulin-Like (CML) Genes in Wild-Growing Grapevine Vitis amurensis. Plants. 8: 602.

El Mahi, H., Pérez-Hormaeche, J., De Luca, Anna, Villalta, I., Espartero, J., Gámez-Arjona, F., Fernández, J., Bundó, M., Mendoza, I., Mieulet, D., Lalanne, E., Lee, S., Yun, D., Guiderdoni, E., Aguilar, M., Leidi, E., Pardo, J., Quintero, F., 2019. A Critical Role of Sodium Flux via the Plasma Membrane Na^+/H^+ Exchanger SOS1 in the Salt Tolerance of Rice. Plant Physiology. 180: 1046-1065.

Emenecker, R., Holehouse, A., Strader, L., 2020. Emerging Roles for Phase Separation in Plants. Developmental Cell. 55: 69-83.

Engreitz, J., Pandya-Jones, A., McDonel, P., Shishkin, A., Sirokman, K., Surka, C., Kadri, S., Xing, J., Goren, A., Lander, E., Plath, K., Guttman, M., 2013. The Xist lncRNA Exploits Three Dimensional Genome Architecture to Spread Across the X Chromosome. Science. 341: 1237973.

Feng, Z., Chen, X., Wu, X., Zhang, M., 2019. Formation of biological condensates via phase separation: Characteristics, analytical methods, and physiological implications. J. Biol. Chem. 294(40): 14823-14835.

Foley, S., Gosai, S., Wang, D., Selamoglu, N., Sollitti, A., Koster, T., Steffen, A., Lyons, E., Daldal, F., Garcia, B., Staiger, D., Deal, R., Gregory, B., 2017. A Global View of RNA-Protein Interactions Identifies Post-transcriptional Regulators of Root Hair Cell Fate. Developmental Cell. 41: 204-220.

Fontaine, J., Saladino, F., Agrimonti, C., Bedu, M., Tercé-Laforgue, T., Hirel, B., Restivo, F., Dubois, F., 2006. Control of the Synthesis and Subcellular Targeting of the Two GDH Genes Products in Leaves and Stems of Nicotiana plumbaginifolia and *Arabidopsis thaliana*. Plant Cell Physiology. 47(3): 410-418.

Francisco-Mangilet, A., Karlsson, P., Kim, M., Eo, H., Oh, S., Kim, J., Kulcheski, F., Park, S., Manavella, P., 2015. THO2, a core member of the THO/TREX complex, is required for microRNA production in Arabidopsis. The Plant Journal. 82: 1018-1029.

Fu, Z., Guo, M., Jeong, B., Tian, F., Elthon, T., Cerny, R., Staiger, D., Alfano, J., 2007. A type III effector ADP-ribosylates RNA-binding proteins and quells plant immunity. Nature. 447: doi:10.1038/nature05737

Fujisaki, K., Ishikawa, M., 2008. Identification of an Arabidopsis thaliana protein that binds to tomato mosaic virus genomic RNA and inhibits its multiplication. Virology. 380: 402-411.

Gagliardi, M., Matarazzo, M., 2016. RIP: RNA Immunoprecipitation. Methods in Molecular Biology. 1480: 73-86.

Galon, Y., Nave, R., Boyce, J., Nachmias, D., Knight, M., Fromm, H., 2008. Calmodulin-binding transcription activator (CAMTA) 3 mediates biotic defense responses in Arabidopsis. FEBS Letters. 582: 943-948.

Gaxiola, R., Rao, R., Sherman, A., Grisafi, P., Alper, S., Fink, G., 1999. The *Arabidopsis thaliana* proton transporters, AtNhx1 and Avp1, can function in cation detoxification in yeast. PNAS. 96: 1480-1485.

Gemmill, D., D'souza, S., Meier-Stephenson, V., Patel, T., 2020. Current approaches for RNA-labelling to identify RNA-binding proteins. Biochem. Cell. Biol. 98: 31-41.

Germain, H., Qu, N., Cheng, Y., Lee, E., Huang, Y., Dong, O., Gannon, P., Huang, S., Ding, P., Li, Y., Sack, F., Zhang, Y., Li, X., 2010. MOS11: A New Component in the mRNA Export Pathway. PLOS Genetics. 6(12): e1001250.

Gong, Z., Xiong, L., Shi, H., Yang, S., Herrera-Estrella, L., Xu, G., Chao, D., Li, J., Wang, P., Qin, F., Li, J., Ding, Y., Shi, Y., Wang, Y., Yang, Y., Guo, Y., Zhu, J., 2020. Plant Abiotic Stress Response and Nutrient Use Efficiency. Sci. China Life Sci. 63: 635-674.

Grudzien-Nogalska, E., Kiledjian, M., 2017. New insights into decapping enzymes and selective mRNAdecay. WIREs RNA. 8: 1379.

Grzechowiak, M., Sliwiak, J., Jaskolski, M., Milosz, R., 2020. Structural Studies of Glutamate Dehydrogenase (Isoform 1) From *Arabidopsis thaliana*, an Important Enzyme at the Branch-Point Between Carbon and Nitrogen Metabolism. Front. Plant Sci.. 11: 754.

Gu, L., Jung, H., Kwak, K., Dinh, S., Kim, Y., Kang, H., 2016. An RRM-containing mei2-like MCT1 plays a negative role in the seed germination and seedling growth of Arabidopsis thaliana in the presence of ABA. Plant Physiol. and Biochem.. 109: 273-279.

Guo , T., Wang, N., Xue, Y., Guan, Q., van Nocker, S., Liu, C., Ma, F., 2019. Overexpression of the RNA binding protein MhYTP1 in transgenic apple enhances drought tolerance and WUE by improving ABA level under drought condition. Plant Science. 280: 397-407.

Guo, Y., Halfter, U., Ishitani, M., Zhu, J., 2001. Molecular Characterization of Functional Domains in the Protein Kinase SOS2 That Is Required for Plant Salt Tolerance. The Plant Cell. 13: 1383-1399.

Gutiérrez, R., MacIntosh, G., Green, P., 1999. Current perspectives on mRNA stability in plants: multiple levels and mechanisms of control. Trends in Plant Science. 4: 1360-1385.

Hafner, M., Landthaler, M., Burger, L., Khorshid, M., Hausser, J., Berninger, P., Rothballer, A., Ascano, M., Jungkamp, A., Munschauer, M., Ulrich, A., Wardle, G., Dewell, S., Zavolan, M., Tuschl, T., 2010. Transcriptome-wide Identification of RNA-Binding Protein and MicroRNA Target Sites by PAR-CLIP. Cell. 141: 129-141.

Ham, B., Brandom, J., Xoconostle-Cázares, B., Ringgold, V., Lough, T., Lucas, W., 2009. A Polypyrimidine Tract Binding Protein, Pumpkin RBP50, Forms the Basis of a Phloem-Mobile Ribonucleoprotein Complex. The Plant Cell. 21: 197-215.

Han, J., Gong, P., Reddig, K., Mitra, M., Guo, P., Li, H., 2006. The Fly CAMTA Transcription Factor Potentiates Deactivation of Rhodopsin, a G Protein-Coupled Light Receptor. Cell. 127: 847-858.

Han, J., Lee, K., Lee, K., Jung, S., Jeon, Y., Pai, H., Kang, H., 2015. A nuclear-encoded chloroplast-targeted S1 RNA-binding domain protein affects chloroplast rRNA processing and is crucial for the normal growth of Arabidopsis thaliana. 83: 277-289.

Han, S., Zhao, B.S., Myers, S., Carr, S., He, C., Ting, A. RNA–protein interaction mapping via MS2- or Cas13-based APEX targeting. PNAS 2020, 117(36): 22068-22079.

He, X., Hsu, Y., Zhu, S., Wierzbicki, A., Pontes, O., Pikaard, C., Liu, H., Wang, C., Jin, H., Zhu, J., 2009. An effector of RNA-directed DNA methylation in Arabidopsis is an ARGONAUTE 4- and RNA-binding protein. Cell. 137(3): 498-508.

Helm, M., Motorin, Y., 2017. Detecting RNA modifications in the epitranscriptome: predict and validate. Nature Reviews. 18: 275-291.

Hentze, M., Kuhn, L., 1996. Molecular control of vertebrate iron metabolism: mRNA-based regulatory circuits operated by iron, nitric oxide, and oxidative stress. PNAS. 93: 8175-8182.

Hetherington, A., Brownlee, C., 2004. The Generation of Ca^{2+} Signals in Plants. Annu. Rev. Plant Biol. 55: 401-427.

Hocine, S., Singer, R., Grunwald, D., 2010. RNA Processing and Export. Cold Spring Harbor Perspectives of Biology. 2010: a000752.

Hornyik, C., Terzi, L., Simpson, G., 2010. The Spen Family Protein FPA Controls Alternative Cleavage and Polyadenylation of RNA. Developmental Cell. 18: 203-213.

Huang, H., Weng, H., Chen, J., 2020. The biogenesis and precise control of RNA m(6)A methylation. 36: 44-52.

Huh, S., Paek, K., 2013. Plant RNA binding proteins for control of RNA virus infection. Frontiers in Physiology. 4: 397.

Huh, S., Paek, K., 2013b. Role of Arabidopsis Pumilio RNA binding protein 5 in virus infection. Plant Signaling and Behavior. 8(5): e23975

Hunt, A., 2012. RNA regulatory elements and polyadenylation in plants. Frontiers in Plant Science. 2: 109.

Hunt, A., Xing, D., Li, Q., 2012. Plant polyadenylation factors: conservation and variety in the polyadenylation complex in plants. BMC Genomics. 13: 641.

Jakubiec, A., Yang, S., Chua, N., 2012. Arabidopsis DRB4 protein in antiviral defense against Turnip yellow mosaic virus infection. The Plant Journal. 69: 14-25.

Jiao, X., Chang, J., Kilic, T., Tong, L., Kiledjian, M., 2013. A Mammalian Pre-mRNA 50End Capping Quality Control Mechanism and an Unexpected Link of Capping to Pre-mRNA Processing. Mol. Cell. 50: 104-115.

Jiao, X., Doamekpor, S., Bird, J., Nickels, B., Tong, L., Hart., R., Kiledjian, M., 2017. 5' End Nicotinamide Adenine Dinucleotide Cap inHuman Cells Promotes RNA Decay through DXO-Mediated deNADding. Cell. 168: 1015-1027.

Johansson, H., Liljas, L., Uhlenbeck, O., 1997. RNA Recognition by the MS2 Phage Coat Protein. Seminars in Virology. 8: 176-185.

Jonkhout, N., Tran, J., Smith, M., Schonrock, N., Mattick, J., Novoa, N., 2017. The RNA modification landscape in human disease. RNA. 23: 1754-1769.

Jung, H., Kim, M., Kang, H., 2013. An ABA-regulated putative RNA-binding protein affects seed germination of Arabidopsis under ABA or abiotic stress conditions. Journal of Plant Physiology. 170: 179-184.

Juntawong, P., Sorenson, R., Bailey-Serres, J., 2013. Cold shock protein 1 chaperones mRNAs during translation in Arabidopsis thaliana. The Plant Journal. 74: 1016-1028.

Kadumuri, R., Janga, S., 2018. Epitranscriptomic Code and Its Alterations in Human Disease. Trends in Molecular Medicine. 24: 886-903.

Kaewsapsak, P., Schechner, D., Mallard, W., Rinn, J., Ting, A. Live-cell mapping of organelle-associated RNAs via proximity biotinylation combined with protein-RNA crosslinking. eLife 2017, 6: e29224.

Kall, L., Storey, J., MacCoss, M., Noble, W., 2008. Assigning significance to peptides identified by tandem mass spectrometry using decoy databases. 7: 29-34.

Kargapolova, Y., Levin, M., Lackner, K., Danckwardt, S., 2017. sCLIP—an integrated platform to study RNA–protein interactomes in biomedical research: identification of CSTF2tau in alternative processing of small nuclear RNAs. Nucleic Acids Research. 45(10): 6074-6086.

Keller, A., Nesvizhskii, A., Kolker, E., Aebersold, R., 2002. Empirical statistical model to estimate the accuracy of peptide identifications made by MS/MS and database search. Analytical Chemistry. 74: 5383-5392.

Kiledjian, M., 2018. Eukaryotic RNA 5'-End NAD^+ Capping and DeNADding. Trends in Cell Biology. 28: 454-464.

Kim, H., Abbasi, N., Choi, S., 2013. Bruno-like proteins modulate flowering time via 3′ UTR-dependent decay of SOC1 mRNA. New Phytologist. 198: 747-756.

Kim, H., Lee, J., Kim, A., Park, S., Ma, S., Lee, S., Joung, Y., 2016. Heterologous expression of an RNA-binding protein affects flowering time as well as other developmental processes in Solanaceae. Molecular Breeding. 36: 71.

Kim, Y., Kim, J., Kang, H., 2005. Cold-inducible zinc finger-containing glycine-rich RNA-binding protein contributes to the enhancement of freezing tolerance in Arabidopsis thaliana. The Plant Journal. 42: 890-900.

Kim, Y., Park, S., Gilmour, S., Thomashow, M., 2013. Roles of CAMTA transcription factors and salicylic acid in configuring the low-temperature transcriptome and freezing tolerance of Arabidopsis. The Plant Journal. 75: 364-376.

König, J, Zarnack, K., Rot, G., Curk, T., Kayikci, M., Zupan, B., Turner, D., Luscombe, N., Ule, J., 2014. iCLIP reveals the function of hnRNP particles in splicing at individual nucleotide resolution. Nature Structural and Molecular Biology. 17: 909-915.

Krasensky J., Jonak C., 2012 Drought, salt, and temperature stress-induced metabolic rearrangements and regulatory networks. Journal of Experimental Biology. 63: 1593-1608.

Kudla, J., Becker, D., Grill, E., Hedrich, R., Hippler, M., Kummer, U., Parniske, M., Romeis, T., Schumacher, K., 2017. Advances and current challenges in calcium signaling. New Phytologist. 218: 414-431.

Kwak, K., Kim, Y., Kang, H., 2005. Characterization of transgenic Arabidopsis plants overexpressing GR-RBP4 under high salinity, dehydration, or cold stress. Journal of Experimental Botany. 56(421): 3007-3016.

Laluk, K., Prasad, K., Savchenko, T., Celesnik, H., Dehesh, K., Levy, M., Mitchell-Olds, T., Reddy, A., 2012. The Calmodulin-Binding Transcription Factor SIGNAL

RESPONSIVE1 is a Novel Regulator of Glucosinolate Metabolism and Herbivory Tolerance in Arabidopsis. Plant Cell Physiol. 53: 2008-2015.

Lee, Y., Choe, J., Park, O., Kim, Y., 2020. Molecular Mechanisms Driving mRNA Degradation by m6A Modification. Trends in Genetics. 36: 177-178.

Lee, J., Lee, I., 2010. Regulation and function of SOC1, a flowering pathway integrator. Journal of Experimental Botany. 61(9): 2247-2254.

Levitt, J., 1980 Responses of Plants to Environmental Stresses. New York: Academic Press.

Li, P., Ham, B., Lucas, W., 2011. CmRBP50 Protein Phosphorylation Is Essential for Assembly of a Stable Phloem-mobile High-affinity Ribonucleoprotein Complex. Journal of Biological Chemistry. 286(26): 23142-23149.

Libault, M., Pingault, L., Zogli, P., Schiefelbein, J., 2017. Plant Systems Biology at the Single-Cell Level. Trends in Plant Science. 22(11): 949-960.

Licatalosi, D., Mele, A., Fak, J., Ule, J., Kayikci, M., Chi, S., Clark, T., Schweitzer, A., Blume, J., Wang, X., Darnell, J., Darnell, R., 2008. HITS-CLIP yields genome-wide insights into brain alternative RNA processing. Nature. 456: 464-469.

Lim, F., Downey, T., Peabody, D., 2001. Translational Repression and Specific RNA Binding by the Coat Protein of the Pseudomonas Phage PP7. Journal of Biological Chemistry. 276: 22507-22513.

Lin, C., Miles, W., 2019. Beyond CLIP: advances and opportunities to measure RBP–RNA and RNA–RNA interactions. Nucleic Acids Research. 47(11): 5490-5501.

Liu, J., Ishitani, M., Halfter, U., Kim, C., Zhu, J., 2000 The *Arabidopsis thaliana* SOS2 gene encodes a protein kinase that is required for salt tolerance. PNAS. 97: 3730-3734.

Liu, J., Lenzoni, G., Knight, M., 2020. Design Principle for Decoding Calcium Signals to Generate Specific Gene Expression Via Transcription. Plant Physiology. 182: 1743-1761.

Liu, J., Ye, Y., Han, D., Wang, X., Fu, Y., Zhang, L., Jia, G., Yu, M., Lu, Z., Deng, X., Dai, Q., Chen, W., He, C., 2014. A METTL3–METTL14 complex mediates mammalian nuclear RNA N6-adenosine methylation. Nature Chemical Biology. 10: 93-95.

Liu, J., Zhang, C., Jia, X., Wang, W., Yin, H., 2020. Comparative analysis of RNA-binding proteomes under *Arabidopsis thaliana*-Pst DC3000-PAMP interaction by orthogonal organic phase separation. International Journal of Biological Macromolecules. 160: 47-54.

Liu, J., Zhu, J., 1998. A Calcium Sensor Homolog Required for Plant Salt Tolerance. Science. 280: 1943-1945.

Livak, K., Schmittgen, T., 2001. Analysis of relative gene expression data using real-time quantitative PCR and the 2(-Delta Delta C(T)) Method. Methods. 25(4): 402-408.

Lorkovic, Z., 2009. Role of plant RNA-binding proteins in development, stress response and genome organization. Trends in Plant Science. 14(4): 229-236.

Lu, X., Cheng, Y., Gao, M., Li, M., Xu, X., 2020. Molecular Characterization, Expression Pattern and Function Analysis of Glycine-Rich Protein Genes Under Stresses in Chinese Cabbage (Brassica rapa L. ssp. pekinensis). Frontiers in Genetics. 11: 774.

Lucas, W., Yoo, B., Kragler, F., 2001. RNA as a long-distance information macromolecule in plants. Nature Reviews. 2: 849-887.

Lucero, L., Bazin, J., Melo, J., Ibanez, F., Crespi, M., Ariel, F., 2020. Evolution of the Small Family of Alternative Splicing Modulators Nuclear Speckle RNA-Binding Proteins in Plants. Genes. 11: 207.

Luo, G., MacQueen, A., Zheng, G., Duan, H, Dore, L., Lu, Z., Liu, J., Jia, G., Bergelson, J., He, C., 2014. Unique features of the m6A methylome in *Arabidopsis thaliana*. Nature Communications. 5: 5630.

Lyons, R., Iwase, A., Gansewig, T., Sherstnev, A., Duc, C., Barton, G., Hanada, K., Higuchi-Takeuchi, M., Matsui, M., Sugimoto, K., Kazan, K., Simpson, G., Shirasu, K., 2013. The RNA-binding protein FPA regulates flg22-triggered defense responses and transcription factor activity by alternative polyadenylation. Scientific Reports. 3: 2866.

Ma, Y., Szostkiewicz, I., Korte, A., Moes, D., Yang, Y., Christmann, A., Grill, E., 2009. Regulators of PP2C Phosphatase Activity Function as Abscisic Acid Sensors. Science. 324: 1064-1068.

Mahanta, T., Kumar, P., Bae, H., 2017. Genomics and evolutionary aspect of calcium signaling event in calmodulin and calmodulin-like proteins in plants. BMC Plant Biology. 17: 38.

Mallikaratchy, P., 2017. Evolution of Complex Target SELEX to Identify Aptamers against Mammalian Cell-Surface Antigens. Molecules. 22: 215.

Marlow, M., Dogan, J., Frederick, K., Valentine, K., Wand, J., 2010. The role of conformational entropy in molecular recognition by calmodulin. Nature Chemical Biology. 6: 352-358.

Marmisolle, F., García, M., Reyes, C., 2018. RNA-binding protein immunoprecipitation as a tool to investigate plant miRNA processing interference by regulatory proteins of diverse origin. Plant Methods. 14:9.

Marondedze, C., Thomas, L., Gehring, C., Lilley, K., 2019. Changes in the Arabidopsis RNA-binding proteome reveal novel stress response mechanisms. BMC Plant Biology. 19: 139.

Marondedze, C., Thomas, L., Lilley, K., Gehring, C., 2020. Drought Stress Causes Specific Changes to the Spliceosome and Stress Granule Components. Frontiers in Molecular Biosciences. 6: 163.

Marondedze, C., Thomas, L., Serrano, N., Lilley, K., Gehring, C., 2016. The RNA-binding protein repertoire of *Arabidopsis thaliana*. Scientific Reports. 6: 29766.

Martin, L., Nicolas, P., Matas, A., Shinozaki, Y., Catalá, C., Rose, J., 2016. Laser microdissection of tomato fruit cell and tissue types for transcriptome profiling. Nature Protocols. 11(12): 2376-2388.

Maticzka, D., Ilik, I., Aktas, T., Backofen, R., Akhtar, A., 2018. uvCLAP is a fast and non-radioactive method to identify *in vivo* targets of RNA-binding proteins. Nature Communications. 9: 1142.

McCormack, E., Tsai, Y., Braam, J., 2005. Handling Calcium Signaling: Arabidopsis CaMs and CMLs. Trends in Plant Science. 10: 1360-1385.

McHugh, C., Chen, C., Chow, A., Surka, C., Tran, C., McDonel, P., Pandya-Jones, A., Blanco, M., Burghard, C., Moradian, A., Sweredoski, M., Shishkin, A., Su, J., Lander, E., Hess, S., Plath, K., Guttman, M., 2015. The Xist lncRNA interacts directly with SHARP to silence transcription through HDAC3. Nature. 521: 232-236.

McMahon, A., Rahman, R., Jin, H., Shen, J., Fieldsend, A., Luo, W., Rosbash, M., 2016. TRIBE: Hijacking an RNA-Editing Enzyme to Identify Cell-Specific Targets of RNA-Binding Proteins. Cell. 165: 742-753.

Mei H., Cheng-Qiang H., Nai-Zheng D., 2018 Abiotic Stresses: General Defenses of Land Plants and Chances for Engineering Multistress Tolerance. Front. Plant Sci. 9: 1771.

Melencion, S., Chi, Y., Pham, T., Paeng, S., Wi, S., Lee, C., Ryu, S., Koo, S., Lee, S., 2017. RNA Chaperone Function of a Universal Stress Protein in Arabidopsis Confers Enhanced Cold Stress Tolerance in Plants. International Journal of Molecular Sciences. 18: 2546.

Meyer, K., Patil, D., Zhou, J., Zinoviev, A., Skabkin, M., Elemento, O., Pestova, T., Qian, S., Jaffrey, S., 2015. 5′ UTR m6A Promotes Cap-Independent Translation. Cell. 163: 999-1010.

Meyer, K., Koster, T., Nolte, C., Weinholdt, C., Lewinski, M., Grosse, I., Staiger, D., 2017. Adaptation of iCLIP to plants determines the binding landscape of the clockregulated RNA-binding protein AtGRP7. Genome Biology. 18: 204.

Mitsuda, N., Isono, T., Sato, M., 2003. Arabidopsis CAMTA family proteins enhance V-PPase expression in pollen. Plant and Cell Physiology. 44: 975-981.

Monaghan, J., Germain, H., Weihmann, T., Li, X., 2010. Dissecting plant defence signal transduction: modifiers of snc1 in Arabidopsis. Canadian Journal of Plant Pathology. 32(1): 35-42.

Monaghan, J., Xu, F., Gao, M., Zhao, Q., Palma, K., Long, C., Chen, S., Zhang, Y., Li, X., 2009. Two Prp19-Like U-Box Proteins in the MOS4-Associated Complex Play Redundant Roles in Plant Innate Immunity. PLOS Pathogens. 5(7): e1000526.

Moshelion, M., Altman, A., 2015. Current challenges and future perspectives of plant and agricultural biotechnology. Trends in Biotechnology. 33(6): 337-341.

Mruk, K., Farley, B., Ritacco, A., Kobertz, W., 2014. Calmodulation meta-analysis: predicting calmodulin binding via canonical motif clustering. J. Gen. Physiol. 144: 105-114.

Mukherjee, J., Hermesh, O., Eliscovich, C., Nalpas, N., Franz-Wachtel, M., Macek, B., Jansen, R.P. β-Actin mRNA interactome mapping by proximity biotinylation. PNAS 2019, 116(26): 12863-12872.

Murashige, T., Skoog, F., 1962. A revised medium for rapid growth and bioassays with tobacco tissue cultures. Physiol. Plant. 15: 473-497.

Muthuramalingam, M., Wang, Y., Mahalingam, R., 2016. Interacting protein partners of Arabidopsis RNA-binding protein AtRBP45b. Plant Biology. 19: 327-334.

Nachtergaele, S., He, C., 2018. Chemical Modifications in the Life of an mRNA Transcript. Annu. Rev. Genet. 52: 349-372.

Nagy, E., Rigby, W., 1996. Glyceraldehyde-3-phosphate Dehydrogenase Selectively Binds AU-rich RNA in the NAD^+-binding Region (Rossmann Fold). Journal of Biological Chemistry. 270: 2755-2763.

Nemali, K., Bonin, C., Dohleman, F., Stephens, M., Reeves, W., Nelson, D., Castiglioni, P., Whitsel, J., Sammons, B., Silady, R., Anstrom, D., Sharp, R., Patharkar, O., Clay, D., Coffin, M., Nemeth, M., Leibman, M., Luethy, M., Lawson, M., 2015. Physiological responses related to increased grain yield under drought in the first biotechnology-derived drought-tolerant maize. Plant, Cell, and Environment. 38: 1866-1880.

Nesvizhskii, A., Keller, A., Kolker, E., Aebersold, R., 2003. A statistical model for identifying proteins by tandem mass spectrometry. Anal. Chem. 73: 4646-4658.

Nicolai, M., Duprat, A., Sormani, R., Rodriguez, C., Roncato, M., Rolland, N., Robaglia, C., 2007. Higher plant chloroplasts import the mRNA coding for the eucaryotic translation initiation factor 4E. FEBS Letters. 581(21): 3921-3926.

Nie, H., Zhao, C., Wu, G., Wu, Y., Chen, Y., Tang, D., 2012. SR1, a Calmodulin-Binding Transcription Factor, Modulates Plant Defense and Ethylene-Induced Senescence by Directly Regulating NDR1 and EIN3. Plant Physiology. 158: 1847-1859.

Niranjanakumari, S., Lasda, E., Brazas, R., Garcia-Blanco, M., 2002. Reversible cross-linking combined with immunoprecipitation to study RNA-protein interactions in vivo. Methods. 26: 182-190.

Nostrand, E., Pratt, G., Shishkin, A., Gelboin-Burkhart, C., Fang, M., Sundararaman, B., Blue, S., Nguyen, T., Surka, C., Elkins, K., Stanton, R., Rigo, F., Guttman, M., Yeo, G., 2016. Robust transcriptome-wide discovery of RNA-binding protein binding sites with enhanced CLIP (eCLIP). Nature Methods. 13(6): 508-514.

Palma, K., Zhao, Q., Cheng, Y., Bi, D., Monaghan, J., Cheng, W., Zhang, Y., Li, X., 2007. Regulation of plant innate immunity by three proteins in a complex conserved across the plant and animal kingdoms. Genes and Development. 21: 1484-1493.

Pan, H., Liu, S., Tang, D., 2012. HPR1, a component of the THO/TREX complex, plays an important role in disease resistance and senescence in Arabidopsis. The Plant Journal. 69: 831-843.

Pandey, N., Ranjan, A., Pant, P., Tripathi, R., Ateek, F., Pandey, H., Patre, U., Sawant, S., 2013. CAMTA 1 regulates drought responses in *Arabidopsis thaliana*. BMC Genomics. 14: 216.

Park, C., Kim, K., Shin, R., Park, J., Shin, Y., Paek, K., 2004. Pathogenesis-related protein 10 isolated from hot pepper functions as a ribonuclease in an antiviral pathway. The Plant Journal. 37: 186-198.

Park, S., Fung, P., Nishimura, N., Jensen, D., Fujii, H., Zhao, Y., Lumba, S., Santiago, J., Rodrigues, A., Chow, T., Alfred, S., Bonetta, D., Finkelstein, R., Provart, N., Desveaux, D., Rodriguez, P., McCourt, P., Zhu, J., Schroeder, J., Volkman, B., Cutler, S., 2009. Abscisic Acid Inhibits Type 2C Protein Phosphatases via the PYR/PYL Family of START Proteins. Science. 324: 1068-1071.

Park, S., Jeong, J., Redillas, M., Jung, H., Bang, S., Kim, Y., Kim, J., 2013. Transgenic overexpression of UIP1, an interactor of the 30 untranslated region of the Rubisco small subunit mRNA, increases rice tolerance to drought. 7: 83-90.

Park, H., You, Y., Lee, A., Jung, H., Jo, S., Oh, N., Kim, H., Lee, H., Kim, J., Kim, Y., Jung, C., Cho, H., 2020. OsFKBP20-1b interacts with the splicing factor OsSR45 and participates in the environmental stress response at the post-transcriptional level in rice. The Plant Journal. 102: 992-1007.

Parry, G., Ward, S., Cernac, A., Dharmasiri, S., Estelle, M., 2006. The Arabidopsis Suppressor of Auxin Resistance Proteins are Nucleoporins with an Important Role in Hormone Signaling and Development. The Plant Cell. 18: 1590-1603.

Perez-Perri, J., Rogell, B., Schwarzi, T., Stein, F., Zhou, Y., Rettel, M., Brosig, A., Hentze, M., 2018. Discovery of RNA-binding proteins and characterization of their dynamic responses by enhanced RNA interactome capture. Nature Communications. 9: 4408.

Pfalz, J., Bayraktar, O., Prikryl, J., Barkan, A., 2009. Site-specific binding of a PPR protein defines and stabilizes 50 and 30 mRNA termini in chloroplasts. The EMBO Journal. 28: 2042-2052.

Ping, X., Sun, B., Wang, L., Xiao, W., Yang, X., Wang, W., Adhikari, S., Shi, Y., Lv, Y., Chen, Y., Zhao, X., Li, A., Yang, Y., Dahal, U., Lou, X., Liu, X., Huang, J., Yuan, W., Zhu, X.,

Cheng, T., Zhao, Y., Wang, X., Danielsen, J., Liu, F., Yang, Y., 2014. Mammalian WTAP is a regulatory subunit of the RNA N6-methyladenosine methyltransferase. Cell Research. 24: 177-189.

Popescu, S., Popescu, G., Bachan, S., Zhang, Z., Seay, M., Gerstein, M., et al., 2007. Differential binding of calmodulin related proteins to their targets revealed through high-density Arabidopsis protein microarrays. PNAS. 104: 4730-4735.

Prasad, K., Abdel-Hameed, A., Xing, D., Reddy, A., 2016. Global gene expression analysis using RNA-seq uncovered a new role for SR1/SR1 transcription factor in salt stress. Scientific Reports. 6: 27021.

Preiss, T., Sang, A., Chrzanowska-Lightowlers, Z., Lightowlers, R., 1995. The mRNA-binding protein COLBP is glutamate dehydrogenase. FEBS Letters. 367: 291-296.

Qi, J., Song, C., Wang, B., Zhou, J., Kangasjarvi, J., Zhu, J., Gong, Z., 2018. Journal of Integrative Plant Biology. 60: 805-826.

Qiu, Y., Xi, J., Du, L., Suttle, J., Poovaiah, B., 2012. Coupling calcium/calmodulin-mediated signaling and herbivore-induced plant response through calmodulin-binding transcription factor AtSR1/SR1. Plant Mol. Biol. 79: 89-99.

Queiroz, R., Smith, T., Villanueva, E., Marti-Solano, M., Monit, M., Pizzinga, M., Mirea, D., Ramakrishna, M., Harvey, R., Dezi, V., Thomas, G., Willis, A., Lilley, K., 2019. Comprehensive identification of RNA–protein interactions in any organism using orthogonal organic phase separation (OOPS). Nature Biotechnology. 37: 169-178.

Quintero, F., Martinez-Atienza, J., Villalta, I., Jiang, X., Kim, W., Ali, Z., Fujii, H., Mendoza, I., Yun, D., Zhu, J., Pardo, J., 2010. Activation of the plasma membrane Na/H antiporter

Salt-Overly-Sensitive 1 (SOS1) by phosphorylation of an auto-inhibitory C-terminal domain. PNAS. 108: 2611-2616.

Raghavendra A., Gonugunta, V., Christmann, A., Grill, E., 2010. ABA Perception and Signaling. Trends in Plant Science. 15: 395-401.

Ramanathan, M., Porter, D., Khavari, P., 2019. Methods to study RNA–protein interactions. Nature Methods. 16: 225-234.

Ranty, B., Aldon, D., Galaud, J., 2006. Plant Calmodulins and Calmodulin-Related Proteins. Plant Signaling and Behavior. 1: 96-104.

Reddy A., Ali G., Celesnik H., Day I., 2011. Coping with Stresses: Roles of Calcium- and Calcium/Calmodulin-Regulated Gene Expression. The Plant Cell. 23: 2010-2032.

Reddy, A., 2001. Calcium: a silver bullet in signaling. Plant Science. 160: 381-404.

Reddy, A.S.N., Marquez, Y., Kalyna, M., Barta, A., 2013. Complexity of the alternative splicing landscape in plants. Plant Cell. 25(10): 3657-3683.

Reddy, A., Reddy, V., Golovkin, M., 2000. A Calmodulin Binding Protein from Arabidopsis Is Induced by Ethylene and Contains a DNA-Binding Motif. Biochemical and Biophysical Research Communications. 279: 762-769.

Reed, E., Hammer, D., 2018. Redox Sensitive Protein Droplets from Recombinant Oleosin. Soft Matter. 14(31): 6506-6513.

Reichel, M., Liao, Y., Rettel, M., Ragan, C., Evers, M., Alleaume, A., Horos, R., Hentze, M., Preiss, T., Millar, A., 2016. In Planta Determination of the mRNA-Binding Proteome of Arabidopsis Etiolated Seedlings. The Plant Cell. 28: 2435-2452.

Ren, G., Chen, X., Yu, B., 2012. Uridylation of miRNAs by HEN1 SUPPRESSOR1 in Arabidopsis. Current Biology. 22: 695-700.

Roads, A., Friedberg, F., 1997. Sequence Motifs for Calmodulin Recognition. FASEB J. 11: 331-340.

Roundtree, I., Evans, M., Pan, T., He, C., 2017. Dynamic RNA Modifications in Gene Expression Regulation. Cell. 169: 1187-1200.

Rowley, J., Bohmdorfer, G., Wierzbicki, A., 2013. Analysis of long non-coding RNAs produced by a specialized RNA Polymerase in Arabidopsis thaliana. Methods. 63(2): 160-169.

Ruiz, M., Hubbard, K., Gardner, M., Jung, H., Aubry, S., Hotta, C., Mohd-Noh, N. Robertson, F., Hearn, T., Tsai, Y., Dodd, A., Hannah, M., Carré, I., Davies, J., Braam, J., Webb, A., 2018. Circadian oscillations of cytosolic free calcium regulate the Arabidopsis circadian clock. Nature Plants. 4: 690-698.

Ruwe, H., Wang, G., Gusewski, S., Schmitz-Linneweber, C., 2016. Systematic analysis of plant mitochondrial and chloroplast small RNAs suggests organelle-specific mRNA stabilization mechanisms. Nucleic Acids Research. 44(15): doi: 10.1093/nar/gkw466.

Saéz-Vásquez, J., Delseny, M., 2019. Ribosome Biogenesis in Plants: From Functional 45S Ribosomal DNA Organization to Ribosome Assembly Factors. The Plant Cell. 31: 1945-1967.

Saveliev, S., Woodroofe, C., Sabat, G., Adams, C., Klaubert, D., Wood, K., et al., 2013. Mass spectrometry compatible surfactant for optimized in-gel protein digestion. Anal. Chem. 85: 907-914.

Schmid, L., Ohler, L., Mohlmann, T., Brachmann, A., Muino, J., Leister, D., Meurer, J., Manavski, N., 2019. PUMPKIN, the Sole Plastid UMP Kinase, Associates with Group II Introns and Alters Their Metabolism. Plant Physiology. 179: 248-264.

Schoning, J., Streitner, C., Page, D., Hennig, S., Uchida, K., Wolf, E., Furuya, M., Staiger, D., 2007. Auto-regulation of the circadian slave oscillator component AtGRP7 and regulation of its targets is impaired by a single RNA recognition motif point mutation. The Plant Journal. 52: 1119-1130.

Schwartz, S., Mumach, M., Jovanovic, M., Wang, T., Maciag, K., Bushkin, G., Mertins, P., Ter-Ovanesyan, D., Habib, N., Cacchiarelli, D., Sanjana, N., Freinkman, E., Pacold, M., Satija, R., Mikkelsen, T., Hacohen, N., Zhang, F., Carr, S., Lander, E., Regev, A., 2014. Perturbation of m6A Writers RevealsTwo Distinct Classes of mRNA Methylation at Internal and 5' Sites. Cell Reports. 8: 284-296.

Scopes, R., 1974. Measurement of protein by spectrophotometry at 205 nm. Analytical Biochemistry. 59: 277-282.

Scutenaire, J., Deragon, J., Jean, V., Benhamed, M., Raynaud, C., Favory, J., Merret, R., Bousquet-Antonelli, C., 2018. The YTH Domain Protein ECT2 Is an m6A Reader Required for Normal Trichome Branching in Arabidopsis. The Plant Cell. 30: 986-1005.

Searle, B., Turner, M., Nesvizhskii, A., 2008. Improving sensitivity by probabilistically combining results from multiple MS/MS search methodologies. 7: 245-253.

Seifikalhor, M., Aliniaeifard, S., Shomali, A., Azad, N., Hassani, B., Lastochkina, O., Li, T., 2019. Calcium signaling and salt tolerance are diversely entwined in plants. Plant Signaling and Behavior. 1665455.

Shang, X., Cao, Y., Ma, L., 2017. Alternative Splicing in Plant Genes: A Means of Regulating the Environmental Fitness of Plants. Int. J. Mol. Sci. 18: 432.

Shi, H., Ishitani, M., Kim, C., Zhu, J., 2000. The *Arabidopsis thaliana* salt tolerance gene SOS1 encodes a putative Na^+/H^+ antiporter. PNAS. 97: 6896-6901.

Shi, H., Lee, B., Wu, S., Zhu, J., 2002. Overexpression of a plasma membrane Na^+/H^+ antiporter gene improves salt tolerance in *Arabidopsis thaliana*. Nature Biotechnology. 21: 81-85.

Shi, H., Quintero, F., Pardo, J., Zhu, J., 2002b. The Putative Plasma Membrane Na/H Antiporter SOS1 Controls Long-Distance Na Transport in Plants. The Plant Cell. 14: 465-477.

Shi, H., Wei, J., He, C., 2019. Where, When, and How: Context-Dependent Functions of RNA Methylation Writers, Readers, and Erasers. Molecular Cell. 74: 640-650.

Shi, Z., Barna, M., 2015. Translating the genome in time and space: specialized ribosomes, RNA regulons, and RNA-binding proteins. Annu. Rev. Cell Dev. Biol. 31:31-54.

Silva, O., 1994. CG-1, a parsley light-induced DNA-binding protein. Plant Molecular Biology. 25: 921-924.

Slavkovic, S., Churcher, Z., Johnson, P., 2018. Nanomolar binding affinity of quinine-based antimalarial compounds by the cocaine-binding aptamer. Bioorg Med Chem. 1(26): 5427-5434.

Snedden, W., Fromm, H., 2001. Calmodulin as a versatile calcium signal transducer in plants. New Phytologist. 151: 35-66.

Song, K., Backs, J., McAnally, J., Qi, X., Gerard, R., Richardson, J., Hill, J., Bassel-Duby, R., Olson, E., 2006. The Transcriptional Coactivator CAMTA2 Stimulates Cardiac Growth by Opposing Class II Histone Deacetylases. Cell. 125: 453-466.

Sonmez, C., Baurle, I., Magusin, A., Dreos, R., Laubinger, S., Weigel, D., Dean, C., 2011. RNA 3′ processing functions of Arabidopsis FCA and FPA limit intergenic transcription. PNAS. 108(20): 8508-8513.

Sun, H., Tan, W., Zu, Y., 2016. Aptamers: versatile molecular recognition probes for cancer detection. Analyst. 141: 403.

Staiger, 2001. RNA-Binding Proteins and Circadian Rhythms in Arabidopsis thaliana. Phil. Trans. R. Soc. Lond. 356: 1755-1759.

Staiger, D., Zecca, L., Wieczorek Kirk, D., Apel, K., Eckstein, L., 2003. The circadian clock regulated RNA-binding protein AtGRP7 autoregulates its expression by influencing alternative splicing of its own pre-mRNA. The Plant Journal. 33(2): 361-371.

Steffen, A., Elgner, M., Staiger, D., 2019. Regulation of Flowering Time by the RNA-Binding Proteins AtGRP7 and AtGRP8

Streitner, C., Danisman, S., Wehrle, F., Schoning, J., Alfano, J., Staiger, D., 2008. The small glycine-rich RNA binding protein AtGRP7 promotes floral transition in Arabidopsis thaliana. The Plant Journal. 56(2): 239-250.

Streitner, C., Koster, T., Simpson, C., Shaw, P., Danisman, S., Brown, J., Staiger, D., 2012. An hnRNP-like RNA-binding protein affects alternative splicing by in vivo interaction with transcripts in Arabidopsis thaliana. Nucleic Acids Research. 40: 22.

Takenaka, M., Verbitskiy, D., van der Merwe, J., Zehrmann, A., Plessmann, U., Urlaub, H., Brennicke, A., 2007. *In vitro* RNA editing in plant mitochondria does not require added energy. FEBS Letters. 581(14): 2743-2747.

Tan, Y., Qin, Y., Li, Y., Li, M., Ma, F., 2014. Overexpression of MpGR-RBP1, a glycine-rich RNA-binding protein gene from Malus prunifolia (Willd.) Borkh., confers salt stress tolerance and protects against oxidative stress in Arabidopsis. Plant Cell Tissue Organ Culture. 119: 635-646.

Tatavarty, V., Ifrim, M., Levin, M., Korza, G., Barbarese, E., Yu, J., Carson, J., 2012. Single-molecule imaging of translational output from individual RNA granules in neurons. Mol. Biol. Cell. 23(5): 918-929.

Téllez, S., Kanhonou, R., Bellés, C., Serrano, R., Alepuz, P., Ros, R., 2020. RNA-Binding Proteins as Targets to Improve Salt Stress Tolerance in Crops. Agronomy. 10: 250.

Tercé-Laforgue, T., Clément, G.. Marchi, L., Restivo, F., Lea, P., Hirel, B., 2015. Resolving the Role of Plant NAD-Glutamate Dehydrogenase: III. Overexpressing Individually or Simultaneously the Two Enzyme Subunits Under Salt Stress Induces Changes in the Leaf Metabolic Profile and Increases Plant Biomass Production. Plant Cell and Physiology. 56(10): 1918-1929.

Tercé-Laforgue, T., Dubois, F., Ferrario-Méry, S., Pou de Crecenzo, M., Sangwan, R., Hirel, B., 2004. Glutamate Dehydrogenase of Tobacco is Mainly Induced in the Cytosol of Phloem Companion Cells When Ammonia is Provided Either Externally or Released during Photorespiration. Plant Physiology. 136: 4308-4317.

Tian, B., Manley, J., 2017. Alternative polyadenylation of mRNA precursors. Nat Rev Mol Cell Biol. 18(1): 18-30.

Tian, L., Chou, H., Fukuda, M., Kumamaru, T., Okita, T., 2020. mRNA Localization in Plant Cells. Plant Physiology. 182: 97-109.

Tian, L., Chou, H., Zhang, L., Hwang, S., Starkenburg, S., Doroshenk, K., Kumamaru, T., Okita, T., 2018. RNA-Binding Protein RBP-P Is Required for Glutelin and Prolamine mRNA Localization in Rice Endosperm Cells. The Plant Cell. 30: 2529-2552.

Tian, Y., Zheng, H., Zhang, F., Wang, S., Ji, X., Xu, C., He, Y., Ding, Y., 2019. PRC2 recruitment and H3K27me3 deposition at FLC require FCA binding of COOLAIR. Science Advances. 5: eaau7246.

Truman, W., Sreekanta, Lu, Y., Bethke, G., Tsuda, K., Katagiri, F., Glazebrook, J., 2013. The CALMODULIN-BINDING PROTEIN60 Family Includes Both Negative and Positive Regulators of Plant Immunity. Plant Physiology. 163: 1741-1751.

Ule, J., Jensen, K., Ruggiu, M., Mele, A., Ule, A., Darnell, R., 2003. CLIP Identifies Nova-Regulated RNA Networks in the Brain. Science. 302: 1212-1215.

Uniacke, J., Zerges, W., 2008. Stress Induces the Assembly of RNA Granules in the Chloroplast of Chlamydomonas reinhardtii. J. Cell Biol. 182(4): 641-646.

Vermel, M., Guermann, B., Delage, L., Grienenberger, J., Maréchal-Drouard, L., Gualberto, J., 2002. A family of RRM-type RNA-binding proteins specific to plant mitochondria. PNAS. 99(9): 5866-5871.

Wallander, M., Leibold, E., Eisenstein, R., 2006. Molecular control of vertebrate iron homeostasis by iron regulatory proteins. Biochimica et Biophysica Acta. 1763: 668-689.

Walley, J., Coughlan, S., Hudson, M., Covington, M., Kaspi, R., Banu, G., Harmer, S., Dehesh, K., 2007. Mechanical Stress Induces Biotic and Abiotic Stress Responses via a Novel cis-Element. PLOS Genetics. 3: 1800-1812.

Walters, R., Matheny, T., Mizoue, L, Rao, B., Muhlrad, D., Parker, R., 2017. Identification of NAD^+ capped mRNAs in Saccharomyces cerevisiae. PNAS. 114: 480-485.

Wang, B., Wang, G., Shen, F., Zhu, S., 2018. A Glycine-Rich RNA-Binding Protein, CsGR-RBP3, Is Involved in Defense Responses Against Cold Stress in Harvested Cucumber (Cucumis sativus L.) Fruit. Frontiers in Plant Science. 9: 540.

Wang, S., Wang, R., Liang, D., Ma, F., Shu, H., 2012. Molecular characterization and expression analysis of a glycine-rich RNA-binding protein gene from Malus hupehensis Rehd. Molecular Biology Reports. 39: 4145-4153.

Wang, T., Xie, Y., Xiao, G., 2014. dCLIP: a computational approach for comparative CLIP-seq analyses. Genome Biology. 15: R11.

Wang, X., Lu, Z., Gomez, A., Hon, G., Yue, Y., Han, D., Fu, Y., Parisien, M., Dai, Q., Jia, G., Ren, B., Pan, T., He, C., 2014. N6-methyladenosine-dependent regulation of messenger RNA stability. Nature. 505: 117-120.

Wang, Y., Li, S., Zhao, Y., You, C., Le, B., Gong, Z., Mo, B., Xia, Y., Chen, X., 2019. NAD^+-capped RNAs are widespread in the Arabidopsis transcriptome and can probably be translated. PNAS. 116: 12094-12102.

Wang., X., Zhao, B., Roundtree, I., Lu, Z., Han, D., Ma, H., Weng, X., Chen, K., Shi, H., He, C., 2015. N6-methyladenosine Modulates Messenger RNA Translation Efficiency. Cell. 161: 1388-1399.

Webb, A., McAinsh, M., Taylor, J., Hetherington, A., 1996. Calcium Ions as Intracellular Second Messengers in Higher Plants. Advances in Botanical Research. 22: 45-96.

Wei, L., Song, P., Wang, Y., Lu, Z., Tang, Q., Yu, Q., Xiao, Y., Zhang, X., Duan, H., Jia, G., 2018. The m6A Reader ECT2 Controls Trichome Morphology by Affecting mRNA Stability in Arabidopsis. The Plant Cell. 30: 968-985.

Wierzbicki, A., Ream, T., Haag, J., Pikaard, C., 2009. RNA Polymerase V transcription guides ARGONAUTE4 to chromatin. Nature Genetics. 41(5): 630-634.

Xing, D., Li, Q., 2011. Alternative polyadenylation and gene expression regulation in plants. WIREs RNA. 2(3): 445-458.

Xing, D., Wang, Y., Hamilton, M., Ben-Hur, A., Reddy, A., 2015. Transcriptome-Wide Identification of RNA Targets of Arabidopsis SERINE/ARGININE-RICH45 Uncovers

the Unexpected Roles of This RNA Binding Protein in RNA Processing. The Plant Cell. 27: 3294-3308.

Xiong, J., Sun, Y., Yang, Q., Tian, H., Zhang, H., Liu, Y., Chen, M., 2017. Proteomic analysis of early salt stress responsive proteins in alfalfa roots and shoots. Proteome Science. 15:19. DOI 10.1186/s12953-017-0127-z

Xu, F., Xu, S., Wiermer, M., Zhang, Y., Li, X., 2012. The cyclin L homolog MOS12 and the MOS4-associated complex are required for the proper splicing of plant resistance genes. The Plant Journal. 70: 916-928.

Xu, W., Rahman, R., Rosbash, M., 2018. Mechanistic implications of enhanced editing by a HyperTRIBE RNA-binding protein. RNA. 24: 173-182.

Yamada, K., Nagano, A., Ogasawara, K., Hara-Nishimura, I., Nishimura, M., 2009. The ER body, a new organelle in *Arabidopsis thaliana*, requires NAI2 for its formation and accumulates specific β-glucosidases. Plant Signaling and Behavior. 4(9): 849-852.

Yamaguchi, T., Aharon, G., Scottosanto, J., Blumwald, E., 2005. Vacuolar Na^+/H^+ antiporter cation selectivity is regulated by calmodulin from within the vacuole in a Ca^{2+-} and pH-dependent manner. PNAS. 102: 16107-16112.

Yamaguchi, T., Apse, M., Shi, H., Blumwald, E., 2003. Topological analysis of a plant vacuolar Na^+/H^+ antiporter reveals a luminal C terminus that regulates antiporter cation selectivity. PNAS. 100: 12510-12515.

Yang, D., Kwak, K., Kim, M., Park, S., Yang, K., Kang, H., 2013. Expression of Arabidopsis glycine-rich RNA-binding protein AtGRP2 or AtGRP7 improves grain yield of rice (Oryza sativa) under drought stress conditions. Plant Stress. 214: 106-112.

Yang, T., Poovaiah, B., 2000. An early ethylene up-regulated gene encoding a calmodulin-binding protein involved in plant senescence and death. Journal of Biological Chemistry. 275: 38467-38473.

Yang, T., Poovaiah, B., 2002. A Calmodulin-binding/CGCG Box DNA-binding Protein Family Involved in Multiple Signaling Pathways in Plants. Journal of Biological Chemistry. 277: 45049-45048.

Yang, W., Yu, M., Zou, C., Lu, C., Yu, D., Cheng, H., Jiang, P., Feng, X., Zhang, Y., Wang, Q., Zhang, H., Song, G., Zhou, Z., 2019. Genome-wide comparative analysis of RNA binding Glycine-rich protein family genes between Gossypium arboreum and Gossypium raimondii. PLOS One. 14(6): e0218938

Yasuda, K., Zhang, H., Loiselle, D., Haystead, T., Macara, I., Mili, S., 2013. The RNA-binding protein Fus directs translation of localized mRNAs in APC-RNP granules. J. Cell Biol. 203(5): 737-746.

Yi, W., Li, J., Zhu, X., Wang, X., Fan, L., Sun, W., Liao, L., Zhang, J., Ye, J., Chen, F., Taipale, J., Chan, K., Zhang, L., Yan, J. CRISPR-assisted detection of RNA–protein interactions in living cells. Nature Methods 2020, 17: 685-688.

Yin, Q., Cui, Y., Zhang, G., Zhang, H., Wang, X., Yang, Z., 2012. The Arabidopsis pentatricopeptide repeat protein PDM1 is associated with the intergenic sequence of S11-rpoA for rpoA monocistronic RNA cleavage. Chinese Science Bulletin. 57: 3452-3459.

Yoo, J., Park, C., Kim, J., Heo, W., Cheong, M., Park, H., Kim, M., Moon, B., Choi, M., Kang, Y., Lee, J., Kim, H., Lee, S., Yoon, H., Lim, C., Yun, D., Lee, S., Chung, W., Cho, M., 2005. Direct Interaction of a Divergent CaM Isoform and the Transcription Factor,

MYB2, Enhances Salt Tolerance in Arabidopsis. Journal of Biological Chemistry. 280: 3697-3706.

Yosef, I., Irihimovitch, V., Knopf, J., Cohen, I., Orr-Dahan, I., Nahum, E., Keasar, C., Shapira, M., 2004. RNA Binding Activity of the Ribulose-1,5-bisphosphate Carboxylase/Oxygenase Large Subunit from Chlamydomonas reinhardtii. Journal of Biological Chemistry. 279(11): 10148-10156.

Yuenyong, W., Chinpongpanich, A., Comai, L., Chadchawan, S., Buaboocha, T., 2018. Downstream components of the calmodulin signaling pathway in the rice salt stress response revealed by transcriptome profiling and target identification. BMC Plant Biology. 18: 335.

Yuenyong, W., Roytrakul, S., Chadchawan, S., Wutipraditkul, N., Chaicherdsakul, T., Limpaseni, T., Buaboocha, T., 2017. Proteomic analysis of transgenic rice overexpressing a calmodulin calcium sensor reveals its effects on redox signaling and homeostasis. 26: 235-245.

Zambelli, F., Pavesi, G., 2015. RIP-Seq Data Analysis to Determine RNA-protein Associations. Methods in Molecular Biology. 1269: 293-303.

Zarnegar, B., Flynn, R., Shen, Y., Do, B., Chang, H., Khavari, P., 2015. irCLIP platform for efficient characterization of protein–RNA interactions. Nature Methods. 13(6): 489-492.

Zeevaart, J., 1980. Changes in the Levels of Abscisic Acid and Its Metabolites in Excised Leaf Blades of Xanthium strumarium during and after Water Stress. Plant Physiol. 66: 672-678.

Zhang, Y., Cheng, Y., Bi, D., Palma, K., Li, X., 2005. MOS2, a Protein Containing G-Patch and KOW Motifs, Is Essential for Innate Immunity in Arabidopsis thaliana. Current Biology. 15: 1936-1942.

Zhang, Y., Gu, L., Hou, Y., Wang, L., Deng, X., Hang, R., Chen, D., Zhang, X., Zhang, Y., Liu, C., Cao, X., 2015. Integrative genome-wide analysis reveals HLP1, a novel RNA-binding protein, regulates plant flowering by targeting alternative polyadenylation. Cell Research. 25: 864-876.

Zhang, Y., Li, X., 2005. A Putative Nucleoporin 96 is Required for Both Basal Defense and Constitutive Resistance Responses Mediated by suppressor of npr1-1, constitutive 1. The Plant Cell. 17: 1306-1316.

Zhang, X., Shi, Y., Powers, J., Gowda, N., Zhang, C., Ibrahim, H., Ball, H., Chen, S., Lu, H., Mount, S., 2017. Transcriptome analyses reveal SR45 to be a neutral splicing regulator and a suppressor of innate immunity in Arabidopsis thaliana. BMC Genomics. 18: 772.

Zhang, H., Zhong, H., Shang, S., Shao. X., Ni, M., Chen, X., Xia, Y., 2019. NAD tagSeq reveals that NAD^+-capped RNAs are mostly produced from a large number of protein coding genes in Arabidopsis. PNAS. 116: 12072-12077.

Zhang, X., Wang, T., Liu, M., Sun, W., Zhang, W., 2018. Calmodulin-like gene MtCML40 is involved in salt tolerance by regulating MtHKTs transporters in Medicago truncatula. Environmental and Experimental Botany. 157: 79-90.

Zhang, Z., Sun, W., Shi, T., Lu, P., Zhuang, M., Liu, J., 2020. Capturing RNA–protein interaction via CRUIS. Nucleic Acids Research. 48(9): e52.

Zhang, Z., Boonen, K., Ferrari, P., Schoofs, L., Janssens, E., van Noort, V., Rolland, F., Geuten, K., 2016. UV crosslinked mRNA-binding proteins captured from leaf mesophyll protoplasts. Plant Methods. 12: 42.

Zhao, Y., Yu, Y., Zhai, J., Ramachandran, V., Dinh, T., Meyers, B., Mo, B., Chen, X., 2012. The Arabidopsis Nucleotidyl Transferase HESO1 Uridylates Unmethylated Small RNAs to Trigger Their Degradation. Current Biology. 22(8): 689-694.

Zhao, C., Zhang, H., Song, C., Zhu, J., Shabala, S., 2020. Mechanisms of Plant Responses and Adaptation to Soil Salinity. The Innovation. 1(1). https://doi.org/10.1016/j.xinn.2020.100017.

Zhu, J., 2001. Current Opinion in Plant Biology. 4: 401-406.

Zhu, J., 2016 Abiotic Stress Signaling and Responses in Plants. Cell. 167: 314-324.

Zhu, Y., Rowley, J., Bohmdorfer, G., Wierzbicki, A., 2013. A SWI/SNF Chromatin-Remodeling Complex Actsin Noncoding RNA-Mediated Transcriptional Silencing. Molecular Cell. 49: 298-309.

Zuo, Y., Feng, F., Qi, W., Song, R., 2019. Dek42 encodes an RNA-binding protein that affects alternative pre-mRNA splicing and maize kernel development. Journal of Integrative Plant Biology. 61(6): 728-748.